UNIVERSITY OF CASSINO AND SOUTHERN LAZIO
DEPARTMENT OF CIVIL AND MECHANICAL ENGINEERING
DOCTORAL COURSE IN "METHODS, MODELS AND TECHNOLOGIES FOR ENGINEERING"

CHARACTERIZATION OF AIRBORNE AND RESPIRATORY PARTICLES IN INDOOR ENVIRONMENTS

ING-IND/11, BUILDING PHYSICS AND BUILDING ENERGY SYSTEMS

PhD Candidate:
ELISA CARACCI

Tutor:
PROF. GIORGIO BUONANNO

Co-tutor:
PROF. LUCA STABILE

XXXVI CYCLE

UNIVERSITY OF CASSINO AND SOUTHERN LAZIO
DEPARTMENT OF CIVIL AND MECHANICAL ENGINEERING
DOCTORAL COURSE IN "METHODS, MODELS AND TECHNOLOGIES FOR ENGINEERING"

Date:	16/01/2024
Author:	**Elisa Caracci**
Title:	**Characterization of airborne and respiratory particles in indoor environments**
Department:	**Civil and Mechanical Engineering**
Degree:	**Philosophiae Doctor**

Permission is herewith granted to University to circulate and to have copied for non-commercial purposes, the above title upon the request of individuals or institutions.

Signature of Author

TABLE OF CONTENTS

LIST OF TABLES

LIST OF FIGURES

SUMMARY

The understanding of the relationship between human health and indoor air quality (IAQ) is a never-ending challenge. For decades the main design parameters of efficient buildings were the energy efficiency and, in case, the protection from outdoor pollutants whereas the possible health treat of indoor sources was mostly underestimated. In fact, building occupants are not properly aware of the indoor air quality, of their exposure to pollutants or pathogens and, consequently, of how much they contribute to reducing the indoor air quality through their habits and activities. In addition, modern lifestyles pushed people to spend most of time in indoor microenvironments respect to outdoor ones, and consequently expose them to high pollutant concentrations. Outdoor pollutants are affected by physical and chemical processes, driven by complex meteorology and photochemistry. In contrast, indoor ones are a function of outdoor pollutants, indoor source strength, removal and deposition rate within the structure, indoor mixing, and chemical reaction. All these factors make the study of indoor environment more than challenging, and worthy of attention.

Airborne particles represent one of the main pollutants negatively affecting the IAQ, ranging in size from nanometers to millimeters. They can be generated by different indoor sources (e.g., cooking activities or biomass burning, etc.), produced by indoor reactions (e.g., ozone-initiated reactions occurring during cleaning activities) or penetrating from outdoor spaces. They are capable to cross the respiratory system, carrying toxic compounds, depositing in the deepest airways, and provoking negative health effects. Recently, smaller particles were recognized as most critical for human health and the related metrics (number and surface area) being more representative of the health effects with respect to particle mass (e.g., PM_{10}). For this reason, an in-depth measurement and monitoring of particle concentrations, particle size distributions and relative composition is having more and more attention.

Indoor air quality also involves the presence of biological contaminants, fungi (including yeasts), pathogens, allergens (from fungi, pets, insects, and other sources, including pollen) and toxins. Indoor air biological contamination may have different sources, namely outdoor air, the human

body, bacteria growing indoors, and pets. Concerning indoor environments, the most important biologic contaminants are microorganisms, allergens, and toxins. Recently, the severe acute respiratory syndrome coronavirus 2 (SARS-CoV-2) pandemic has brought renewed attention to virus-laden *respiratory particles* in disease transmission (airborne transmission). The measurement of expelled respiratory particles represents the preliminary step to apply the existing risk models of infection in indoor environments and/or in close-proximity configurations. Indeed, such models are strongly dependent on the viral emission of the infected subject which is, in turn, influenced by the viral load carried by the respiratory particles (that can be obtained from PCR tests) and by the number of emitted particles.

In this thesis work, some currently missing aspects regarding airborne and respiratory particles were explored and discovered, with the aim to fill some knowledge gap in terms of characterization of *emission*, its associated *risk*, and possible *eco-feedback* approach with the goal of spreading awareness related to indoor air quality-issues. In Chapter 1, a general overview of aerosol dynamics, classification, measurement, health effects and regulatory framework is provided. In Chapter 2, a description of airborne and respiratory particles, the related risks, and methods to improve people's awareness is detailed. Considering that airborne particles represent one of the most significant environmental risks people have to face, different airborne particle indoor sources (e.g., candles, incenses, mosquito coils) where physically and chemically analyzed according to their size through a detailed experimental analysis presented in Chapter 3. Indeed, the existing risk models on human health (e.g., related to the occurrence of lung cancer) revealed a strong correlation with the sub-micron airborne particles (with respect to super-micron ones) related to the exposure of different sources, especially cooking activities that represent the main contributor to the emission of sub-micron airborne particles in free-smoking homes. To this end, a simplified approach to evaluate the lung cancer risk related to airborne particles emitted by indoor sources was developed and presented in Chapter 4. If it is true that knowledge is fundamental, its transfer is even more important, especially for those who are not directly part of the scientific community. Indeed, an Eco-Feedback strategy, usually adopted in energy savings, was designed for indoor air quality issues, with the objective to increase awareness and stimulate behavioral changes among occupants. The success of the strategy emerged both in terms of promoting behavioral changes of the occupants and reducing the concentration levels while airborne particle emitting sources (i.e., cooking) were in operation as shown in Chapter 5. Finally, as concern the respiratory particles, since the quantification of emitted respiratory particles is critical in calculating the risk of infection in

confined environments and few studies are currently available in the literature on children, an experimental analysis aimed at measuring the respiratory particles emitted by children during speaking activities was carried out and here presented (Chapter 6).

Chapter 1:
AEROSOL CHARACTERIZATION

Aerosol is defined as a metastable suspension of solid or liquid particles (airborne particles) in a carrier gas. The time scales affecting the dynamic and thermodynamic phenomena of airborne particles are generally very short and thus confer the characteristic of instability on the aerosol to which the adjective "metastable" refers. In environmental field, the presence of particles in gaseous exhausts or in the atmosphere can be defined as smoke, fog, particulate matter (PM), etc.

1.1 Particle size classification

Size classification is one of the most relevant for airborne particles. The minimum particle size is not strictly defined perhaps in part because technological limitations do not allow particles smaller than 2 nm to be detected with acceptable efficiency. Nevertheless, the size range of airborne particles is from a few nanometers to tens of micrometers. Particles with a characteristic size between 2.5 and 10 μm are commonly referred to as "coarse particles", those smaller than 2.5 μm as "fine particles", and those smaller than 100 nm as "ultrafine particles" (UFPs) [1].

Since the direct measurement method of particle concentration consists of weighing particles deposited on filter following size selection by impactor, it is also useful to recall the definitions of the different PM (particulate matter) fractions. In fact, Council Directive 2008/50/EC of May 21, 2008, on ambient air quality limit values for sulphur dioxide, nitrogen dioxide, nitrogen oxides, particulate matter, and lead defines PM_{10} and $PM_{2.5}$ as the mass fractions of particles that penetrate through a size-selective inlet with a 50 percent of cut-off efficiency for an aerodynamic diameter of 10 and 2.5 μm, respectively. Similarly, particles less than 100 μm in diameter are more generically referred to as "total suspended particles" (TSPs) [2].

The characteristic particle size referred to the size classification just proposed is the diameter. The shape of aerosol particles (sampled in ambient or emission) is not purely spherical (Figure 1-1), therefore, a characteristic parameter of particle size needs to be identified. Different equivalent diameters were introduced by referring to properties of the same measurable particles: the best

known is certainly the equivalent aerodynamic diameter (d_{ae}), defined as the diameter of the sphere of unit density (ϱ_0 = 1 g cm^{-3}) that has the same settling velocity as the particle under consideration. Similarly, referring for example, to the ability of particles to move in an electric field or in a diffusive field, it is possible to define equivalent diameters of a particle, assumed to be spherical, that exhibits the same mobility as the particle under consideration.

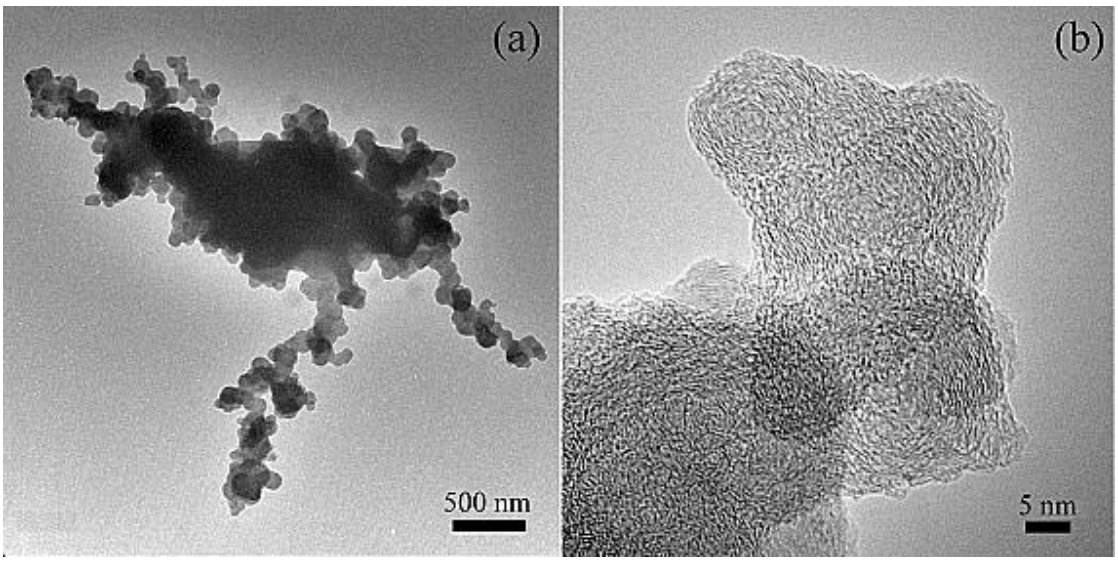

Figure 1-1. TEM images of a soot particle. (a) A chain-like soot aggregate. (b) High-resolution TEM image shows the typical aggregate structures [3].

1.2 Particle size distribution

Aerosol particles, whether sampled in the environment or in emission from plants, typically are not dimensionally monodisperse. On the contrary, they vary over a size range from a few nanometers to tens or hundreds of micrometers according to a concentration distribution that, in terms of number, surface area, and volume, has peaks (or modes), in different areas of the size range under consideration. An example of particle concentration distribution in number, surface area and volume for an urban aerosol is shown in Figure 1-2. In general, the distribution in number is strongly shifted toward smaller diameters with a very large number of small particles despite a small number of large particles, which, however, make the largest contribution in terms of volume/mass.

According to the different origin of aerosol (mechanical, from combustion phenomena, etc.) the distribution in particle number has one or more characteristic modes. In the typical size range of sub-micrometer particles, three typical modes can be distinguished: *nucleation mode*, *Aitken mode*

and *accumulation mode*. The typical *nucleation mode* includes particles generated directly from gas-particle conversion phenomena: these are "fresh" particles emitted by the combustion phenomena (primary aerosol) or formed photochemically in the atmosphere (secondary aerosol) and are in the size range of a few tens of nanometers. The *Aitken mode* includes typically growing particles whose typical size is several tens of nanometers. *Nucleation mode* and *Aitken mode* usually dominate the number distributions of particles. *Accumulation mode* includes "aged" particles that have virtually ended their growth phase, or, at any rate, whose growth rate has drastically decreased. This mode is typically in the range of 100 nm to a few hundred nanometers and dominates the distribution of particles in surface area.

In defining typical aerosol modes, reference was made to the origin of the particles and the relative different shape of size distributions. In addition to size, aerosol particles can also be classified with reference to the source of emission. They may have a natural or anthropogenic origin if their emission is attributable to natural sources (rock erosion, particle resuspension from the ground, etc.) or due to combustion phenomena based in energy conversion processes (vehicular traffic, power plants, etc.). In addition, aerosol can be classified according to origin into primary and secondary aerosol: aerosol directly emitted from the source into the atmosphere is defined as primary, whereas aerosol generated photochemically in the atmosphere from precursor gases is defined as secondary.

Natural sources can have a mass contribution far greater than the anthropogenic contribution [5], [6] but, the latter, constitutes the main source in terms of sub-micrometer particles. It should also be noted that, except for long-range transport, particles influence humans and the environment essentially on a local scale. In this sense, although particles emitted from natural sources are globally much higher than those emitted anthropogenically, they do not have significant effects on human health and the environment. In contrast, particles emitted from anthropogenic sources are being investigated since these sources are close to urban settlements with higher population densities. Thus, in general, it can be argued that mechanically generated particles are mainly of the super-micrometer type, while the formation of sub-micrometer particles is due to nucleation phenomena that are based in combustion processes by condensation of low-volatile vapors (gas-particle conversion) and/or in chemical reactions of precursor gases in the atmosphere that give rise to condensable species (secondary particles).

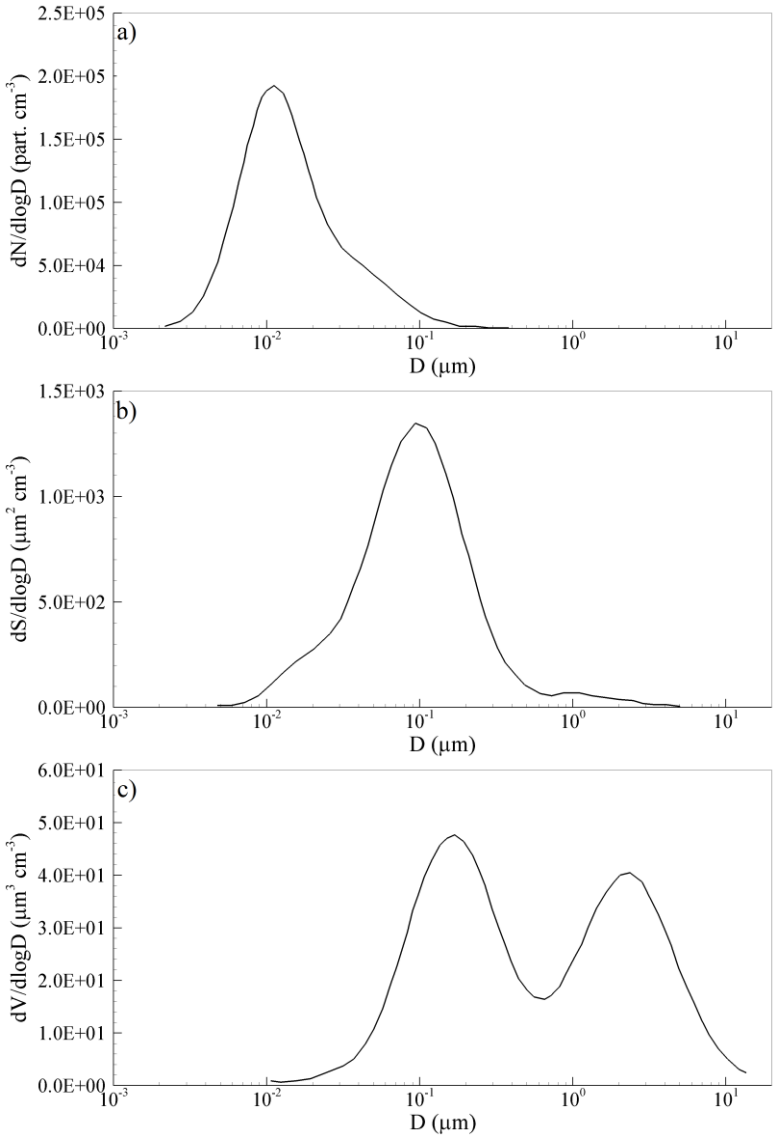

Figure 1-2. Size distributions in terms of number (a), surface area (b), and volume (c) for an urban aerosol [4].

1.3 Aerosol dynamics

In the definition of the atmospheric aerosol introduced at the beginning of the chapter, emphasis was placed on the characteristic of meta-stability, which requires the aerosol to be considered as a nonstationary system due to the sudden thermodynamic and dynamic phenomena affecting the particles. The position of the modes in the distribution of an aerosol (not already "aged") can also vary very rapidly by virtue of the different dynamics of the particles in the different

modes of the size spectrum. The formation of new particles is due to nucleation phenomena driven by the formation of a condensed phase from supersaturated vapors: the typical size of these particles is represented by the nucleation mode. Such gas-particle conversion phenomena are characteristic of both combustion processes (primary particles) and photochemical reactions in the atmosphere from precursor gases (secondary particles). The time evolution of the particles from their formation to deposition is shown in Figure 1-3.

Particles typical of the nucleation mode tend to grow by moving, thus, onto the *Aitken mode* and then, finally, into the accumulation mode region. This growth phenomenon occurs by condensation of vapors on the stable nucleus already formed (the number of particles remains constant) or, also, by coagulation between particles (with relative decrease in the number of particles). In the accumulation region, the particles are now "aged", and their growth process is greatly slowed down. Therefore, the formation of coarse particles is not due to the evolution of fine particles but, as previously shown, to mechanical phenomena.

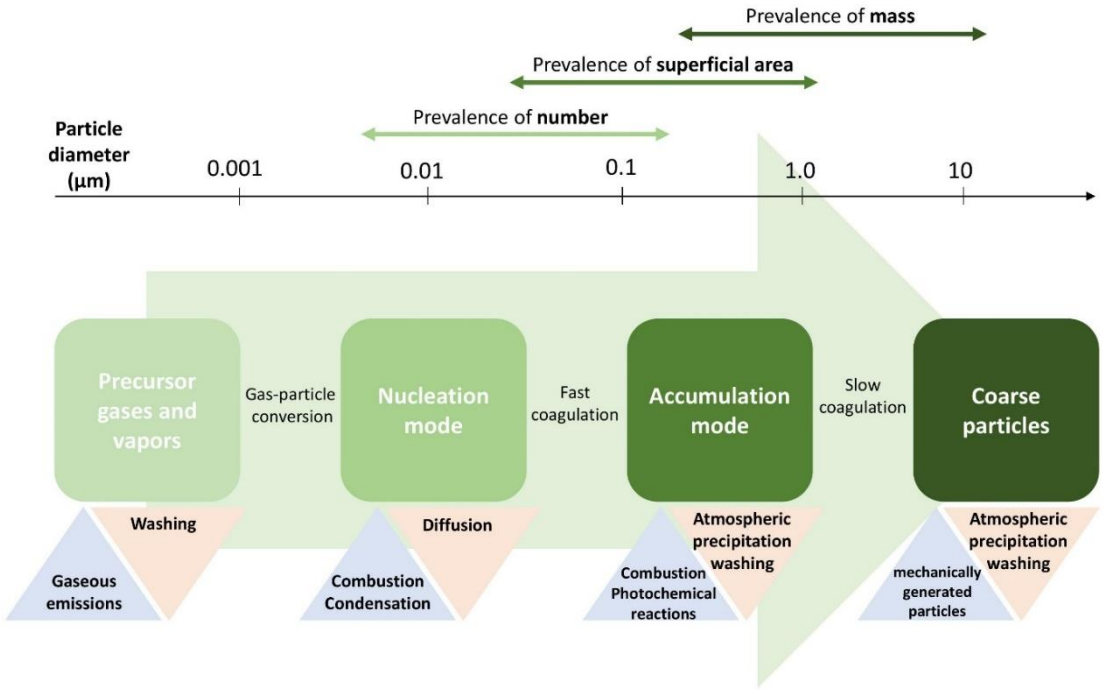

Figure 1-3. Evolution of aerosol particles for different modes: the mechanisms of formation, growth, and removal.

Alongside the phenomena of particle size evolution, removal processes occur that act simultaneously with those of particle formation and growth by influencing aerosol distribution [1].

Removal phenomena are different according to the size of the particles under consideration: deposition processes typical of ultrafine particles are diffusive while, as particles increase in size, they are subject to removal phenomena by inertial means (gravitational settling, washing by atmospheric precipitation, etc.).

1.4 Concentrations and size distributions particle measurement

The interest in ever smaller particle sizes from an epidemiological and toxicological point of view has necessitated, on the one hand, the updating of emission limits and ambient concentrations for the protection of human health (see section 1.6), and on the other hand, the development of measurement technologies and methodologies capable of assessing total concentrations and size distributions of particles both in emission from plants and in the environment (outdoor and indoor).

The method defined by EU regulations as the reference for mass measurement of particles is, as previously described, the gravimetric method, whose characteristic parameters are represented by the different PM fractions ($PM_{2.5}$, PM_{10}). This technique cannot be used automatically and, moreover, gives no indication as to the concentration distribution over the size range of interest being representative only of the fraction of particles that has a significant contribution by mass. However, the research in the epidemiological field has shifted from the mass fraction alone to particle concentration in terms of particle number and surface area. This need has resulted in the development of optical sensing techniques and in the simultaneous refinement of particle size classification methodologies, then applied in instrumentation capable of measuring total particle number concentration and particle size distribution. It seems clear, therefore, that there is a need to measure in the size range of ultrafine particles. In terms of health effects, for example, the importance of knowing the distribution over the entire size range, in addition to the integral value of the total mass concentration, is demonstrated by the different deposition of particles in different regions of the respiratory system because of their size [7].

This section will describe the operation of measuring devices used in the methodology of the case studies dedicated to particle size characterization that can assess, in a quasi-instantaneous manner, the total concentration and size distribution in terms of aerosol number, surface area, and volume. Because of the different motion and deposition dynamics that characterize particles of different sizes, various instruments are used in measuring in the different particle size ranges. For particles larger than a micrometer in size, sizing techniques directly related to particle inertia can be

used (the measurement principle behind the *Aerodynamic Particle Sizer*, APS, spectrometer); in contrast, particles on the order of a few hundred nanometers, or smaller are not directly classifiable due to their inertia, because, the dynamics affecting their motion do not depend on inertial phenomena, and it is necessary, therefore, to first electrostatically classify and, subsequently, count the particles (measurement principle underlying the *Scanning Mobility Particle Sizer*, SMPS). However, the cost and bulk of the APS and SMPS instruments make them unenforceable for workplace use and more appropriate for lab-based applications. This aspect has led to the development of "portable aerosol instruments" consisting of devices in a small and light format. Among these, handheld condensation particle counter (CPC), Aerasense Nano Tracer and TSI AeroTrak are used for measuring the particle counts. NanoScan scanning mobility particle sizer (NanoScan SMPS), portable aerosol mobility spectrometer (PAMS), and optical particle sizers (OPS) can be used to provide a more detailed assessment of workplace environments, including the particle counts and size distributions [8].

1.4.1 Lab-based instruments

Principle of particles classification

Most of the lab-based instruments accomplish the classification of sub-micrometric particles by applying an electrostatic force to the particles and thereby controlling their trajectory. To properly classify the particles contained in a volume of aerosol properly sampled, a known electric charge must be imparted to the particles themselves and, once charged, their field of motion can be altered by varying the strength of an external electric field. The main conventional techniques used to electrically charge aerosol particles can be classified as follows: by *static electrification*, using a flame (*flame charging*), by ion diffusion (*diffusion charging*) and by the effect of an external electric field (*field charging*). The sub-micrometer particle charging technique exploited in the classification and measurement devices described below is *bipolar diffusion charging* (neutralization) achieved by ion generation due to the decay (radiation decay) of radioactive material. Bipolar diffusion charging and neutralization phenomena require a high concentration of bipolar ions, which the classical corona discharging method, which can be used only in the case of unipolar ion generation, cannot provide. Radioactive decay allows positive and negative ions to be produced, which will then be attracted to oppositely charged particles to obtain, after sufficient residence time, an equilibrium charge distribution. The equilibrium is reached after the evolution of two phenomena, specifically the collision of ions already presents in the air (roughly equally distributed between positive and negative ions) imparting an unknown charge distribution to the aerosol and likewise way, the loss

of charge for particles attracting oppositely charged ions. The two competing phenomena tend, at equilibrium, to give a stationary charge distribution which, under the assumption of equal concentration of positive and negative ions, is referred to as a distribution of Boltzmann equilibrium or, also, bipolar equilibrium charge distribution. It estimates the probability (fn) that particles of a given size d_p possess n electric charges elementary *e*.

The Boltzmann distribution is symmetric with respect to the n = 0 condition, and this is due to the assumption of positive and negative ions present in equal concentration in the charging environment. Positive and negative ions have different mobility because of their different molecular weights and different propensity to form a condensed phase around them. Therefore, ions of different polarity tend to bind with particles differently. The effects of different mobility of ions and their ability to bind to aerosol particles have been studied by Gunn [9], Fuchs [10], and Hoppel and Frick [11], [12], and the resulting charge distributions at equilibrium exhibit a slight asymmetry. In the case of Aerosol Neutralizers 3077 (TSI Inc.), the equilibrium charge distribution used is that proposed by Wiedensohler based on Gunn's formulas (Table 1-1).

Aerosol classification techniques based on electrostatic charge work best for sub-micrometer particles since larger particles have too high a probability of acquire multiple charges. In the case of sub-micrometer particles, the probability of multiple charges is smaller and, in any case, can be estimated by equilibrium charge probability distributions as the of the size of the particles themselves. The incorrect estimation of the number of charges on the particle results in an inaccurate assessment of the electrical mobility of the Z_p particle: particles of equal size but with different charge distribution have a different rate of migration electric and, therefore, a different trajectory in the applied electric field and, in conclusion, are classified as particles of different sizes.

Classification by techniques that exploit electric mobility is, for practical purposes, usable only for sub-micrometer particles also because of their high migration rate, which makes this rapid sizing method. On the other hand, the particles under consideration are also those that most easily tend to deposit diffusively compromising the measurement. The time (τ) required for a particle subjected to electric field forces travels a distance *b*, based on the definition of the electrical migration velocity, is estimated as

$$\tau = \frac{b}{Z_p E} \qquad (1)$$

where E represents the electric field strength. Aerosol classification, the charging of which is the preliminary process, is practiced in an electrostatic classifier consisting of an Aerosol

Neutralizer and a particle sampling column better known as a Differential Mobility Analyzer (DMA). The DMA, in its cylindrical version (Figure 1-4), consists of two coaxial steel electrodes, one external grounded and the other, internal, to which a high voltage is applied such as to create a radial electric field whose intensity (*E*) varies along the radius of the cylinder according to the law:

$$E(r)=\frac{V}{r\ln\frac{r_2}{r_1}} \qquad (2)$$

where V is the applied voltage varying from 0 to -11 kV and r_1 and r_2 represent the polar coordinates of the inner and outer electrode, respectively.

Table 1-1. Equilibrium charge distribution of aerosol particles evaluated by Wiedensohler [13].

	Probability of the particle to possess *n* elementary charges												
***d_p* (μm)**	**-6**	**-5**	**-4**	**-3**	**-2**	**-1**	**0**	**+1**	**+2**	**+3**	**+4**	**+5**	**+6**
0.01						5.14	90.75	4.11					
0.02					0.02	10.96	80.57	8.64	0.01				
0.04					0.54	19.50	64.79	14.86	0.31				
0.06				0.02	1.92	24.32	54.13	18.51	1.09	0.01			
0.08				0.11	3.73	26.81	46.75	20.46	2.10	0.05			
0.10				0.37	5.63	27.31	42.28	20.91	3.30	0.17			
0.20		0.05	0.53	3.40	12.38	25.49	29.66	19.51	7.26	1.53	0.18	0.01	
0.40	0.27	1.14	3.60	8.54	15.24	20.46	20.65	15.66	8.93	3.83	1.24	0.03	0.05
0.06	1.21	3.00	6.19	10.53	14.82	17.25	16.60	13.20	8.69	4.73	2.13	0.79	0.24
0.08	2.42	4.64	7.71	11.12	13.90	15.06	14.15	11.53	8.15	4.99	2.65	1.22	0.49
1.00	3.56	5.84	8.53	11.13	12.96	13.45	12.46	10.30	7.59	5.00	2.93	1.54	0.92

A flow of dimensionally polydisperse aerosol (*Qa*) is sampled and, before entering the Electrostatic Classifier (EC3080, TSI Inc.), passed through an impactor capable of removing particles larger than a given size by inertial impact. The removal of particles of sufficiently large aerodynamic diameter is important, because, they have a high probability of carrying multiple charges. At the inlet of the Electrostatic Classifier, the *Qa* flow rate is passed through a charge neutralizer that can impart an equilibrium charge distribution to the aerosol. The polydisperse aerosol with an equilibrium charge distribution is fluxed from above and fed into the classification region between the two electrodes, according to a laminar flow, where it comes into contact, without mixing, with a flow of filtered air (*Qs, sheath flow*), also characterized by a laminar flow, which drives the *Qa* flow rate downward from the classification region confining it to an area close to the outer cylinder.

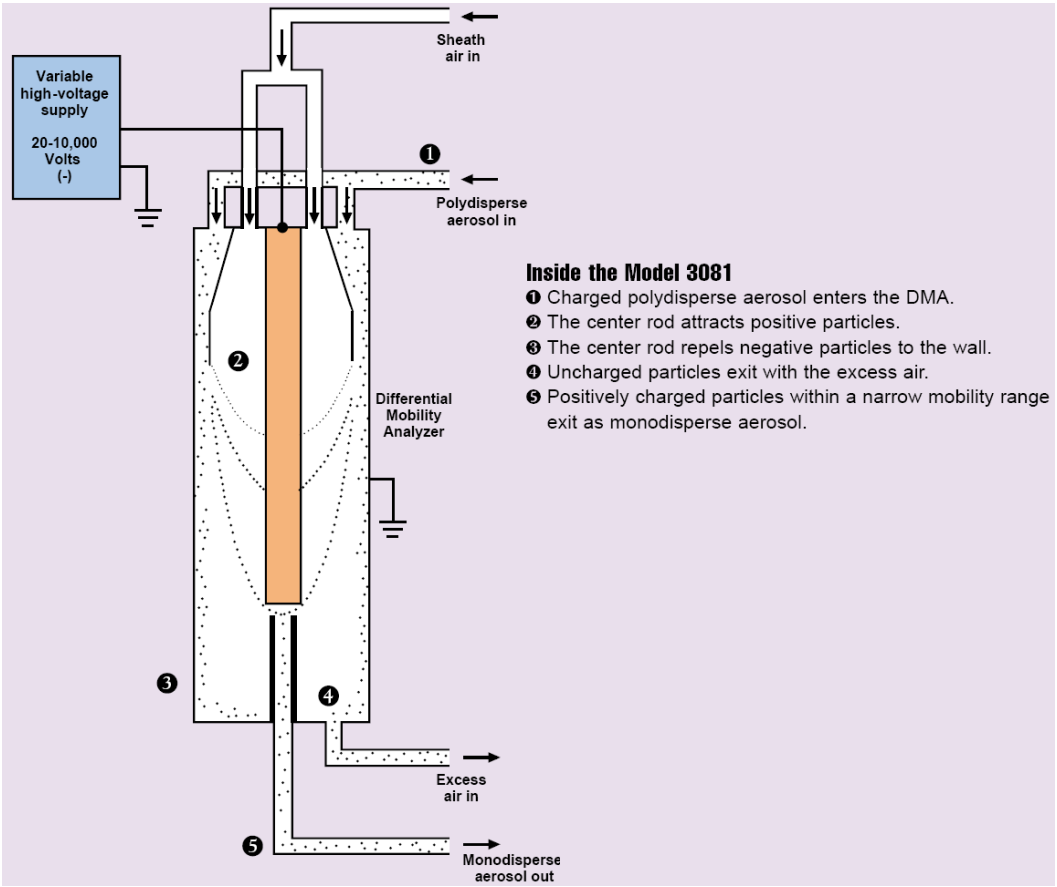

Figure 1-4. DMA function scheme (Long-DMA 3081, TSI Inc.).

The applied electric field attracts positively charged particles to the inner electrode. The ability of the particles to move in such an electric field is, by definition, expressed through the electric mobility of the particles (1) and depends on the aerosol flow rate present in the classification region and the geometry of the classifier. Smaller particles, characterized by high electrical mobility high, are attracted more rapidly toward the negative electrode, whereas larger particles, with lower electric mobility, are affected more by the forces of the momentum field succeeding, therefore, accomplish a longer trajectory in the classification region. Specifically, given the geometry of the classification region and the flow rates *Qa* and *Qs*, to each assigned voltage (*V*) corresponds to a characteristic electric mobility and, therefore, a characteristic particle size whose trajectory (trade-off between electrical and momentum forces) terminates in a gap (exit slit) arranged immediately downstream of the lower end of the central electrode. The aerosol flow rate consisting of particles of a desired size (monodisperse aerosol, *Qm*) thus collected can be sent to a counter. The remaining aerosol flow rate (excess flow rate, *Qe*), characterized by particles larger than those selected, is collected

clean and reused as sheath flow (Qs) as described in the operation diagram of the Electrostatic Classifier (EC 3080, TSI Inc.) in Figure 1-5.

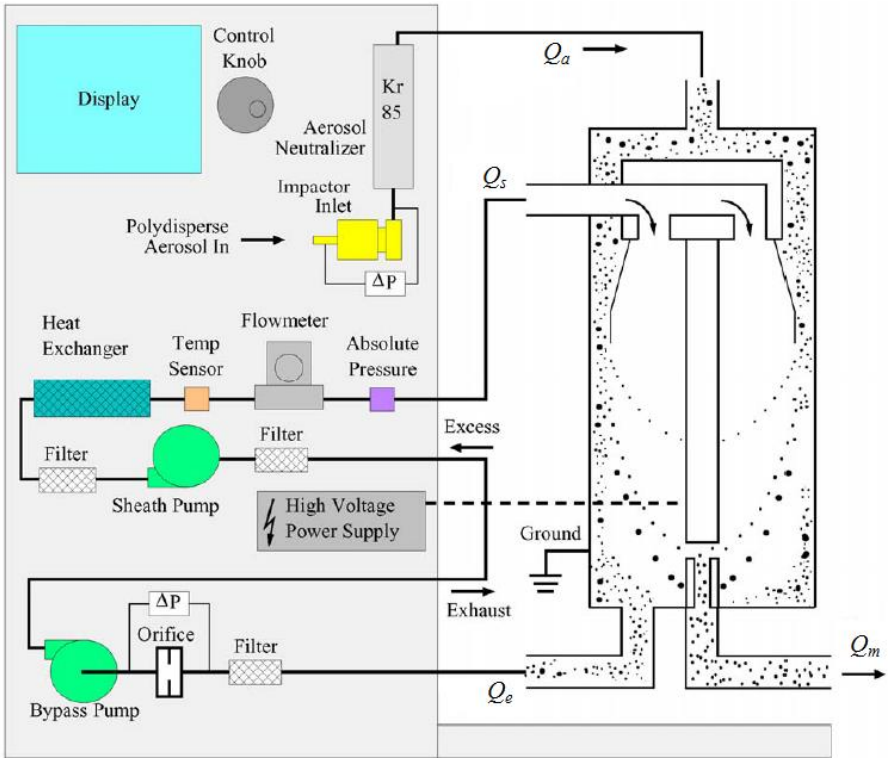

Figure 1-5. Operation scheme of the Electrostatic Classifier (EC 3080, TSI Inc.).

Particle counts: Condensation Particle Counter (CPC)

Particle counting by vapor condensation, which targets particle accretion, was introduced to make up for the threshold limits of detectability of particles optically. Counting by condensation techniques is carried out in special counters, better known as *Condensation Particle Counter* (CPC) or *Condensation Nuclei Counter* (CNC), through three processes: the creation of a supersaturated environment with respect to a working fluid, particle growth by vapor condensation, and particle detection by optical technique. There are three different techniques used to activate condensation: adiabatic expansion, cooling (or heating in the case of water CPCs) and mixing of hot and cold air streams.

The operation of the cooling CPC is described below, as it is, to date, the most widely used type downstream of a particle classification device (Electrostatic Classifier) in a configuration known as Scanning Mobility Particle Sizer (SMPS) and used for the determination of aerosol size distributions.

The cooling CPC consists of a saturator, a condenser, and an optical detector; an alcohol (butanol, ethanol, and methanol) is typically used as the working fluid. A volumetric flow rate of aerosol is continuously flushed by means of a suction pump placed in the outlet section of the instrument so that the aerosol first passes into a saturator, which, in the case of butanol, must be maintained at a temperature of 39°C so that the air becomes saturated with butanol vapors. Next, the aerosol flow is sent into a condenser, that is, a duct maintained at a low temperature (14°C) by conduction cooling the outer surface. In this section, the aerosol becomes supersaturated with butanol vapor, and the greater the degree of supersaturation (*S*) achieved, the more easily the individual particle can be enlarged by condensation. The particles, having reached a size of a few micrometers, are easily detected by an optical counter, which, in the case of low concentrations, counts the particles individually by producing a single-pass signal (single particle counting) while, in the case of high concentrations, it uses a photometric-type counting technique by which the total light scattered (total light scattering) by the particles is converted to total concentration on the basis of an appropriate calibration factor.

As an example, Figure 1-6 shows the operating schematic of CPC 3775 TSI Inc. Following the path that the aerosol takes in such a device, downstream of the inlet section, the sampled aerosol is divided into two flow rates: an aerosol flow rate that undergoes the thermodynamic transformations previously described, and a flow rate that is cleaned of aerosol by HEPA filters and eventually used as a by-pass flow rate so that the pump operates at a constant flow rate.

The CPC can operate in two different input flow modes: low-flow (low-flow) or high-flow (high-flow). In the case of high-flow mode, the input flow rate is 1.5 L min^{-1} of which 1.2 L min^{-1} is used as by-pass and the remaining 0.3 L min^{-1} is analyzed. In the case of low-flow mode, the inlet flow rate is 0.3 L $min^{-1,}$ and this is sent entirely to the saturator, the remaining 1.2 L min^{-1} flow rate required by the pump is sucked in separately (make-up air) and filtered by HEPA filter. The ability to work in high-flow mode allows for reduced response time and minimized diffusive losses in the ducts. Such a motion regime is, therefore, used in the case of operation disjointed from a classifier when, that is, one is interested in the integral value of total concentration. In the case where the CPC is used downstream of a classifier, the use of either flow condition depends on the size range one wishes to monitor.

One of the critical aspects of particle counting is the non-homogeneous distribution of temperature, and hence saturation ratio *S*, along the condenser radius. The minimum diameter for which the condensation process can be activated depends, therefore, also on the radial position of

the particles along the condenser duct, leading to lower counting efficiency at smaller diameter particles. The definition of a minimum diameter detectable by the CPC and the decrease in counting efficiency of smaller particles is due, in addition, to the higher saturation ratio required to realize a condensation phenomenon in the case of particles with the highest radius of curvature. In the case of CPC 3775 (TSI Inc.), the minimum detectable diameter is about 4 nm; as for counting efficiency as a function of size, instrument management software corrects measurement data based on efficiency curves reported in various scientific studies ([14]–[18]): Figure 1-7 shows the typical counting efficiency curve for CPC 3775.

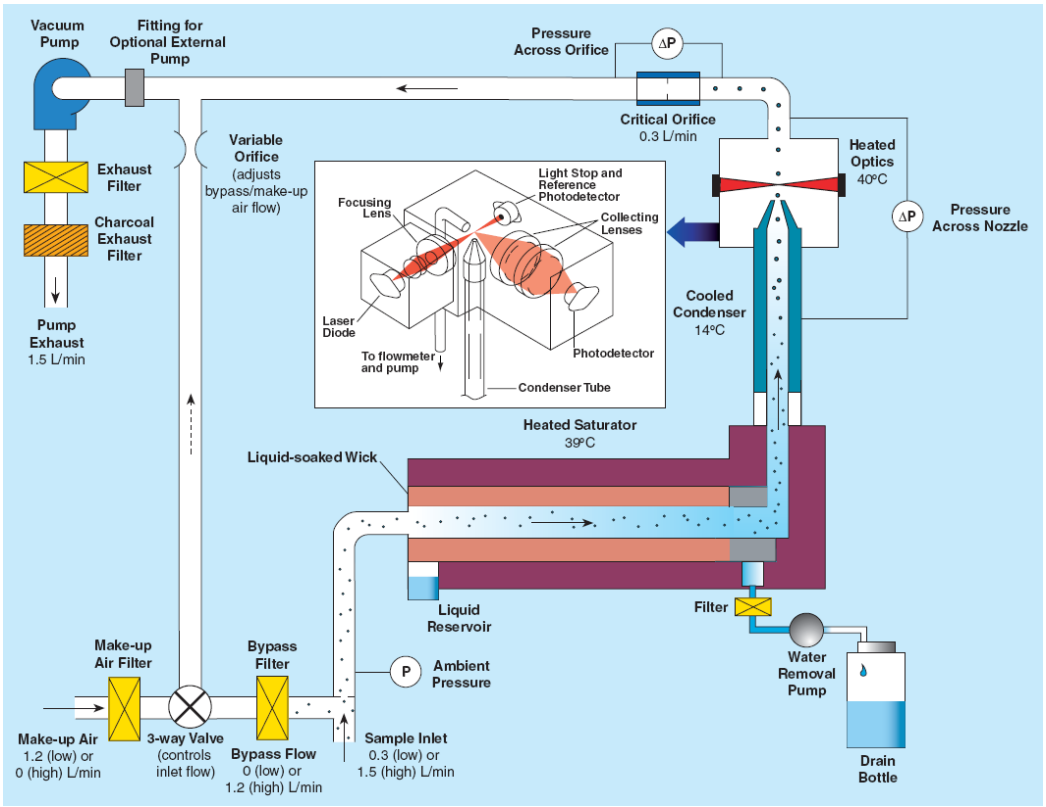

Figure 1-6. Operation scheme of the Condensation Particle Counter (CPC3775 TSI Inc.).

Another critical issue in the measurement of particle concentration by CPC is the statistical error in counting if very low particle concentrations are measured. The uncertainty associated with this statistical error is evaluated using a Poisson distribution [19] as $\sqrt{n}/n$ having denoted by n the total particle concentration.

Errors in the measurement of aerosol concentration can also occur in the measurement of concentrations that are too high, in which case, in fact, the probability of particle coincidence, i.e.,

simultaneous presence of multiple particles in the optical detection region, increases. The CPC can correct for coincidence errors by means of a "*live-time*" correction. *Live-time* is the time between two electrical pulses, i.e., the time interval of the total measurement except the time during which the counter is engaged with one or more particles in the optical sensor's measurement range (dead time). Coincidence correction is made in the CPC by relating the number of particles counted to the live-time only and the aerosol flow rate.

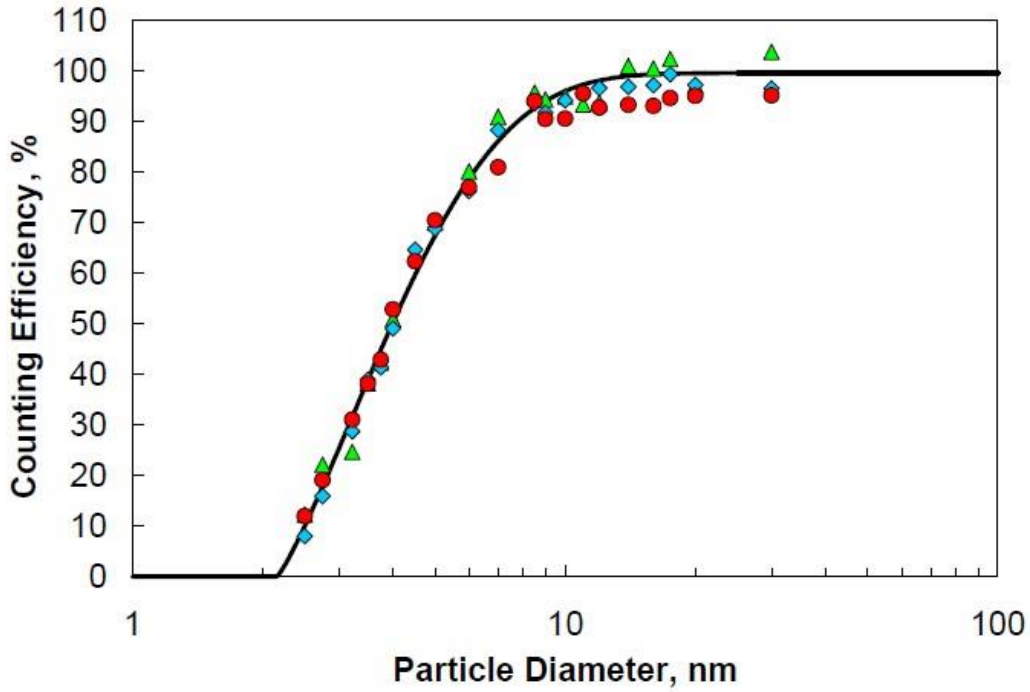

Figure 1-7. Counting efficiency CPC 3775 (TSI Inc.).

Scanning Mobility Particle Sizer (SMPS)

The evolution of the particle classification technique proposed by Knutson and Whitby [20], in conjunction with improvements in the field of optical particle detection (the introduction of the first CNC is due to Agarwal and Sem, [21]), allowed the development of techniques for measuring aerosol distribution. Specifically, the first system consisting of Electrostatic Classifier and CPC, marketed by TSI Inc. was the Differential Mobility Particle Sizer (DMPS 3932). This device allowed aerosol distribution to be measured automatically by applying different voltage steps while having to, however, wait for the sampled aerosol to reach a new steady state at each voltage. This required too long measurement times (more than ten minutes) and, therefore, the actual temporal changes in the aerosol could not be assessed. A further and decisive development in the automatic

measurement of aerosol size distribution is due to Wang and Flagan [22] who improved the system using a dynamic voltage scan that reduced the instabilities allowing faster measurements: this instrument is known as the Scanning Electrical Mobility Spectrometer and, since 1993, has been marketed (TSI Inc.) as the Scanning Mobility Particle Sizer (SMPS).

Figure 1-8 shows the operation diagram of the SMPS 3936 spectrometer (TSI Inc.) consisting of a Long-DMA 3081 (TSI Inc.) and CPC 3775 (TSI Inc.). The operation diagrams of the Electrostatic Classifier and CPC have been described in Figure 1-5 and Figure 1-6, respectively, so Figure 1-8 merely illustrates the connection between the classifier and counter.

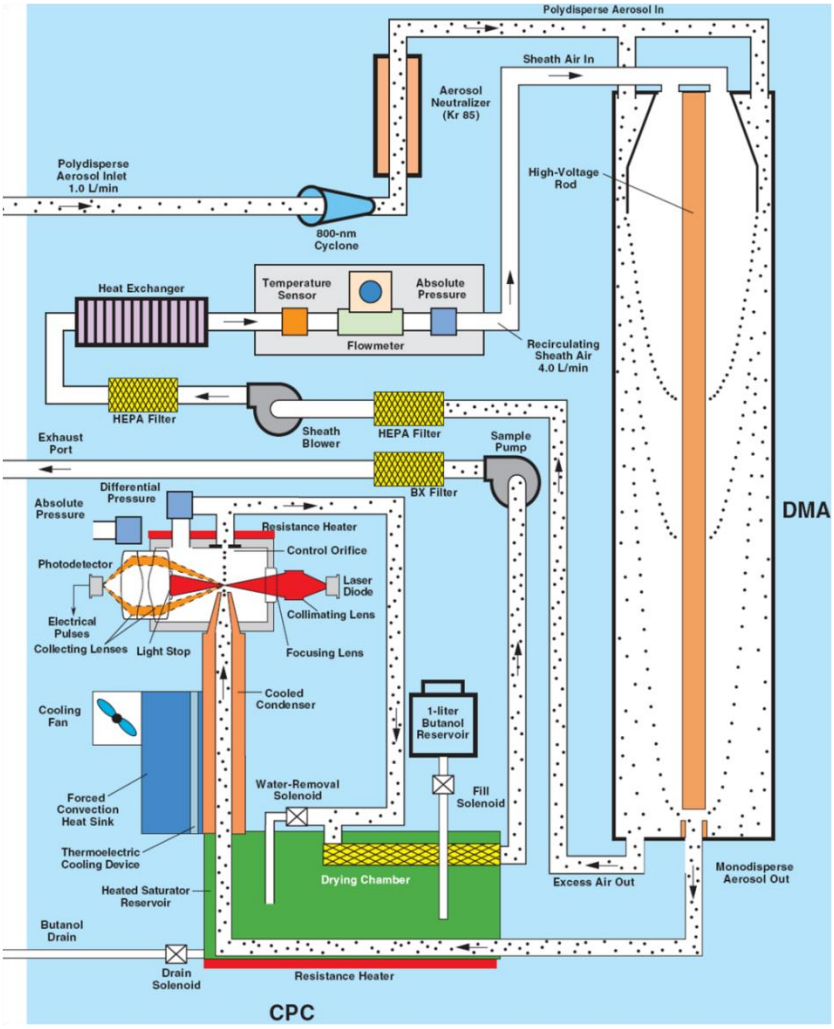

Figure 1-8. Schematic of operation of the SMPS 3936 spectrometer (TSI Inc.) consisting of Long-DMA (DMA 3081, TSI Inc.) and CPC 3775 (TSI Inc.).

In the sections on the operation of the Electrostatic Classifier and the CPC the dependence of the instrument resolution on the residence time of the aerosol in the ducts and, therefore, on the

flow rates was emphasized. In the classification region of the Long-DMA, a ratio between the flow rates of monodisperse aerosol and filtered air of 1:10 must be ensured. The CPC, on the other hand, can operate under two different flow modes: low-flow (0.3 L min^{-1}) and high-flow (1.5 L min^{-1}). It follows that an SMPS 3936 can operate under two flow rate conditions: aerosol flow rate 0.3 L min^{-1} and sheath flow 3.0 L min^{-1}, or aerosol flow rate 1.5 L min^{-1} and sheath flow 15.0 L min^{-1}.

Table 1-2. Measurement range as a function of aerosol and sheath flow rate and impactor used for SMPS 3936 (with Long-DMA 3081 and CPC 3775).

Theoretical measuring range (nm)	**Aerosol flow rate, Q_a (L min^{-1})**	**Sheath flow, Q_s (L min^{-1})**	**Impactor size (cm)**
13 – 838	0.3	3.0	0.0457
5.7 – 239	1.5	15.0	0.071

Control of the inlet aerosol flow rate is provided by a mechanical impactor through the pressure drop downstream of the same impactor. Such an impactor is also used to remove too large particles that could carry, therefore, multiple electrical charges. Impactors of different diameters (holes of 0.0457 cm, 0.0508 cm, and 0.071 cm) can be used; in particular, Table 1-2 shows the range that can be examined as aerosol and sheath flow rates and the impactor used vary. Using higher flow rates can classify smaller diameters but, in that case, the measurement range narrows considerably.

Aerodynamic Particle Sizer (APS) (measurement of particle distribution > 1 μm)

As illustrated in the case of the SMPS spectrometer, advances in optical sensing are of great support in particle counting but do not allow direct sizing of particles over the entire range of interest, because there is no particle property directly related to the amount of scattered light (light scattering) over the entire particle size spectrum.

In the case of sub-μm particles, measurement methodologies are based on a combination of optical sensing techniques and manipulation of the particles' flow field. In that size range, the particle trajectory can be more easily modified by electric and diffusive fields, which, on the other hand, have less applicability for particles >1 μm.

In the case of particles >1 μm, the parameter that best defines the behaviour of the particles themselves is the aerodynamic diameter as it is best related to phenomena of physical interest such as gravitational sedimentation, filtration, and deposition in the respiratory system [23], [24].

With the advent of laser techniques, measurement devices capable of determining real-time aerosol size distributions in the range d_p >1 μm have been developed. Specifically, the instrument

that has had, arguably the greatest following, and has been progressively refined over the years, is the Aerodynamic Particle Sizer (APS) spectrometer produced by TSI Inc.

Figure 1-9 shows the operating schematic of the APS 3321 spectrometer (TSI Inc.) introduced in 2001.

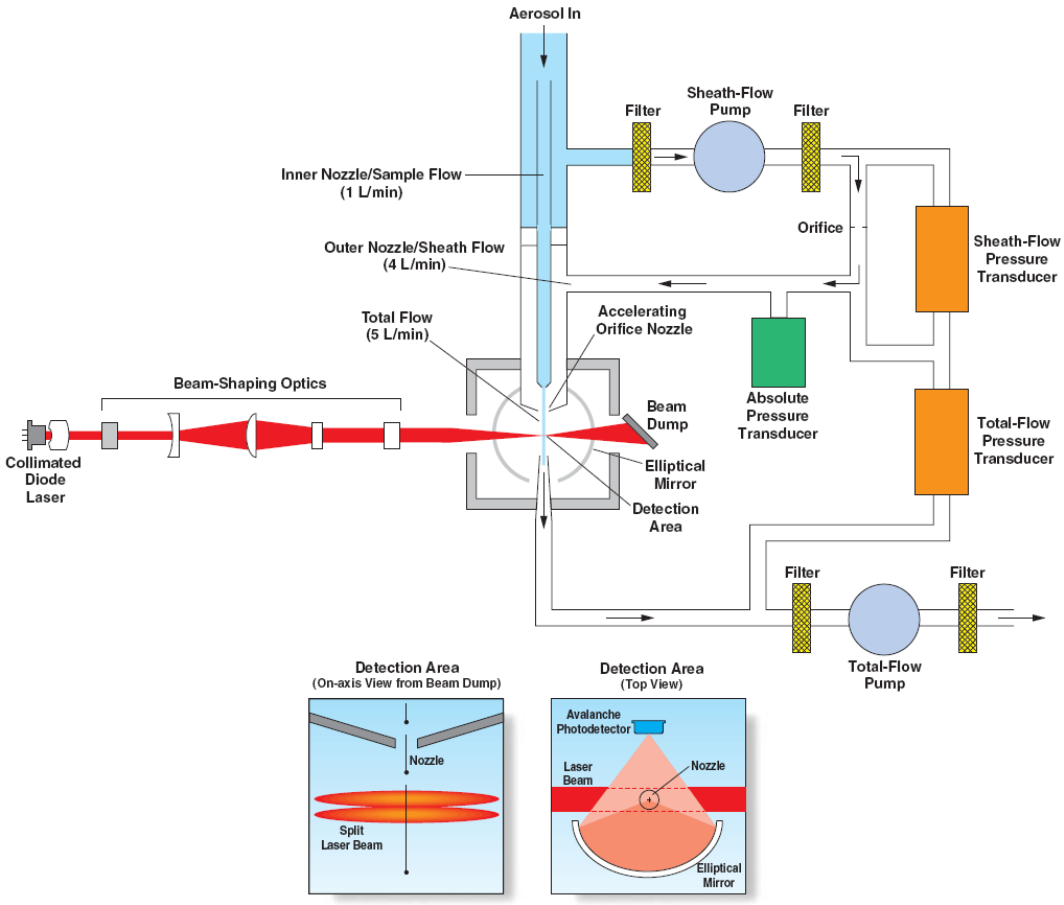

Figure 1-9. Scheme of operation of APS 3321 (TSI Inc.).

At the inlet of the APS spectrometer, the flow of sampled aerosol (aerosol in, 5 L min^{-1}) is divided into two flow rates: a sample aerosol flow rate (aerosol sample, 1 L min^{-1}) and a support air flow rate (sheath flow, 4 L min^{-1}) that is cleaned of particles by HEPA filtering. The sample aerosol flow rate is flushed into an internal duct at the end of which is a converging nozzle that increases the aerosol velocity. The flow of clean air is flushed into an outer duct that is also converging. In the area near the outlet orifice of the inner nozzle, a vacuum is created that accelerates the sample aerosol to ultra-stokesian regimes of motion.

The size (and thus the inertia) of the particles determines their ability to accelerate and, therefore, to follow the gas more easily to the exit of the accelerating duct. At the exit of the converging duct, the particles enter the optical sensing region where they pass through two partially overlapping laser beams. As the particle passes through, the amount of light from the lasers is scattered and an elliptical mirror, placed at 90° to the axis of the laser beams, collects it by concentrating it on an avalanche photodiode (*avalanche photodetector*, APD) capable of converting the received pulses into electrical signals.

The two laser beams provide a signal consisting of two peaks: the time taken by the particles to pass through the two laser beams is called *time of flight*, TOF. The frequency signal is measured with a resolution of 4 ns to which corresponds a threshold size detectable by the instrument of 0.523 μm.

Figure 1-10 also shows the response in terms of light scattering of the particle; in fact, in addition to the frequency signal, the APS 3321 spectrometer is also able to detect the amplitude of the signal obtained as the particle passes through; it is proportional to the intensity of scattered light (Figure 1-10). Attempting to trace the size of particles by means of the light scattered by them can, in fact, be misleading because of the dependence of the light scattering signal on the refractive index and the shape of the particles, therefore, the instrument provides the light scattering measurement data separately from that in terms of TOF and used by experts in the field in order to obtain further information about the composition of the aerosol.

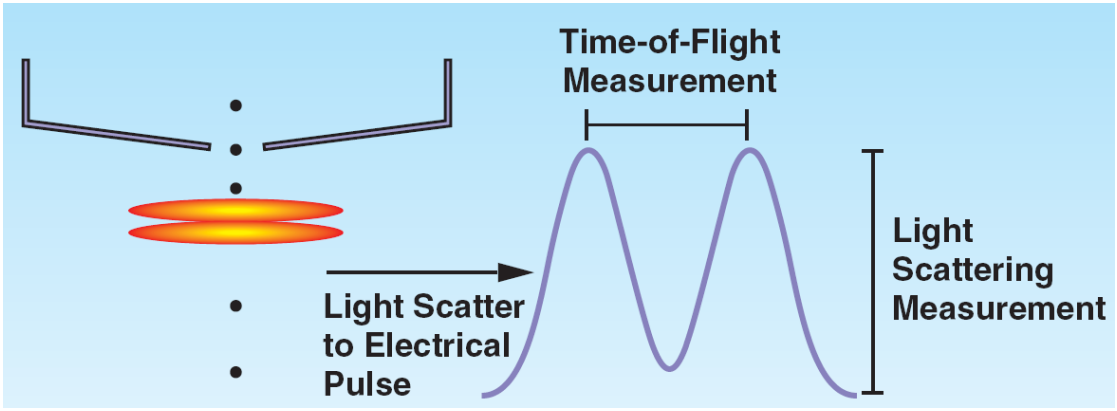

Figure 1-10. Particle detection methods used by the APS 3321 spectrometer (TSI Inc.).

The signal in TOF provided by the APS 3321 spectrometer (TSI Inc.) is susceptible to coincidence errors; these are signaled by more than two peaks higher than the detectability threshold (amplitude signal, detection threshold) at the passage of a (believed) single particle. The

instrument processing program is able, therefore, to recognize such of coincidence and enumerate these events separately. Particles whose aerodynamic diameter is less than 0.523 μm are categorized in a particular size channel (<0.523 μm) and not counted for size distribution purposes; such particles are identified by the instrument as small particles because they have, typically, only one peak above the optical detection threshold. The maximum time within which two peaks due to the passage of a particle can be recorded is 4.096 μs from which it follows that particles that take a longer time are classified as large particles. A crossing time of 4.096 μs corresponds to an aerodynamic diameter of about 20 μm, therefore, the size range that can be analyzed by APS 3321 (TSI Inc.) is from 0.523 to 20 μm in aerodynamic diameter. The different types of signals in amplitude and frequency obtained at the passage of the newly classified particle are summarized in Figure 1-11.

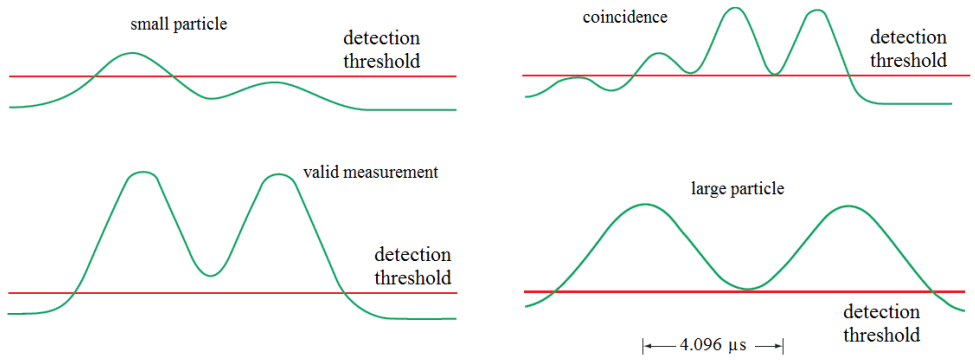

Figure 1-11. Different case histories of TOF signal decoding achieved by APS 3321 (TSI Inc.): single peak (small particle, d_{ae} < 0.523 μm); double peak (valid measurement); triple peak (coincidence); double peak beyond the maximum passage time between the two lasers.

1.4.2 Portable aerosol instruments

Portable aerosol instruments can exploit different measurement principles depending on the type of variable to be measured. In this section, portable devices that were adopted in the case studies shown below are described.

DiSCmini

The DiSCmini is a portable and battery-powered instrument based on electrical diffusion charging of the particles. It is able to determine particle number concentration, mean particle size and alveolar LDSA concentration with a 1-s time resolution [25]. The instrument draws the sampling aerosol with a flow rate of 1 $Lmin^{-1}$ through an optional impactor with a cut-off diameter of 700 nm. DiSCmini charges the aerosol in a unipolar diffusion charger, through a corona wire, which is held at a positive high voltage. A wire mesh separates the corona area from the area where

the particle flow passes by to avoid particle losses due to electrostatic precipitation. Some of the produced ions by the corona penetrates the grid and may then attach to the particles. The current produced by ions I_{ion} arriving at the electrode on the opposite side is constant by controlling the corona voltage. The coefficient K represents the probability of an ion attachment to a particle, proportionally inverse to the mobility b of the particles. Simplifying and by assuming that the attachment coefficients for ions and neutral molecules are equal, the average charge $\bar{q}$ that a particle carry will be proportional to K and thus b^{-1}. Ions that don't attach the particles are removed in a subsequent ion trap by a small electric field, the diffusion stage, consisting of several stainless-steel grids. The current measured in the diffusion stage I_{diff} depends on the particle number concentration N, the average particle charge, and the deposition probability by diffusion. Average charge and diffusion coefficient cancel, and as a result the measured current is directly proportional to the particle number concentration. Particles penetrating the diffusion stage are captured in the following absolute filter, which is also connected to an electrometer. This amplifier measures the current I_{filt}. The current I_{filt} is related to larger particles, I_{diff} to smaller ones. The ratio of the two currents is therefore a measure of the average particle size. The ratio of filter current I_{filt} to the diffusion current I_{diff} can be calculated as function of the mean particle diameter [26].

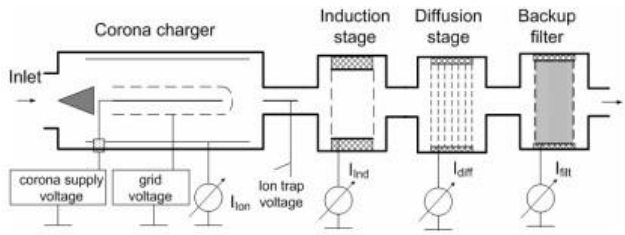

Figure 1-12. Set-up of the diffusion classifier.

DustTrak

DustTrak is a photometer, operating on the basis of a light scattering technique, to measure PM_{10} concentrations with a 1-s time resolution. The TSI Inc (Figure 1-13). DustTrak 8534 is hand-held and, therefore, highly portable direct-reading real-time monitor incorporating a light scattering laser photometer. The light emitted from the laser diode is scattered by particles drawn through the unit in a constant stream; the amount of light scatter determines the particle mass concentration ([27]), based on a calibration factor. The instrument has a mass resolution of ±0.1% or 1 μg m^{-3} (whichever is greater) and a detection range of 0.1–10 μm ($PM_{0.1–10}$).

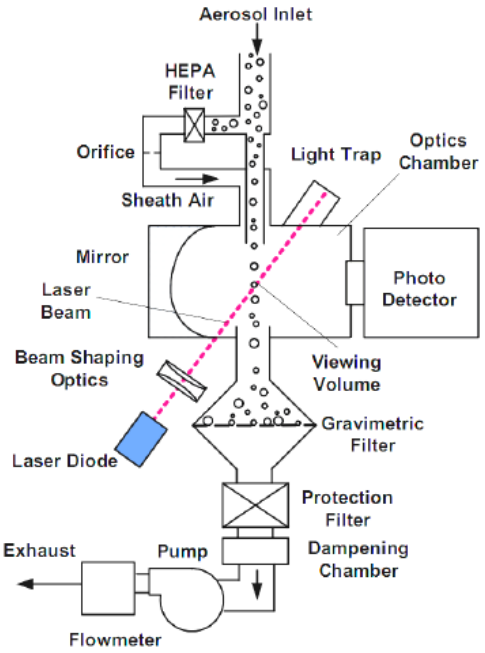

Figure 1-13. Principle of the experimental device: Dust Trak Aerosol Monitor (TSI Inc.).

1.5 Particle chemical characterization and size dependency

Airborne particle dynamics and composition are strongly affected by their size, with smaller particles recently recognized as most critical for human health and the related metrics (number and surface area) being more representative of the health effects with respect to particle mass (e.g. PM_{10}) [28]–[31]. Among the different airborne particle-bound toxic compounds, heavy metals (HMs) and polycyclic aromatic hydrocarbons (PAHs) were recognized as highly detrimental for human health. As an example, long-term exposure to HMs can cause several adverse health effects including human developmental retardation, kidney damage, etc. [32]–[35]. Analogously, exposure to PAHs can increase the risk of respiratory cardiovascular diseases, cognitive development delay, genetic mutations, etc. [34], [36]–[38]. Moreover, some HMs (e.g. As, Cd, Cr, Ni) and PAHs are classified as Group 1 human carcinogens by the IARC (International Agency for Research on Cancer) [39].

Since airborne particle chemical composition and dynamics are size-dependent [40], investigating the size-resolved chemical composition of the entire airborne particle size range [41], [42], i.e. including also sub-micron particles, is a key research issue in view of a more detailed risk assessment related to the exposure to indoor-generated airborne particles [43]–[45].

Studies focused on the chemical characterization of the airborne particles emitted by indoor sources are fewer; some studies revealed the presence of dibenzo-p-dioxins/dibenzofurans, PAHs

and HMs during incense, candles and mosquito coil burning and cooking activities [46]–[58], nonetheless the data provided are still scarce also considering the several parameters potentially affecting the emission. As an example, recently it was carried out an innovative approach to evaluate the lung cancer risk related to airborne particles emitted by indoor sources [44] which relies upon particle and related carcinogenic compound emission rates of the sources: one of the main limitations we faced was the limited information on the chemical analysis of the particles emitted by such sources. Moreover, it was also pointed out that detailed size-segregated chemical compositions of the particles emitted by indoor sources, currently non available, would be extremely important: they would avoid the oversimplifying assumptions considering chemical composition of the emitted particles invariant to the particle size.

1.6 Health effects

Aerosol characterization in terms of size, physics, and chemistry arose from the need to assess the harmful effects of particles on humans and the environment. The exposure to air pollution can increase the risk of developing several acute and health chronic diseases. This is due to the deposition of particles inside the respiratory apparatus that can be divided into three regions differing in anatomical function, duct structure and sensitivity to particle deposition. The first region includes the upper respiratory tract (nose, mouth, pharynx and larynx) and is known as the extrathoracic region; in this region, inhaled air is heated and humidified. The second region is known as the tracheobronchial region and includes the pulmonary ducts, that is, the airways from the trachea to the bronchioles. The third and final region is the alveolar region responsible for the exchange of air between lungs and blood. Larger particles (> 10 μm) are retained in the oropharyngeal region and larynx due to impaction mechanism. Particles between 2 and 10 μm are normally deposited in the tracheobronchial region. Particles of size 0.5–2 μm are deposited in the alveoli and small conducting airways due to gravitational sedimentation. Particles that do not settle significantly and are exhaled are only those between about 100 nm and about 1μm. Below 10 nm, particles are deposited at 90% or more. The particle deposition related to the respiratory tract is shown in Figure 1-14. The magnitude of deposition of inhaled particles in lungs depends on particle parameters (diameter and density), breathing parameters (particle velocity and residence time), and morphometric parameters (branching angle airway radius and gravity angle). Impaction is most effective when air and particle velocities are higher than in the peripheral region of the lungs.

However, in the alveolar region, particle deposition is mainly guided by diffusion and sedimentation due to smaller velocities and hence longer residence times [59].

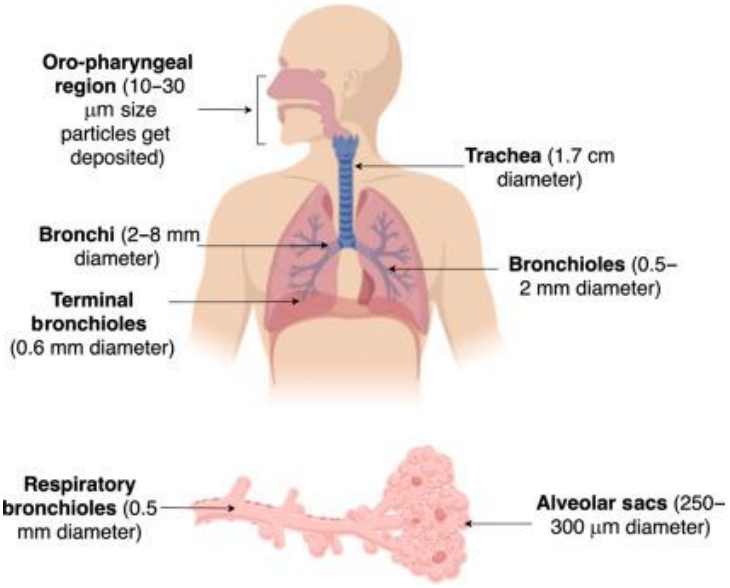

Figure 1-14. Particle deposition in different parts of the respiratory tract [59].

The total deposition inside the entire respiratory apparatus was experimentally estimated by the inhaled concentration distributions from people in different conditions (sitting person, in light or intense exercise), both experimentally and through the support of mathematical models of deposition. In Figure 1-15 deposition curves for the extrathoracic, tracheobronchial, and alveolar regions evaluated by the International Commission on Radiological Protection ([60]) for lightly exercised adults (data averaged for men and women). It can be seen from the proposed deposition curves that particles > 1 μm in diameter are almost totally removed in the extrathoracic region, whereas UFPs deposit, essentially diffusively, in all regions of the respiratory system. The total deposition curve shows an overall reduction in deposition for particles on the order of a few hundred nanometers. Therefore, the resulting size distribution exhaled by people is unimodal with peak at the minimum of the deposition curve (Figure 1-15).

Considering the exposed population, children, older adults, and people with chronic issues represent the most vulnerable classes [7], [61], [62]. Scientific reports highlight the link between exposure, particulate matter (i.e., PM_{10}, $PM_{2.5}$) and health diseases, including fetal growth characteristics [63], [64], ischemic heart diseases [65], respiratory and circulatory mortality [66] and lung cancer [67]–[69], brain disease, mutagenic and carcinogenic impacts, asthma, chronic obstructive pulmonary disease (COPD), pulmonary fibrosis, type-2 diabetes, neurodegenerative

diseases and even obesity [70]. Inhalation of UFPs may also contribute to cardiovascular effects due to their ability to penetrate deep into the lungs and enter the bloodstream [71]. In addition,

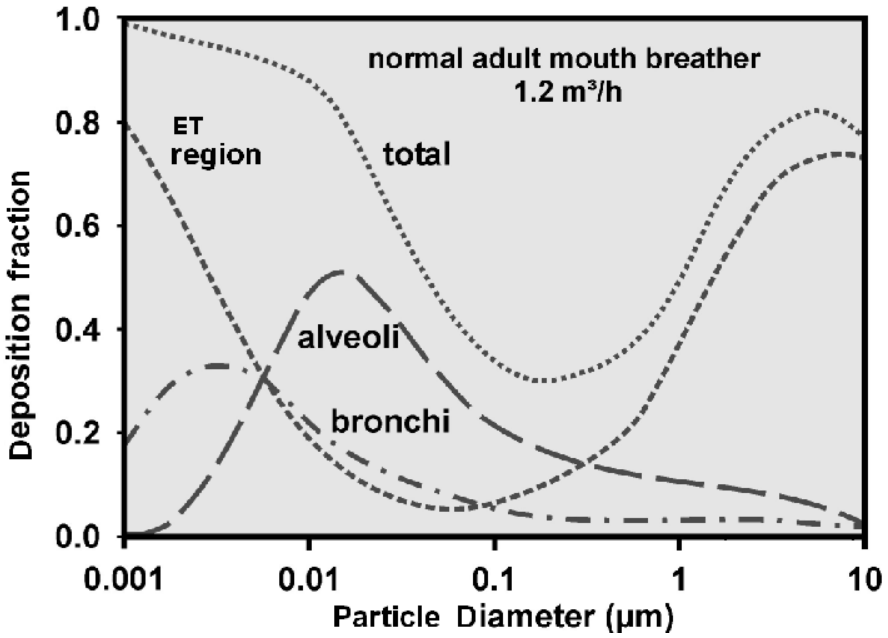

Figure 1-15. Average predicted total and regional lung deposition based on ICRP 1 deposition model for nose breathing for light exercise breathing condition. Highest deposition (ET region for 0.001 and 10 μm particles, bronchi region for 0.005 to 0.007 μm particle [72]).

considering that most of the population spend 80 to 90% time in the indoor environment and UFPs are emerging as the most dominant and abundant particulate matter and, human exposure to these particles has increased dramatically. Due to the small size, these particles may provoke more dangerous and aggressive health impacts, ranging from normal transient of respiratory problems to cardiovascular and respiratory mortality and morbidity. Due to the large surface area, these particles can transport a variety of toxins causing tissue and cell injury, leading to enhanced oxidative stress and inflammation [73]. For this reason, the scientific community is orienting more and more research in their investigation, with the objective to introduce air quality guidelines with the aim to increase awareness among the exposed population.

1.7 Regulatory framework

The purpose of the legislation is to control emission and ambient concentration of airborne particles for the protection of human health. The presence of condensation nuclei was confirmed by the end of XIX century and the research focused interest on human health also due to tragic environmental disasters such as the one recorded in London in 1952. In that circumstance, the

exposure to high levels of particles concentrations due to residential outdoor pollution and unfavorable conditions (excessive thermal stability, no wind, high humidity) caused the deaths of several people.

In Italy scenario, the problem of air quality was introduced in 1994 with the concept of PM_{10}. In 2002, with the Ministerial Order n.60, transposed by the European Directive, identified a concentration of 50 μg m^{-3} as the daily limit value of PM_{10} for the protection of human health. It was stipulated that this limit value should be reached by 2005 and could not be exceeded more than 35 times per year, with a daily limit of 40 μg m^{-3}. These limits have been confirmed with the enactment of the European Directive 2008/50/CE transposed in Italy by Legislative Decree No. 155 of August 13, 2010 [74] and was added another limitation regarding the $PM_{2.5}$, with annual limit concentration set at 25 μg m^{-3}. Along with the European Directive 2008/50/CE the gravimetric method was pinpointed as reference to ensure traceability to the International System of Measurements. It consists of a sampling of particulate matter using a low porosity filter inside a volumetric sampler; the filter is weighed before and after sampling under controlled thermohygrometric conditions obtaining by difference the mass of particulate matter deposited [75]. The monitoring of PM_{10} and $PM_{2.5}$ is performed through the fix sampling stations, equally dislocated according to the number of inhabitants. Recently, given the importance and health impact of UFPs, the recent proposal for a Directive of the European Parliament and of the Council on ambient air quality and clean air for Europe suggests that UFPs shall be monitored at selected locations in addition to other air pollutants (at least 1 sampling point per 5 million inhabitants shall be established).

Nowadays, in addition to residential pollution, vehicular traffic represents the main pollutant outdoor source [76]–[78]. For this reason, the environmental policy was focused in reducing the car and power plant emissions [79]. Over time the authorities had imposed limits (e.g., Euro 6 regulation) on particulate matter emitted by vehicular traffic, especially for diesel vehicles (approximately the 50% of the entire car fleet on the road) responsible of soot particles of 20-30 nm. This led to mandatory installation of particulate filters on all diesel engines that guarantee the abatement of the mass fraction of particles. In addition to vehicular sources, the authorities also instituted regulations for the emission from combustion of waste from incineration plants, with a maximum limit for the total suspended particles (TSP) of daily 10 mg m^{-3} and 30 mg m^{-3} on a semi-hourly basis. It should be noted that the actual TSP emissions for most incineration plants are far below these limit values [80], [81].

Nevertheless, the mentioned legislation is directed toward outdoor environments, and coarse (PM_{10}) and fine particles ($PM_{2.5}$). Indeed, in Italy (also in Europe) specific directive legislative framework on the quality of indoor air is not yet available, despite the presence of pre-legislative initiatives, guidelines, and documents. Considering the high permanence in indoor environments (90%) [82], the presence of several pollutant sources respect to outside [83] and poor ventilation practices [84] it is necessary to adopt and implement measures to combat air pollution at the source.

Chapter 2:
EMISSION, RISK AND ECO-FEEDBACK APPROACH

In this chapter, a more detailed description about the dynamics interacting between airborne and respiratory particles and the exposed population is provided, in terms of *emission*, *exposure*, *risk,* and *eco-feedback* strategy.

2.1 Airborne particles

Indoor aerosol consists of particles penetrating from outside, emitted from indoor sources, and formed through reactions between precursors in gas phase [85]–[89]. In order to evaluate the interaction between the emissive source and the population exposed, it is necessary paying attention to some key aspects. Firstly, the exposure is a vital element of risk assessment, that depends on the pollutant concentration (i.e., the numerical value of the amount of an individual pollutant per unit volume of air at a particular point in time or averaged over a period of time) multiplied by the time over which a person is in contact with that pollutant. The pollutant concentration in a specific environment is related to several boundary conditions (e.g., room size, room ventilation) and the emission rates (i.e., the amount of a specific pollutant emitted per unit time).

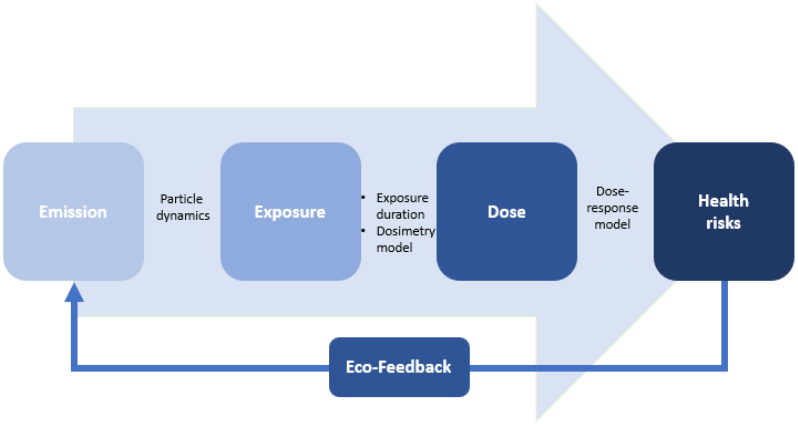

Figure 2-1. Particle dynamics, from emission to risk, through an Eco-feedback approach.

When the concentration is time-varying, an average concentration is used for exposure calculation. Subsequently, the *dose* is a product between the *exposure* and *dosimetry factors* (e.g., inhalation rate, regional surface area of the lung or breathing pattern) and quantifies the amount of substance available for interference with metabolic processes or biologically significant receptors.

Dose-response is the magnitude of the response of an individual to a given dose of pollutant. *Lifetime individual risk* (which applies specifically to carcinogenic pollutants) is a product of lifetime average daily dose and *dose-response*. Risk of *exposed population* is a quantitative assessment which considers *lifetime individual risk* of the population groups affected and specific *exposure scenarios* of the population. The main objective of health risk assessment is to link the hazard with the risk to the exposed population in a quantitative way, and thus provide the basis for risk management [90]. Finally, considering that the management of indoor environments is influenced by occupant's actions, try to make a behavioural change could reduce the related health risks, through "eco-feedback" strategies (Chapter 5) (Figure 2-1).

In the following sections, a more in-depth explanation is provided both for airborne and respiratory particles.

2.1.1 Emission of airborne particles by indoor sources

Airborne particles can be generate by several indoor activities and, especially, by combustion phenomena occurring when cooking, smoking, using heating systems, incenses, candles or using cleaning products etc., [91]–[96], that can increase the level of particle concentration and, in particular, number and surface area concentrations with respect to mass [97]–[101]. Cooking activities represent the main contributor to the emission of sub-micron and ultrafine particles in free-smoking homes [102], [103]. For example, Buonanno et al. [97] measured the particle emissions produced during grilling and frying as a function of the food, source, cooking temperature and type of oil. It was found that when grilling, the gas stove generated more particles (1.5×10^{12} part. min^{-1}) than the electric stove (1.2×10^{12} part. min^{-1}), with relevant differences in emission factors from heating the empty grill at maximum (2.5×10^{12} part. min^{-1}) and minimum power (1.5×10^{12} part. min^{-1}) on the gas stove. Furthermore, the type of food used for grilling did significantly affect emission rates, with foods containing a higher percentage of fat generating higher emission rates. Grilling cheese may cause the generation of more particles (3.4×10^{12} part. min^{-1}) respect to eggplants (2.6×10^{12} part. min^{-1}). It was also observed that the temperature is a non-negligible parameter of influence that may increase the number of particles in every condition, regardless the type of food, oil, or technology involved. Experiments to determine the influence of

oil type on gas frying found that sunflower oil generated the lowest number, surface area and mass emission factors, whilst olive oil emitted the highest. The emission factors obtained from using an electrical frying pan with the same three oils were found to be well below those observed for frying using a gas stove.

Mainstream aerosol linked to smoking activities represent the main route in the occurrence of lung cancer risk [104], [105]. In fact, more than 70 compounds including Polycyclic Aromatic Hydrocarbons (PAHs) are emitted by cigarette combustion, others, namely tobacco-specific N-nitrosamines, are mainly produced during the curing process of tobacco [105]. Even electronic cigarettes (e-cigs), commercialized with the aim of eliminating the intake of such carcinogenic compounds (e.g., carbonyl compounds, among which formaldehyde, tobacco-specific N-nitrosamines NNN and NNK and metals, such as Pb, Cd and Ni), present harmful compounds in their aerosol, even if at 9-450 levels lower than for tobacco cigarettes [106], [107]. Besides the mainstream aerosol, the second-hand aerosol represents a real risk for the exposed population. In order to characterize the emission of second-hand aerosol, Avino et al. [108] measured particle number concentrations and size distributions, PM_{10} and Black Carbon (BC), and the relevant emission rates during smoking activities. Median emission rates of smokers and vapers in terms of particle number were 4.3×10^{11} part. min^{-1} (2.80×10^{12} part. cig^{-1}) and 9.62×10^{10} part. min^{-1} (5.51×10^{11} part. cig^{-1}), respectively. Significant PM_{10} (4.92 mg min^{-1}; 32.0 mg cig^{-1}) and BC (66.2 μg min^{-1}; 430 μg cig^{-1}) emissions were estimated for tobacco cigarette smokers, whereas the relevant vaper emissions were negligible.

The combustion of candles and incenses and mosquito coils can produce high concentrations of particles. To this end, Stabile et al. [96] evaluated the emission factors in terms of number, surface area and PM fraction concentration. The results reveal that Emission factors due to incenses and anti-mosquito products were higher than 10^{14} part. h^{-1} and 48 mg h^{-1} in terms of number and PM_{10} concentrations, respectively. Differently, PM fraction emissions from candle burning were well below 1 mg h^{-1}. Nonetheless, BC emission rate and distribution measurements showed that candle flaming combustion produces mainly carbonaceous particles (BC/PM_{10} ratio higher than 80%). Differently, smoldering combustion processes, like incense and mosquito coils
product combustions, showed a negligible amount of BC.

Another potential pollutant source is attributable to house cleaning activities. Despite their aim is to provide a level of hygiene for health and productivity, they are not necessarily related to an adequate IAQ. Indeed, the presence of air pollutants related to the use of cleaning products is due

to the ozone-initiated reactions of volatile organic compounds (VOCs), such as terpenes and terpenoids (e.g., d-limonene)[109]–[114] and glycol ethers [115].

In the following section, an estimation of the average *emission factor* that can be adopted for airborne particles sources is shown.

Emission factors calculating

Before evaluating the *emission factor*, a particle concentration balance equation, taking into consideration the contributions from indoor and outdoor sources, the deposition rate of particles on indoor surfaces and the AER, should be used as follows ([116]–[118]):

$$\frac{dC_{in}}{dt} = P \cdot AER \cdot C_{out} + \frac{Q_S}{V} + (AER + k) \cdot C_{in} \quad (3)$$

where C_{in} and C_{out} are the indoor and outdoor particle concentrations, respectively, P is the penetration efficiency, k is the deposition rate, Q_s is the indoor particle generation rate, t is time and V is the efficient volume of the laboratory.

The estimation of the average *emission factor*, through the equation (3), can be simplified by using average values instead of functions, and also by making further assumptions about the experimental conditions reported in He et al. [119] as follows:

$$ER = V\left[\frac{C_{in} - C_{in,0}}{\Delta t} + \left(\overline{AER + k}\right) \cdot \overline{C_{in}} - AER \cdot C_{in,0}\right] \quad (4)$$

Where C_{in} and $C_{in,0}$ represent the peak and initial indoor particle concentrations, respectively, AER is the air exchange rate, $\left(\overline{AER + k}\right)$ is the average total removal rate due to both particle exfiltration (related to the *AER*) and particle deposition (evaluated by means of the particle deposition rate, k), Δt is time difference between initial and peak concentration, $\overline{C_{in}}$ is the average indoor particle concentration in the room, and V is the volume of the room. This equation ignores the effects of particle dynamics such as condensation, evaporation, and coagulation, since these are considered to be minor, particularly under the conditions normally encountered in residential environments.

2.1.2 Exposure and dose to airborne particles in indoor environments

People's activities (e.g. use of pollutant sources, manual airing of the rooms, etc.) and building characteristics (e.g. building ventilation system, airtightness of the envelope, etc.) [91], [120], [121] can influences the indoor concentrations of air pollutants and contaminants and, thus, the related exposure of occupants [122]. The exposure in homes is also affected by the seasonality effect with highest pollutant concentrations measured in colder periods due to the low ventilation rates and

insufficient outdoor air supply [92], [123]–[125]. Indeed, residential buildings are becoming increasingly airtight to avoid heat losses and to achieve high energy efficiency ratings [126] but most of them are not equipped with ad-hoc ventilation systems [127], [128]. Stabile et al. [129] measured the exposure to different airborne particle metrics (including both sub- and super-micron particles) and attached carcinogenic compounds in dwellings where three different heating systems were used: open fireplaces, closed fireplaces and pellet stoves. Measurements in terms of particle number, lung-deposited surface area, and PM fraction concentrations were measured during the biomass combustion activities. The results showed hourly particle surface area extra-doses received by people (evaluated as most probable values through a Monte Carlo simulation) resulted equal to 56 $mm^2\ h^{-1}$, 5 $mm^2\ h^{-1}$, and 3 $mm^2\ h^{-1}$ for exposure to open fireplaces, closed fireplaces, and pellet stoves, respectively. Such dose values due to open fireplaces resulted extremely high when compared to other indoor sources. Pacitto et al. [128] assessed the daily doses in terms of particle surface area received by different Western populations in order to show the effect of the age, gender, microenvironment, and nationality (lifestyle, culture, and built-up environment) on the overall daily dose. Data on particle concentration levels demonstrate a high exposure during cooking and eating activities for all the populations investigated. The main parameter influencing the dose received by people is the lifestyle: the time spent in highly-polluted microenvironments (e.g. during cooking and eating activities), as already observed in Buonanno et al. [130], which strongly affect the total daily dose. On the contrary, the outdoor air quality in studied cities has low impact on the dose received by people, due to both short exposure time and not significantly high concentration levels (when compared to indoor sources/exposures).

Exposure and dose calculating

As abovementioned, once the exposure is noted, the *dose* (e.g., the daily tracheobronchial and alveolar deposited fraction of airborne particles) can be calculated as reported in Buonanno et al. [130]:

$$\delta_{A,x} = \sum_{j=1}^{n} \left\{ IR_{activity} \cdot \left[\int_0^{\infty} \varphi_A(IR_{activity}, D) \cdot \frac{dx(D)}{dD} \cdot dD \right] T_j \right\} \quad (5)$$

Where x can be *N* or *S* for particle number and surface area concentration, $IR_{activity}$ is the inhalation rate depending on the human activity, $\varphi_A(IR_{activity}, D)$ is the fractional alveolar deposition depending on inhalation rate and particle diameter, $dx(D)/\ dD$ *D* is the particle number size distribution for each microenvironment and T_j is the time spent for an activity in a defined

location. It possible to deduce that the *exposure* is an environmental parameter, while the *dose* is depending on personal activity respect the surrounding space.

2.1.3 Lung cancer risk in indoor environments

Since the indoor exposure represents a risk to human health (section 1.6), it is useful to perform a-priori risk assessments for indoor environments where highly-emitting sources are adopted. In terms of lung cancer risk related to airborne particles, such assessment can be performed adopting a model developed by Sze-To et al. [131] which allows to estimate the Excess Lifetime Cancer Risk (ELCR), i.e. "additional risk of developing lung cancer" for people exposed lifetime (typically assumed of 70 years) to carcinogen-laden particles, including the contribution of both sub-micron and super-micron particles. In particular, in the ELCR model, particle surface area and mass (PM_{10}) concentrations are adopted as dosimetry parameters for sub- and super-micron particles, respectively.

The ELCR model is quite straightforward and could be a valuable tool for air quality experts since it can be compared to the maximum tolerable ELCR established by the WHO (1×10^{-5}, i.e. a new case of lung cancer on 100000 people exposed [132]) to determine critical exposure scenarios. As an example, it was applied the ELCR model in previous papers to simulate different exposure scenarios, both indoor and outdoor, including schools, homes, transport microenvironments [129], [133], allowing to assess the relative contribution of each micro-environment to the lifetime lung cancer risk and, then, to compare mitigation solutions to reduce such risk [133]–[135]. In Stabile et al. [129], the corresponding lifetime extra risk due to the exposure to open fireplaces, closed fireplaces and pellet stoves for a typical exposure in Italy were estimated equal to 8.8×10^{-3}, 1.1×10^{-3}, and 1.4×10^{-3}, respectively. They were significantly larger than the EPA acceptable lifetime risk (10^{-5}): in particular, the risk due to the open fireplace is not negligible with respect to the lung cancer risk of typical Italian population estimated by Buonanno et al. [133]. In the latter study the ELCR for females (2.18×10^{-2}) was statistically higher ($p< 0.01$) than for males (1.63×10^{-2}), however this should not be considered as an intrinsic "gender effect" since it can be related to the different lifestyles of females and males in Italy. For example, females often spend more time in indoor environments, where exposure levels are higher, particularly during cooking activities. Most of the lung cancer cases in Italy not attributable to smoking were found to be attributable to airborne particle inhalation.

Nonetheless, such model is readily applicable when the particle concentrations (both surface area and mass) in the microenvironment and their chemical composition (i.e., mass fraction of the

carcinogenic compounds) are measured. Thus, a-priori estimates of the ELCR can hardly be performed. As an example, the particle concentration in a given microenvironment is affected by several boundary conditions including source emission rate, room size, and room ventilation [86], [90], [136]–[145]; therefore, even when the same source is considered, the concentration to which people is exposed to may differ greatly as a function of the microenvironment. On the contrary, the emission rates, i.e. the amount of particle surface area, mass, and chemical compounds emitted per unit time, are specific parameters of the type of source (once they are properly characterized, [97], [99], [146], [147], [148, p. 202]); therefore, linking the risk of the exposed population to the emission rates of the source would allow an immediate risk assessment through simplified simulations of exposure scenarios. Based on these considerations, Stabile et al. [149] proposed a new approach, introducing the concept of Emitted Risk (ER) of airborne particle sources, and applied it to outdoor sources in order to estimate the overall lung cancer risk of airborne particles emitted in a city. The usefulness of this novel approach lies in the ability to summarize both the particle emission and the particle carcinogenic potential in a single parameter, which is the lung cancer risk "emitted" by the source (Chapter 4).

2.1.4 Eco-feedback strategies in IAQ issues

Considering that emitted risk is also related to occupants' behavior (e.g., type of source and relative usage time, etc.) that provoke a significant influence on IAQ [121], [150], people are often not aware about how their everyday behavior affects the environment where they live and vice versa [151], especially for air pollutants that are both odorless and colorless [152]. For this reason, acting on behavioral change could reduce the exposure to airborne particles in indoor environments [128], [153]. Actually, understanding people environmental behavior is a complex topic spanning many disciplines including education, economics, sociology, psychology and philosophy other than engineering and metrology [154], [155].

Among the different behavior change methods categorized in literature, education, and awareness (EAA) is the most common used, instead of outreach and relationship building (ORB), social influence (SI), nudges and behavioral insights (NBI) and incentives. It consists of providing information (also through materials such as handouts, newsletters, advertising campaigns, etc., [156]) allowing individuals to explore environmental issues, engage in problem solving and participate in actions to restore and protect the environment [157], [158].

Within EAA methods, the "eco-feedback" strategies are promising tools [154] as they are able to bridge the gap between the lack of awareness and the understanding how their behaviors affect

the environment [159]. Indeed, the "eco-feedback" is a correcting strategy applied to different environmental contexts that helps modifying specific behaviors, promoting habit modifications and, more largely, supports the transformation of a particular action into an automatic reflex (internalization) [160]. Actually, the eco-feedback was defined and applied for the very first time in the energy saving context [161] and, so far, the scientific community has applied eco-feedback approaches to different environmental contexts such as excessive domestic energy and water consumption as well as waste disposal [162]–[165]. Different studies demonstrated the rapid effectiveness of eco-feedback approaches to reduce energy consumptions [162], [166], [167]: as an example, Canale et al. [162] observed average reductions of cold water, hot water, electricity and heating energy consumptions in Danish apartments equal to 17%, 23%, 12% and 17%, respectively, barely using in-home displays (IHDs, i.e. a digital device allowing accessing real-time energy data of smart meters) to increase the occupant awareness. Certainly, providing end-users with feedback is increasingly possible in recent years thanks to the advancements in information communication technology [163]; however, simply providing qualitative information about energy consumptions or indoor air quality could not be an effective strategy for a behavioral change [168]–[170]. Indeed, using easy-to-use meters, also in association with IHDs, allow to turn numeric data into a meaningful representation of information so that users can easily understand what is happening in their homes (awareness), what it means to them (understanding), and what to do with the information (action) [151], [171], [172]. Despite metrological performances, desirable features of these devices are cheapness, long operating life, miniaturized size and low operating noise [120], [169].

When it comes to the quality of the indoor environment the application of eco-feedback approaches is more complex [173]. Indeed, with the exception of thermal comfort, which people feel and can tell whether it is appropriate or not, the presence of air pollutants and contaminants is not always sensed by people [120], [174]; moreover, the instrumentations adopted to measure the different airborne particle metrics are not as cheap and easy-to-use as the energy meters, also in case of low-cost sensors [175]. This poses a first question about the need to increase the sensitivity and the awareness on the exposure to airborne particles and, more generally, to IAQ [151], [176], [177]. Indeed, in terms of IAQ, the eco-feedback has been successfully applied mostly in view of reducing smoking indoors [169] nonetheless, air-quality feedback could have a huge potential in view of significantly improving the exposure of occupants to airborne particles [155], [178].

2.2 Respiratory particles

2.2.1 Emission of respiratory particles by human activities

In addition to airborne particles in indoor environment, respiratory particles present another factor to taking account in IAQ issues, especially since the SARS-CoV-2 pandemic highlighted the importance of the airborne transmission route for respiratory pathogens [179]–[184]. Measurement of respiratory particles is a parameter to consider in the risk of infection due to airborne transmission, caused by the emission of virus-laden respiratory particles by infected subjects during their respiratory activities (e.g., breathing, speaking, singing, coughing, sneezing).

Recent studies have highlighted that, for a given exposure scenario (e.g., volume of the indoor space, distance amongst subjects, ventilation of the indoor space, exposure time, etc.), the risk of infection of exposed subjects is mostly affected by the strength of the emission [185]–[191] and, thus, by the number of respiratory particles emitted during a specific respiratory activity. Consequently, the pertinence of predictive models (e.g., zero-dimensional well-mixed models or three-dimensional close-contact models) in estimating the risk of infection for specific exposure scenarios strongly relies upon the knowledge of the emission of respiratory particles [185], [186], [192], [193]. Several studies have described the formation (in the respiratory tract) and the consequent emission of respiratory particles during different respiratory activities [194], [195]. These studies show that different physical processes occurring in different regions of the respiratory system led to the formation of specific particle size modes. The three main modes that have been identified are those involving particles forming in the bronchioles, larynx, and mouth [194], [195]. Nonetheless, the measurement of respiratory particle emissions is not an easy task because the particles undergo sudden thermodynamic processes (e.g., complex and interconnected effects of inertia, gravity, and evaporation) leading to possible artefacts when measured in ambient air after the emission [196]–[198].

Studies that focus on the evaluation of respiratory particle emissions can be classified in two main categories: fluid-dynamic visualization and respiratory particle quantification. Fluid-dynamic visualizations (e.g., high-speed photography, particle image velocimetry etc.) provide useful information for understanding the dynamics of the exhaled flow as soon as it is released in ambient air, and also show how far the particles can travel [181], [194], [199]. However, they do not provide quantification of the particle emissions. In contrast, respiratory particle quantification studies are conducted using particle counters (e.g., with different measurement techniques, including optical and time-of-flight methods) to measure respiratory particle number concentrations and size

distributions in the exhaled air [195], [198], [200]–[203]. Nonetheless, these challenges in measuring the respiratory particles and the difficulty of recruiting and working with human participants have resulted in a limited number of studies reporting on respiratory particle emission characteristics with a limited number of subjects (generally fewer than 20) and a range of different methodologies. The experimental apparatus has varied; in some studies volunteers were asked to speak into a sampling funnel directly connected to the particle counter (the experiments were conducted in a HEPA filtered laminar flow hood, in a cleanroom, or in ambient air) [204]–[207]. In other studies the subjects had to speak into a large duct, where a constant airflow was generated by suction of a filter fan unit, and the measurement probe was placed at a certain distance from the volunteer [202], [203]. Other researchers adopted a small wind tunnel equipped with HEPA filters into which the volunteers placed their head to perform respiratory activities while the particle counter sampled the aerosol from the wind tunnel [200], [201]. There have also been major differences in the testing protocols. For example, respiratory activities (breathing, speaking, singing, coughing, and shouting) were performed by pronouncing specific phonemes [205], [208] or multiphonetic text (e.g., "Rainbow passage") [208] with or without sound pressure level control [209]. Finally, volunteers involved in the studies have mainly included adolescents [202] and adults [201], [208], [210], whereas little information on children aged 12 years and younger is currently available [203], [207], [211].

2.2.2 Exposure to respiratory particles and related dose and risk of infection

The measurement of the emission due to respiratory particles makes possible the application of risk models in closed environments [212], [213]. The key aspects already described (Chapter 2) and intended for airborne particles (Figure 2-1) can be applied even for respiratory particles, in terms of *emission* (i.e., associated to one or more infected people, namely "quanta emission rate", ERq), *exposure* (i.e., exposure to quanta concentration in the microenvironment), *dose* (i.e., dose of quanta received by exposed susceptible subjects), *dose-response* (i.e., the probability of infection) and *risk* (i.e., he individual risk of the exposed person) [187].

Recently, Buonanno et al. [186] proposed a forward emission approach to estimate the quanta emission rate of an infectious subject on the basis of the viral load in the sputum and the concentration of droplets expired during different activities. A quantum is defined as the dose of airborne droplet nuclei required to cause infection in 63% of susceptible persons. The quanta emission rate (ER_q, quanta h^{-1}) is evaluated as:

$$ER_q = c_v \cdot c_i \cdot IR \cdot V_d = c_v \cdot \frac{1}{c_{RNA} \cdot c_{PFU}} \cdot IR \cdot V_d \quad (6)$$

where c_v is the viral load in the sputum (RNA copies mL^{-1}), c_i (quanta RNA copies^{-1}) is a conversion factor defined as the ratio between one infectious quantum and the infectious dose expressed in viral RNA copies, IR is the inhalation rate (m^3 h^{-1}), and V_d is the droplet volume concentration expelled by the infectious person (mL m^{-3}).

The droplet volume concentration V_d is a function of the expiratory activities (i.e., breathing, speaking, singing, etc.). Experimental data on the droplet volume emitted are not definitive and the sampling method itself can affect the results due to the rapid dehydration occurring to the large particles emitted [214]–[216]. With reference to the SARS-CoV-2 viral load in the mouth, researchers have recently found c_v values in the range 10^3-10^{11} copies mL^{-1}, for both symptomatic and asymptomatic persons, which is also variable in the same patient during the course of the disease [217]–[221].

The second step in evaluating the probability of infection is the calculation of the quanta concentration to which a susceptible subject is exposed. The quanta concentration at time t, $n(t)$, in an indoor environment is based on the quanta mass balance proposed by [212], and can be evaluated as:

$$n(t, ER_q) = n_0 \cdot e^{-IVRR \cdot t} + \frac{ER_q \cdot I}{IVRR \cdot V} \cdot (1 - e^{-IVRR \cdot t}) \quad \text{(quanta m}^{-3}\text{)} \quad (7)$$

where $IVRR$ (h^{-1}) represents the infectious virus removal rate in the space investigated, n_0 represents the initial quanta concentration (i.e., at time t=0), I is the number of infectious subjects, V is the volume of the indoor environment considered, and ER_q is the quanta emission rate (quanta h^{-1}) for the specific disease/virus under investigation. The infectious virus removal rate is the sum of three contributions [216]: the air exchange rate (AER) via ventilation, the particle deposition on surfaces (k, e.g. via gravitational settling), and the viral inactivation (λ).

The dose of quanta received by a susceptible subject exposed to a certain quanta concentration, $n(t,ER_q)$, for a certain time interval, T, can be evaluated by integrating the quanta concentration over time as:

$$D_q(ER_q) = IR \int_0^T n(t)dt \quad \text{(quanta)} \quad (8)$$

It can be concluded from Eq. (8) that the dose of quanta received by a susceptible subject is affected by the inhalation rate (IR) and subsequently by their activity level. As an example, for the same

exposure scenario [i.e. identical $n(t,ER_q)$ and T], the dose of quanta received by subjects performing at a light activity level (IR = 1.38 $m^3\ h^{-1}$; e.g. slowly walking) is more than double that received by people just sitting or standing (IR = 0.54 $m^3\ h^{-1}$).

The fourth and final step in evaluating the probability of infection is the adoption of a dose–response model. Several dose–response models are available in the scientific literature for assessing the probability of infection of airborne-transmissible pathogens [222], [223], including deterministic and stochastic models, and threshold and non-threshold models.

The best-suited dose–response models for airborne transmission of pathogens are the stochastic models [223]. In particular, exponential models have been mostly adopted in previous studies because of their suitability and simplicity [224]. Such models consider the pathogens as discrete bundles (i.e., quanta) distributed in a medium (e.g., saliva/sputum) in a random manner described by the Poisson probability distribution. When the medium is aerosolized, the pathogen distribution in the aerosols, and hence their distribution in the air, also follows the Poisson probability distribution. The complex Poisson summation equations can be simplified in an exponential equation [223]–[225], i.e. the exponential dose–response model, which evaluates the probability of infection, P_I (%), of susceptible people as:

$$P_I = 1 - e^{-D_q} \quad (\%) \tag{9}$$

For a unit dose of quanta (D_q = 1), the probability of infection P_I is equal to 63%, from which derives the definition of "quantum" as the "amount of infectious material to infect $1\text{-}e^{-1}$ (i.e. 63%) of the people in an enclosed space" [212], [226].

In the exponential dose–response model, the variation of host sensitivity to the pathogen is not considered. More complex models, such as the Beta-Poisson probability distribution, could take this factor into account [223]–[225].

The illustrated four-step approach was applied in [185] for quantitative assessment of the individual infection risk of susceptible subjects exposed in indoor microenvironments in the presence of an asymptomatic infected SARS-CoV-2 subject. The proposed approach was used for retrospective assessment of documented outbreaks in a restaurant in Guangzhou (China) and at a choir rehearsal in Mount Vernon (USA), showing that, in both cases, the high attack rate values can be justified only assuming the airborne transmission as the main route of contagion.

2.3 Thesis work objectives

Considering the complexity of the management of an adequate indoor air quality (IAQ) in confined environments, the objectives of the thesis here proposed have attempted to fill some knowledge gaps in airborne and respiratory particles field, in terms of *emission*, *risk* (related to *exposure* and *dose*) and *eco-feedback* strategy. These gaps have been addressed in the case studies hereafter proposed. In particular,

- In the Case Study 1, the size-resolved chemical characterization related to particle emission due to combustion of incenses, candles and mosquito-coils were conducted through the experimental campaign. In order to better characterize the chemical composition of the sources under investigation and considering their typical sub-micrometric emissive size range, an electric low-pressure impactor ELPI+™ was adopted. The collected samples were analyzed to detect and quantify heavy metals and PAHs in airborne particles below 10 μm (Chapter 3).
- In the Case Study 2, a simplified approach to evaluate the lung cancer risk related to airborne particles emitted by indoor sources was proposed. The proposed approach was here applied to different indoor sources (including cooking activities, biomass-burning heating systems, etc.) and considering different scenarios in terms of ventilation and exposure mitigation solutions (Chapter 4).
- In the Case Study 3, in view of bridging the gap of knowledge concerning the IAQ awareness and the effectiveness of eco-feedback on IAQ and exposure to airborne particles, a quantification of the effect of an eco-feedback strategy on different airborne particle metrics, including the ultrafine particles, was conducted. In this study, investigating the IAQ awareness of occupants through questionnaire surveys and applying an eco-feedback strategy, based on both a trustworthy information campaign and an experimental campaign, the possible behavioral changes of the occupants and their ability in reducing the concentration levels in the short-term was evaluated (Chapter 5).
- In the Case Study 4, more than 400 children attending primary and secondary schools (aged 6 to 12) were involved in an experimental study aimed at providing emission rates of respiratory particles while speaking at two different intensity levels – "speaking" and "loudly speaking". For this purpose, experimental apparatus and testing protocol were optimized and, indeed, respiratory particle emission rates were obtained by directly measuring respiratory particle

concentration and exhaled flow rate while subjects pronounced a phonetically balanced word list (Chapter 6).

Chapter 3 - CASE STUDY 1:
SIZE SEGREGATED CONTENT OF HEAVY METALS AND POLYCYCLIC AROMATIC HYDROCARBONS IN AIRBORNE PARTICLES EMITTED BY INDOOR SOURCES

Guaranteeing an adequate indoor air quality represents one of the major modern-day challenges for technical and scientific communities involved in designing and managing indoor environments. Considering that airborne particles were recognized as one of the main hazardous pollutants emitted by indoor sources due to their capability to provoke negative health effects and smaller particles recently were recognized as most critical for human health respect to coarse one (e.g., PM_{10}), the size-resolved chemical characterization of airborne particles emitted by indoor combustion sources is useful. Despite the scientific literature carried out several papers characterizing the airborne particle emission rates of indoor sources, the chemical characterization of such particles was poorly investigated; in addition, information on size segregated content of polycyclic aromatic hydrocarbons (PAHs) and heavy metals (HMs) in indoor-generated airborne particles, that would be extremely useful for proper risk assessments, are completely missing.

In the present study, some indoor sources, like candles, incenses, and mosquito coils, were collected through an electrical low-pressure impactor ELPI+™ and then analyzed with gas chromatography–mass spectrometry (GC-MS) and Inductively Coupled Plasma – Atomic Emission Spectroscopy (ICP-AES). The results showed the presence of different PAHs and cancerogenic HMs with a relative mass size distribution in the sub-micron range.

3.1 Aims of the work

In the present study, the size-resolved chemical characterization of airborne particles emitted by indoor combustion sources, i.e., incenses, candles and mosquito-coils were carried out and size dependent HM and PAH contributions to the PM_{10} were provided thanks to an experimental analysis based on airborne particle collection through an electric low-pressure impactor and consequent gas chromatography–mass spectrometry (GC-MS) and Inductively Coupled Plasma – Atomic Emission Spectroscopy (ICP-AES) analyses.

3.2 Materials and methods

3.2.1 Emission source and sampling site description

Three different emission sources were tested during the experimental campaign: incense sticks, candles and mosquito coils. Incenses, candles and mosquito coils commercially available were chosen. In particular, incenses adopted in the experimental campaign are natural benzoin resin sticks, candles were paraffin wax candles without any kind of additives, and mosquito coils were made up of prallethrin (pyrethroid insecticide) with co-formulants and colorants.

Particle sampling experiments were carried out at the Laboratory of Industrial Measurements (LAMI) at the University of Cassino and Southern Lazio, Italy. In particular, samplings were performed in a 1.80 m × 1.20 m × 2.20 m plexiglass chamber presenting a small opening allowing supplying air for combustion phenomena as well as for electrical cables and ducts. The air exchange rate of the chamber in this condition was measured adopting a CO_2 decay method (not reported here for the sake of brevity; [227]) and resulted equal to 0.50±0.05 h^{-1}.

3.2.2 Particle collection: apparatus description and procedure

In order to collect size-resolved mass amounts for post-hoc chemical characterizations (described in sections 3.2.4 and 3.2.3), an electrical low-pressure impactor ELPI+™ (Dekati Ltd.) was employed and placed inside the chamber (whereas its pump was placed outside). The ELPI+™ is a particle spectrometer able to measure airborne particle number distribution (and total concentration) in real-time and simultaneously collect particles with a sampling flow rate of 10 L min^{-1}. Particles are firstly charged with a known charge level in a corona charger, then, they are size classified in a low-pressure cascade impactor according to their aerodynamic diameter. Every impactor stage is electrically insulated, and particles collected in each stage produce an electrical current proportional to number particle concentrations. Particle mass distribution and total concentration were evaluated on the basis of the number distribution data and applying the following particle densities utilizing the filter functions in the $ELPI_{VI}$ software: 1.1 g cm^{-3} for incense and mosquito coils [49], [228], [229] and 1.5 g cm^{-3} for candles [51].

The ELPI+™ presents 15 stages, lower-upper boundary diameter ranges (expressed as 50% efficiency cut-off diameters, D_{50}) are: 6.0-16.7 nm for stage 1, 16.7-31.3 nm for stage 2, 31.3-54.7 for stage 3, 54.7-94.9 for stage 4, 94.9-156 nm for stage 5, 156-258 nm for stage 6, 258-384 nm for stage 7, 384-606 nm for stage 8, 606-952 nm for stage 9, 952 nm-1.64 μm for stage 10, 1.64-2.48 μm for stage 11, 2.48-3.67 μm for stage 12, 3.67-5.39 μm for stage 13, 5.39-9.93 μm for stage 14,

9.93-10 μm for stage 15. The upper boundary of stage 15 depends on the PM inlet sampling head adopted (if any); we have adopted an EN 12341 PM_{10} inlet (downscaled to 10 L min^{-1}), thus, as mentioned above, the upper diameter D_{50} of the stage 15 is actually 10 μm. Stage 1 (6.0-16.7 nm) doesn't allow particle collection; whereas stage 15 (9.93-10 μm) acts as pre-cut stage thus, it is not measured electrically: consequently, particle distributions and concentrations refer to the 6.0 nm-9.93 μm range (14 stages, from stage 1 to 14), whereas particle collection for chemical analyses are available from 16.7 nm to 10 μm (14 stages, from stage 2 to 15). Polycarbonate collection foils (type 23000, dim. 25 mm, Sartorius Stedim Biotech GmbH, Goettingen, Germany) were adopted for particle collection at each ELPI stage.

Table 3-1. Quantity of sources burnt, total sampling period, average particle number and mass concentrations for each sampling and for each source type (sampling 1 (S1) for HM analysis, sampling 2 (S2) for PAH analysis).

Source type	**Quantity**		**Total sampling period (min)**		**Average particle number concentration (part. cm^{-3})**		**Average particle mass concentration (mg m^{-3})**	
	S1	S2	S1	S2	S1	S2	S1	S2
Candles	40	32	889	628	1.68×10^{6}	1.35×10^{6}	29.6	57.6
Incense	10	10	246	246	3.81×10^{6}	3.00×10^{6}	454.6	347.2
Mosquito Coils	4	2	458	347	8.32×10^{6}	9.07×10^{6}	43.4	76.6

Since HM and PAH determination was performed separately, adopting different methods and apparatus, two different samplings were performed: sampling 1 for HM chemical analysis and sampling 2 for PAH chemical analysis. In order to collect an adequate amount of particle mass on each ELPI+™ stage for chemical post-analyses high mass concentrations for long periods were needed. To this end preliminary tests were carried out to check the concentrations reached and estimate the number of sources to burn simultaneously and the total sampling period. Then, we decided to adopt the following procedure for each indoor source and each sampling: several sources (e.g., candles) were lit up simultaneously and the particle collection and measurement with the ELPI+™ was started as well, then, when the sources burnt out, they were replaced with new ones. This procedure was performed several times for each source: the quantity of source burnt, the total sampling period, and the average number and mass concentrations measured by the ELPI+™ during the samplings are summarized in Table 3-1 for each source type for both the samplings. To

avoid any contamination between the sources, the charger and the impactor were cleaned according to the manufacturer suggestions at the end of each sampling. In addition, flush pump was used to keep the ELPI+™ clean between the measurements.

As concern the source combustion, candles were normally burnt, while incenses and mosquito coils were lit by a flame and fanned out so that the glowing ember continue to smolder and burn away the rest of the materials.

3.2.3 HM determination: apparatus description and analytical method

The analysis of HMs in particle mass samples (Sampling 1) involved a preliminary digestion of polycarbonate filters in a microwave digestion system (Mars 5, CEM Corporation, Mathews, North Carolina, USA). The protocol applied was the follow: filters were transferred into Autovent HP-1500 vessel and dissolved with 10 mL of HNO3 (65.0-67.0%, Sigma-Aldrich, Germany) according to the instrumental parameters previously set (600 W, 100% Power, 20 min). The next digested solution was diluted to 10 mL with ultrapure water (18.2 MΩ cm, Milli-Q system, Human Corporation, Seoul, Republic of Korea) before the analysis. Heavy metal concentrations were determinate by Inductively Coupled Plasma – Atomic Emission Spectroscopy (ICP-AES) using Agilent Technologies 4210 MP-AES Atomic Absorption Spectrometer (AAS). The MP-AES method was validated by the construction of calibration curves in the linear range of 0.05-5 ng mL^{-1}. A Custom Multi-Element Mix (1000 mg L^{-1}±0.5 % in 10% HNO_3, O_2Si Smart Solution, North Charleston, SC, USA) containing Cd, Cr, Cu, Pb, Sb, Se, Zn, As, Co, Mn and Ni was used as standard solution. The emission wavelengths selected for each metal analyzed were: 228.802 nm for Cd, 425.433 nm for Cr, 324.754 nm for Cu, 405.781 nm for Pb, 231.147 nm for Sb, 196.026 nm for Se, 213.857 nm for Zn, 193.695 nm for As, 340.512 nm for Co, 403.076 nm for Mn, and 361. 939 nm for Ni. The limit of detection (LOD) and limit of quantification (LOQ) of the method for heavy metal determination were reported in Table 3-2.

Table 3-2. Linear range for calibration curve, limit of detection (LOD) and limit of quantification (LOQ) of the method adopted for for HMs determination.

Heavy metal	**Linear range** (ng mL^{-1})	**LOD** (ng mL^{-1})	**LOQ** (ng mL^{-1})
Cd	0.50-50.00	0.128	0.301
Cr	0.50-50.00	0.240	0.369
Cu	0.50-50.00	0.205	0.378
Pb	0.50-50.00	0.196	0.401

Sb	0.50-50.00	0.257	0.478
Se	1.00-50.00	0.546	0.941
Zn	1.00-50.00	0.492	0.873
As	0.50-50.00	0.156	0.359
Co	0.50-50.00	0.087	0.224
Mn	0.50-50.00	0.174	0.288
Ni	0.50-50.00	0.224	0.362

3.2.4 PAH determination: apparatus description and optimization and validation of the analytical method

The amount of PAHs in particle mass samples (Sampling 2), collected on polycarbonate filters, was extracted by ultrasonic extraction (USAE) procedure. The protocol was performed as follow: filters were placed in a beaker, covered with 2 mL of n-heptane solvent (Riedel-de Haën, Germany), and extracted in ultrasonic bath (Ultrasounds Starsonic 18-35, Liarre s.r.l, Casalfiumanese, Italy) set at 6 min at temperature room for three times. The final extracts were combined in a same vial, dried under the stream flow of nitrogen, and recovered with 500 µL of n-heptane before the GC-MS analysis. A solution of 11 PAHs in acetone (Sigma-Aldrich, Germany) at 500 ng μL^{-1} including acenaphthene, acenaphthylene, fluorene, phenanthrene, anthracene, fluoranthene, pyrene, chrysene, benzo(b)fluoranthene, benzo(k)fluoranthene, benzo(a)pyrene (CPA Chem Ltd., Stara Zagora, Bulgaria) was used as laboratory standard to evaluate the feasibility and reproducibility of the analytical method proposed. PAHs were quantified by means of GC-Ion-Trap MS (GC-IT/MS) analysis using a gas chromatograph Finnigan Trace GC Ultra (ThermFinningan, Bremen, Germany) equipped with a Polaris Q ion trap mass spectrometry detector (Thermo Fisher Scientific, Waltham, MA). The column Meta-XLBTM (30 m length, 0.25 mm internal diameter, 0.25 µm film thickness; TeknokromaTM, Barcelona, Spain) was used for the separation, and He (99.9995% purity) was used as carrier gas at a flow rate of 1.0 mL min^{-1}. The sample injection (Vinj=1 µL) was performed in splitless mode with opening split at 4 min through AI/AS 1310 autosampler. After the injection, the Programmed Temperature Vaporizer (PTV) injector heated from 110 °C to 320 °C at 800 °C min^{-1}. In order to ensure the cleanup of the line, the injector was kept at 320 °C for 10 min after the sample vaporization. The starting oven temperature was 100 °C held for 30 s, then, it was ramped to 150 °C at 20 °C min^{-1} for 2 min and to 290 °C at 20 °C min^{-1} for 10 min. Before the chromatographic separation of PAHs, internal standard solution of dioctyl phthalate (DOP) at 1 ng mL^{-1} was added to the samples.

Detection of PAHs was achieved in selected ion monitoring (SIM) with detector temperature and transfer line set at 250 °C and 270 °C, respectively. Full-scan MS data were acquired over the range m/z 100–400 amu to obtain the fragmentation spectra of the analytes while Thermo Xcalibur Sequence Setup software was used for the data interpretation. The mass to charge (m/z) ratio and retention times of PAHs identified by GC-MS are reported in Table 3-3.

Table 3-3. Linear range for calibration curve, limit of detection (LOD) and limit of quantification (LOQ) of the method adopted for PAHs determination.

PAHs	**Mass to charge** (m/z)	**Retention time**
acenaphthylene	152	6.58
acenaphthene	153	6.87
fluorene	166	7.77
phenanthrene	178	9.36
anthracene	178	9.46
fluoranthene	202	10.90
pyrene	202	11.20
chrysene	228	13.12
benzo(b)fluoranthene	252	14.85
benzo(k)fluoranthene	252	14.97
benzo(a)pyrene	252	15.77

The method adopted was standardized through the construction of calibration curves in linear range from 0.05 to 5.00 ng μL^{-1}. Recoveries of all analytes were found in the range of 87-98% with the error ranging between 8-15%. The limits of detection (LOD) and limits of quantification (LOQ) of the method for PAHs determination are summarized in Table 3-4.

Table 3-4. Linear range for calibration curve, limit of detection (LOD) and limit of quantification (LOQ) of the method adopted for PAHs determination.

PAHs	**Linear range** (ng μL^{-1})	**LOD** (ng μL^{-1})	**LOQ** (ng μL^{-1})
acenaphthene	0.05-5.00	0.020	0.041
acenaphthylene	0.05-5.00	0.018	0.040
fluorene	0.05-5.00	0.021	0.042
phenanthrene	0.05-5.00	0.015	0.025
anthracene	0.05-5.00	0.015	0.027

fluoranthene	0.05-5.00	0.015	0.025
pyrene	0.05-5.00	0.018	0.028
chrysene	0.05-5.00	0.013	0.022
benzo(b)fluoranthene	0.05-5.00	0.028	0.043
benzo(k)fluoranthene	0.05-5.00	0.033	0.048
benzo(a)pyrene	0.05-5.00	0.029	0.045

3.2.5 Data post-processing

In order to perform the data post-processing analysis, $ELPI_{VI}$ software was adopted to extract information about the samplings. PM_{10} particle mass distributions were obtained by averaging particle mass distributions values over the sampling periods for each source.

Mass fractions of the HMs and PAHs concentrations on PM_{10} (expressed as ng/ng) emitted by candles, incense sticks, and mosquito coils were evaluated for each compound found. The HMs and PAHs concentrations, referred to the air sampled, were estimated as follows. Firstly, the HM and PAHs absolute masses (ng), were obtained multiplying the extract concentrations, i.e. the concentrations HMs and PAHs referred to the solution volume (Table 3-7 and Table 3-8), for the solution volume (10 mL and 500 μL, for HM and PAHs, respectively). Then, they were referred to the total sampling volume (depending on ELPI+™ flow rate, 10 L min^{-1}, and sampling periods, Table 3-1).

HMs and PAHs particle mass distributions were calculated referring the HMs and PAHs concentrations to the corresponding channel sizes (section 3.2.2).

All the particle mass distributions were normalized respect to the total mass concentration, in order to highlight the concentration peaks and disengaging from the measurement environment, since that high concentration levels were reached to reduce the sampling time and therefore may be misleading respect to the usual conditions. For this reason, relative particle mass distributions will be discussed.

3.3 Results and discussions

3.3.1 Particle mass distributions

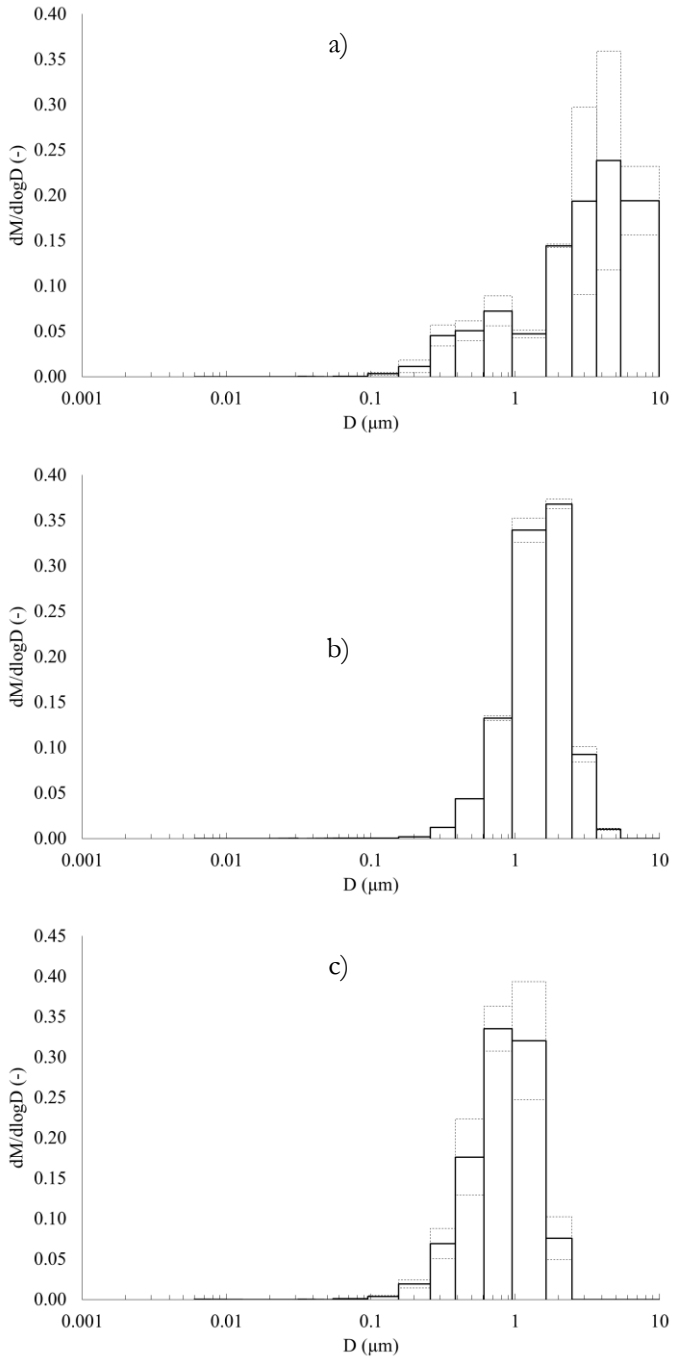

Figure 3-1. Particle mass distributions, normalized to the total concentration, measured during combustion of candles (a), incenses (b) and mosquito coils (c) through ELPI+™ system: solid lines represent average distributions, dashed lines represent standard deviations of the measured distributions.

Particle mass distributions averaged among the two samplings (Sampling 1 for HM analysis and Sampling 2 for PAH analysis) for the sources under investigation are shown in Figure 3-1,

distributions are presented as relative distributions, i.e., normalized to the total mass concentration measured during the samplings.

For all the sources a not negligible contribution of PM_1 fraction was recognized, in particular, the average PM_1 fractions with respect to PM_{10} were equal to 18%, 18%, and 57%, for candles, incenses, and mosquito coils, respectively.

Candles present a bimodal distribution with a main mode at stage 13 (3.67-5.39 μm) and a second mode in the sub-micrometric range (at stage 9, 606-952 nm), on the contrary incenses are characterized by a unimodal distribution with a main mode at stage 11 (1.64-2.48 μm). Mosquito coils produced a unimodal mass distribution as well with a mode in the sub-micrometric range (at stage 9, 606-952 nm).

Actually very few studies were carried out by the scientific community reporting mass distribution of freshly emitted particles from indoor combustion sources: in a previous study the particle mass distributions indoor adopting an SMPS-APS system while using candles, incenses and mosquito coils [230] was measured: a smaller mode (about 300 nm) was measured for candles, incenses and mosquito coils. Such variation can be likely due to the huge variability in the composition of the sources.

3.3.2 HMs and PAHs mass fractions

Table 3-5. Mass fractions of carcinogenic compounds on PM_{10} (expressed as ng/ng) emitted by candles, incenses and mosquito coils and grouped according to their carcinogenic classification by IARC [231].

Source	Group 1				Group 2		Group 3
	As	**Cd**	**Cr (VI)**	**Ni**	**Pb**	**Sb**	**Cu**
Candles	-	-	-	-	4.21×10^{-6}	2.88×10^{-5}	1.15×10^{-5}
Incenses	-	-	-	-	1.65×10^{-6}	7.18×10^{-6}	4.23×10^{-6}
Mosquito coils	2.93×10^{-6}	1.04×10^{-6}	2.43×10^{-5}	8.93×10^{-7}	9.57×10^{-6}	6.32×10^{-5}	6.50×10^{-6}

The analysis of HMs in airborne particles emitted by candles, incenses, and mosquito coils, reported the mainly presence of Cu, Pb, Zn, Sb, Se. Traces of Cd, Cr (hexavalent type), As, and Ni were found in mosquito coil samples while in candles and incenses samples were below the limit of detection (LOD). In addition, the presence of Co, Mn and Ni was not detected except in candles source which showed trace levels of Mn. Nevertheless, in this context the attention was focused on carcinogens compounds Group 1 (As, Cd, Cr, Ni), 2 (Pb, Sb) and 3 (Cu).

In Table 3-5 mass fractions HMs carcinogenic compounds on PM_{10} are reported. The results show that mosquito coils combustion is responsible for the emissions of carcinogenic compounds Group 1, i.e., the most harmful for health, instead of candles and incense sticks. These latter are characterized by Group 2 and 3 HMs emissions. In the current literature, there are not enough data about mass fractions and the existing data concern other sources. Indeed, in Stabile et al. [129] mass fractions of carcinogenic compounds (Group 1) on PM_{10} emitted by wood and pellet combustion phenomena were found and calculated. Their Group 1 mass fractions are similar those reported here, except for As (the mass fraction referred to mosquito coils is higher than two orders of magnitude). Nevertheless, the mass fraction here reported are comparable with those related to the measured concentrations level occurring during typical cooking activities in Italian indoor environments [133], [134]. Regarding PAHs analysis mass fractions, as reported in Table 3-6, only four PAHs were detected and quantified, fluorene, phenanthrene, fluoranthene, pyrene. These PAHs are considered "not classifiable" in terms of carcinogenicity by the IARC [232].

Table 3-6. Mass fractions of PAHs compounds on PM_{10} (expressed as ng/ng) emitted by combustion of candles, incenses, and mosquito coils.

Source	fluorene	phenanthrene	fluoranthene	pyrene
Candles	-	3.93×10^{-6}	-	2.23×10^{-7}
Incenses	1.03×10^{-6}	8.03×10^{-5}	-	-
Mosquito coils	2.64×10^{-7}	3.14×10^{-6}	2.16×10^{-6}	2.26×10^{-6}

3.3.3 HMs and PAHs distributions

HMs

Despite their overall contribution to the total particle mass, a further key information is evaluating the size-resolved mass distribution of HMs. Indeed, different sizes imply different ability of particles to penetrate in the lungs and then carrying there such carcinogenic compounds. In Figure 3-2 mass distributions of As, Cd, Ni, Cr(VI) (Group 1 carcinogenic HMs) and Pb, Sb, Cu (Group 2 and 3 carcinogenic HMs) in freshly emitted particles from mosquito coils combustion (Sampling 1) are shown. The distributions clearly show that the amount of As is exclusively present in the ultrafine particle range with a huge contribution in the stage 2 (16.7-31.3 nm). Similarly, Ni contribution is exclusively due to the sub-micrometric particle range (stages 6 and 7) with a main peak in the 156-384 nm range. Cr(VI) contribution as well was almost completely related to sub-micrometric particles with a clear peak in the range 156-384 nm. On the contrary, the sub-

micrometric particle range contribution to the total amount of Cd is 26% (in the range 94.9-156 nm, stage 5) as other peaks were measured in the stages 11 (1.64-2.48 μm) and 14 (5.39-9.93 μm).

The huge contribution of the sub-micrometric particles emitted by mosquito coil combustion is a critical aspect in terms of people exposure and related lung cancer risk since As, Cd, Ni, Cr(VI) represent the particle-bound compounds with the highest inhalation cancer slope factors [233].

As concern Pb, Sb, and Cu the sub-micrometric contributions are 64%, 26%, and 41%, respectively; in particular, the Pb mass distribution is unimodal with a main peak at 606-952 nm, the Sb distribution is almost uniform, whereas the Cu distribution presents two modes, one in the sub-micrometric (94.9-156 nm) and the other in the super-micrometric range (1.64-2.48 μm).

Pb, Sb, and Cu mass distributions in freshly emitted particles from candle and incense combustion experiments are reported in Figure 3-3; such distributions resulted quite uniform with sub-micrometric range contributions to their total masses around 60% with the exception of Sb for candles whose contribution is completely due to the ultrafine range (main mode at 16.7-31.3 nm).

These results are comparable with those found by Pagels et al. [51], in which the mass distribution of Cu emitted by candles was characterized by a main mode between 0.1 and 1 μm, such as in this study. Regarding mosquito coils, the presence of carcinogenic Group 1 HMs, such as As, Cd, Cr, Ni, were found, in addition to Cd and Pb contents already measured by Roy et al. [52]. These distributions are concentrated below 1 μm, as in the case of Cr and Ni if not below 0.1 micron for As. This raises questions about the presence of carcinogenic Group 1 compounds emitted by mosquito coils and their size distribution toward lower diameters that are associated with worse health effects, as discussed above. This aspect is particularly interesting since that despite their presence was already documented by previous studies, this study, for the very first time, highlight the mass distributions of chemical compounds (in this case PAHs and HMs) for candles, incenses, and mosquito coils. For this reason, a direct comparison with other studies proves not be easy. Moreover, a wide variety of commercially available sources results in a high variability of the emission characteristics of the sources themselves. Even from a legislative point of view, considering for example candles, there are currently no international standards governing the production and sale of candles that include emissions of pollutants carried by air to the stressed combustion of candles. Within the European Union, there are several certification schemes for candle manufacturers, which use a soot index of candles. However, these emission assessments are conducted at constant combustion conditions with a metal shield around the spark plug that

prevents the dispersion of the candle flame. Including assessments of burner emissions under stress, which mimic real-life situations, would allow users to make informed choices and reduce emissions of air pollutants [234].

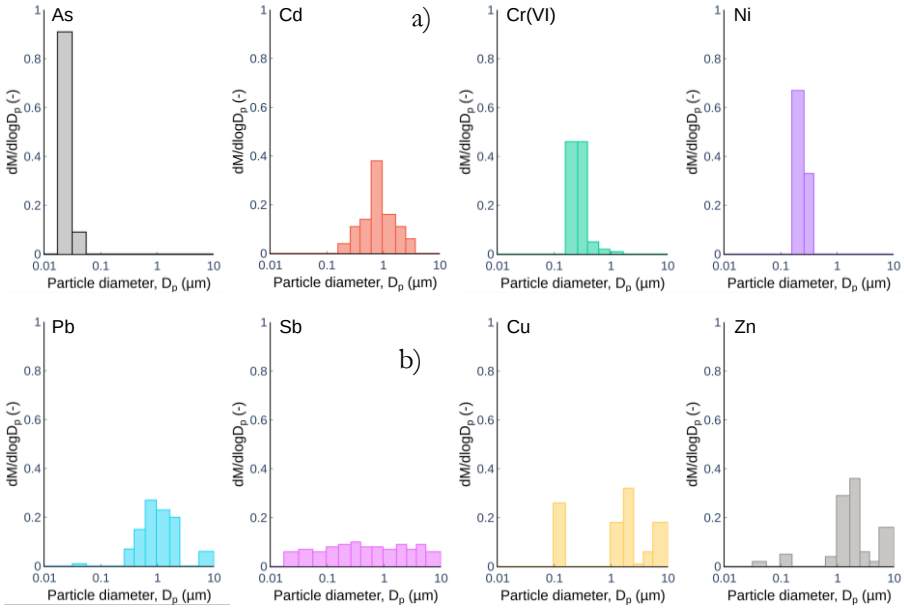

Figure 3-2. Mass distributions (normalized to the total concentration) of As, Cd, Ni, Cr(VI) (a) and Pb, Sb, Cu and Zn (b) in freshly emitted particles from mosquito coils combustion (Sampling 1).

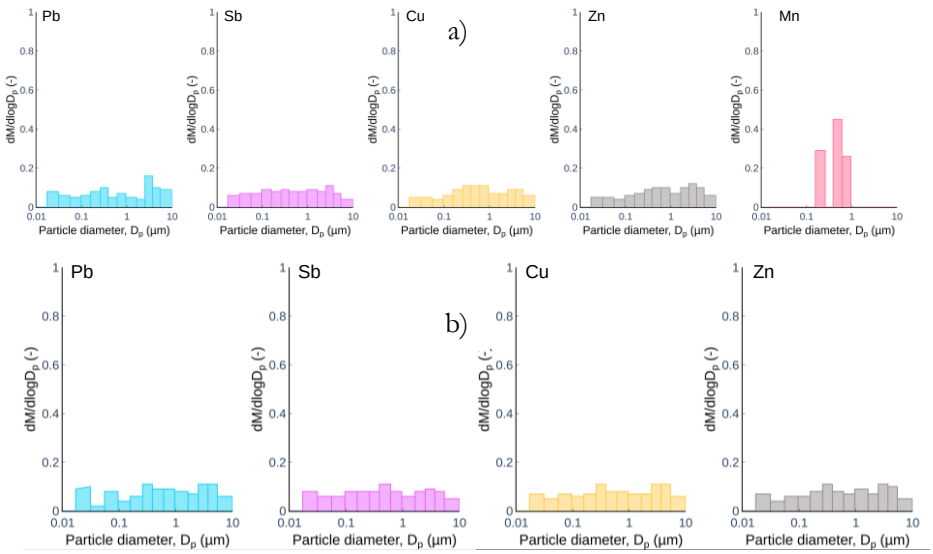

Figure 3-3. Mass distributions (normalized to the total concentration) of Pb, Sb, Cu, Zn and Mn in freshly emitted particles from candle (a) and incense (b) combustions (Sampling 1).

Table 3-7. Heavy metal extract concentrations (ng mL^{-1}) for the different sources.

Sources	Stage	Cd	Cr	Cu	Pb	Sb	Se	Zn	As	Co	Mn	Ni
Candles	2	<LOD	<LOD	27	14	77	1003	98	<LOD	<LOD	<LOD	<LOD
	3	<LOD	<LOD	22	10	76	955	90	<LOD	<LOD	<LOD	<LOD
	4	<LOD	<LOD	19	8	73	941	79	<LOD	<LOD	<LOD	<LOD
	5	<LOD	<LOD	23	9	84	958	95	<LOD	<LOD	<LOD	<LOD
	6	<LOD	<LOD	34	11	81	865	123	<LOD	<LOD	5	<LOD
	7	<LOD	<LOD	35	11	69	840	113	<LOD	<LOD	0	<LOD
	8	<LOD	<LOD	38	7	73	681	144	<LOD	<LOD	7	<LOD
	9	<LOD	<LOD	37	9	66	660	149	<LOD	<LOD	4	<LOD
	10	<LOD	<LOD	30	8	94	544	121	<LOD	<LOD	<LOD	<LOD
	11	<LOD	<LOD	23	5	65	555	137	<LOD	<LOD	<LOD	<LOD
	12	<LOD	<LOD	29	18	80	410	151	<LOD	<LOD	<LOD	<LOD
	13	<LOD	<LOD	27	11	49	293	125	<LOD	<LOD	<LOD	<LOD
	14	<LOD	<LOD	27	15	43	258	118	<LOD	<LOD	<LOD	<LOD
	15	<LOD	<LOD	31	15	59	125	138	<LOD	<LOD	<LOD	<LOD
Incenses	2	<LOD	<LOD	41	23	85	1003	192	<LOD	<LOD	<LOD	<LOD
	3	<LOD	<LOD	28	5	59	955	104	<LOD	<LOD	<LOD	<LOD
	4	<LOD	<LOD	37	16	58	941	153	<LOD	<LOD	<LOD	<LOD
	5	<LOD	<LOD	30	7	66	958	123	<LOD	<LOD	<LOD	<LOD
	6	<LOD	<LOD	34	11	67	865	178	<LOD	<LOD	<LOD	<LOD
	7	<LOD	<LOD	44	17	52	840	200	<LOD	<LOD	<LOD	<LOD
	8	<LOD	<LOD	35	15	86	681	159	<LOD	<LOD	<LOD	<LOD
	9	<LOD	<LOD	34	16	59	660	145	<LOD	<LOD	<LOD	<LOD
	10	<LOD	<LOD	40	16	58	544	225	<LOD	<LOD	<LOD	<LOD
	11	<LOD	<LOD	29	11	54	555	135	<LOD	<LOD	<LOD	<LOD
	12	<LOD	<LOD	44	16	60	410	182	<LOD	<LOD	<LOD	<LOD
	13	<LOD	<LOD	41	17	52	293	174	<LOD	<LOD	<LOD	<LOD
	14	<LOD	<LOD	36	14	47	258	132	<LOD	<LOD	<LOD	<LOD
	15	<LOD	<LOD	7	0	27	125	20	<LOD	<LOD	<LOD	<LOD
Mosquito coils	2	<LOD	<LOD	<LOD	<LOD	105	860	<LOD	54	<LOD	<LOD	<LOD
	3	<LOD	<LOD	<LOD	3	99	855	13	5	<LOD	<LOD	<LOD
	4	<LOD	<LOD	<LOD	<LOD	85	915	<LOD	<LOD	<LOD	<LOD	<LOD
	5	0	<LOD	34	<LOD	110	1082	32	<LOD	<LOD	<LOD	<LOD

6	1	251	<LOD	<LOD	121	1036	<LOD	<LOD	<LOD	<LOD	13
7	2	199	<LOD	11	109	1163	0	<LOD	<LOD	<LOD	5
8	3	25	<LOD	28	92	1127	<LOD	<LOD	<LOD	<LOD	<LOD
9	8	8	<LOD	50	101	1109	26	<LOD	<LOD	<LOD	<LOD
10	4	7	26	52	94	1117	203	<LOD	<LOD	<LOD	<LOD
11	2	<LOD	35	34	100	1170	193	<LOD	<LOD	<LOD	<LOD
12	1	<LOD	1	<LOD	68	1015	28	<LOD	<LOD	<LOD	<LOD
13	0	<LOD	6	0	93	1090	12	<LOD	<LOD	<LOD	<LOD
14	<LOD	<LOD	29	15	98	1241	125	<LOD	<LOD	<LOD	<LOD
15	<LOD	<LOD	2	<LOD	85	1062	<LOD	<LOD	<LOD	<LOD	<LOD

PAHs

Chemical analysis of airborne particles emitted after the combustion of mosquito coils and incenses sources showed the mainly presence of three (fluorene, phenanthrene) and four (fluoranthene, pyrene) ring PAHs while the presence of acenaphthene, acenaphthylene, chrysene, benzo(b)fluoranthene, benzo(k)fluoranthene, benzo(a)pyrene were under of the limit of detection (LOD). The concentration of PAHs quantified by GC-MS are reported in Table 3-8.

The emission of PAHs was already evidenced in previous studies [46], [50], [235]–[237]. Derudi et al. [46] found that PAHs emitted by candles show large differences in similar candles without any clear correlations and the kind of raw material rather than the additives determines the entity of PAHs emissions.

Table 3-8. PAH extract concentrations (ng μL^{-1}) for the different sources.

Sources	Stage	fluorene	phenanthrene	fluoranthene	pyrene
Candles	**2**	< LOD	< LOD	< LOD	< LOD
	3	< LOD	< LOD	< LOD	< LOD
	4	< LOD	0.047	< LOD	< LOD
	5	< LOD	1.058	< LOD	< LOD
	6	< LOD	< LOD	< LOD	< LOD
	7	< LOD	1.478	< LOD	< LOD
	8	< LOD	0.432	< LOD	0.071
	9	< LOD	< LOD	< LOD	< LOD
	10	< LOD	< LOD	< LOD	0.047
	11	< LOD	< LOD	< LOD	0.053
	12	< LOD	< LOD	< LOD	< LOD
	13	< LOD	< LOD	< LOD	< LOD
	14	< LOD	< LOD	< LOD	< LOD
	15	< LOD	< LOD	< LOD	< LOD
Incenses	**2**	< LOD	< LOD	< LOD	< LOD
	3	< LOD	< LOD	< LOD	< LOD
	4	< LOD	< LOD	< LOD	< LOD
	5	< LOD	< LOD	< LOD	< LOD
	6	< LOD	0.137	< LOD	< LOD

Sources	Stage	fluorene	phenanthrene	fluoranthene	pyrene
	7	< LOD	0.26	< LOD	< LOD
	8	< LOD	31.834	< LOD	< LOD
	9	< LOD	29.846	< LOD	< LOD
	10	1.791	37.1	< LOD	< LOD
	11	< LOD	38.97	< LOD	< LOD
	12	< LOD	1.33	< LOD	< LOD
	13	< LOD	0.15	< LOD	< LOD
	14	< LOD	< LOD	< LOD	< LOD
	15	< LOD	< LOD	< LOD	< LOD
	2	< LOD	< LOD	0.044	< LOD
	3	< LOD	< LOD	0.043	< LOD
	4	< LOD	< LOD	0.047	< LOD
	5	< LOD	< LOD	0.073	0.046
	6	< LOD	0.023	0.08	0.094
	7	< LOD	0.642	0.265	0.13
Mosquito	**8**	< LOD	0.463	0.238	0.33
coils	**9**	< LOD	0.514	0.23	0.21
	10	0.142	0.044	0.105	0.285
	11	< LOD	< LOD	0.036	0.118
	12	< LOD	< LOD	< LOD	< LOD
	13	< LOD	< LOD	< LOD	< LOD
	14	< LOD	< LOD	< LOD	< LOD
	15	< LOD	< LOD	< LOD	< LOD

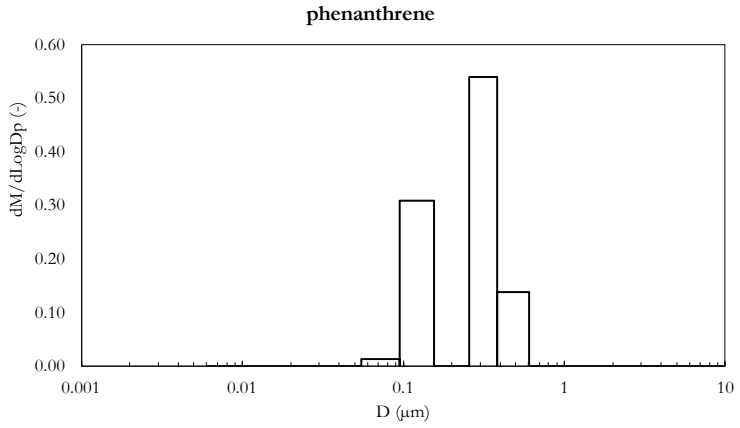

Figure 3-4. Relative mass size distribution of phenanthrene emitted by candles.

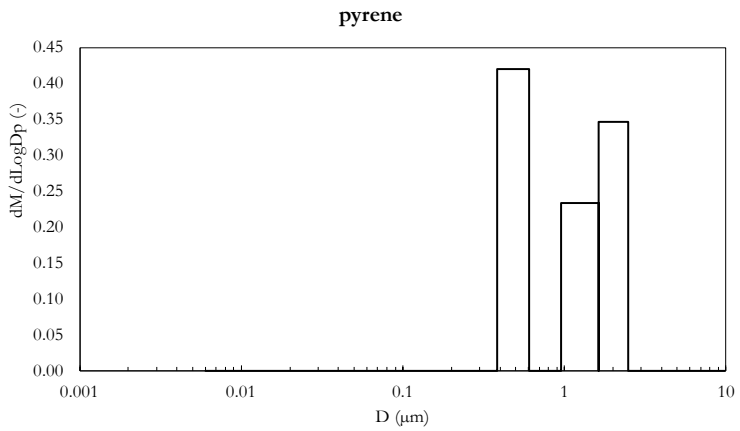

Figure 3-5. Relative mass size distribution of pyrene emitted by candles.

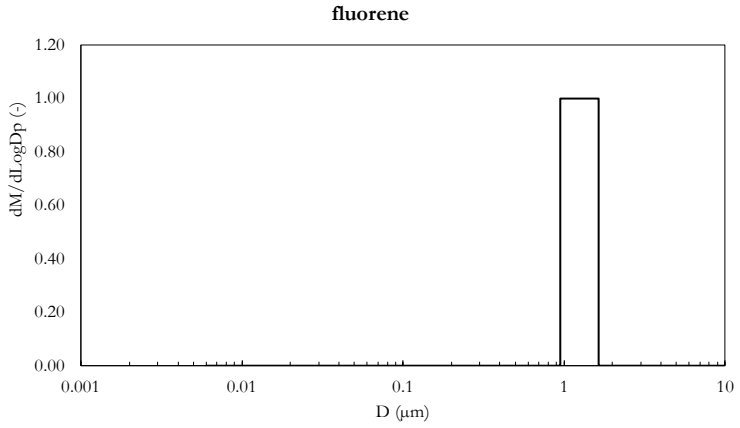

Figure 3-6. Relative mass size distribution of fluorene emitted by incenses.

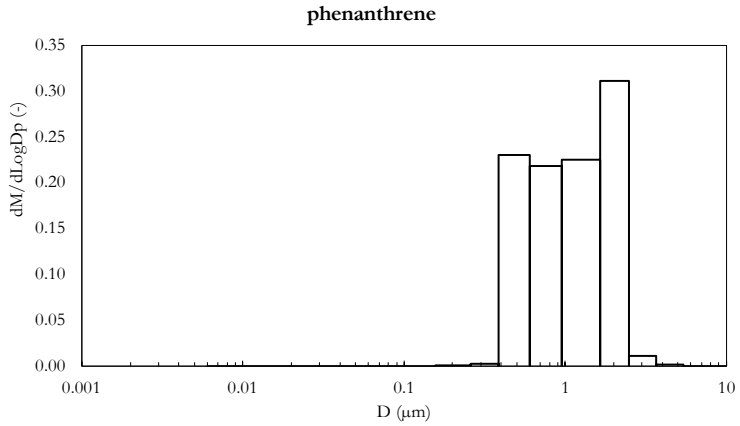

Figure 3-7. Relative mass size distribution of phenanthrene emitted by incenses.

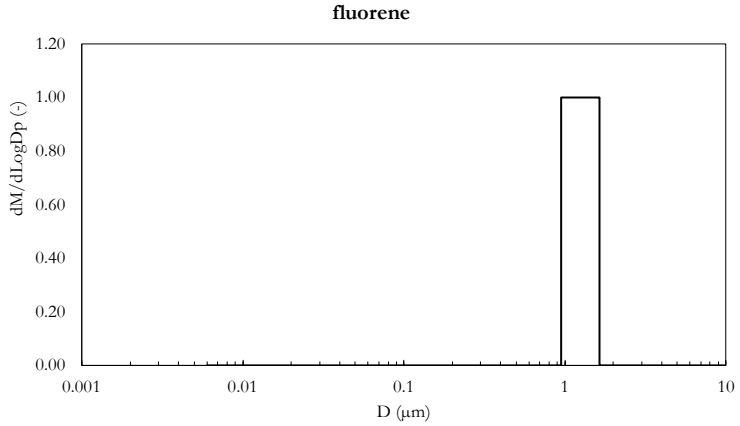

Figure 3-8. Relative mass size distribution of fluorene emitted by mosquito-coils.

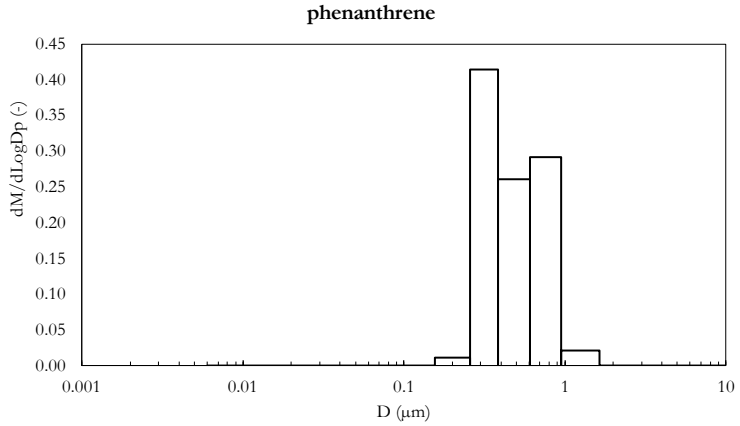

Figure 3-9. Relative mass size distribution of phenanthrene emitted by mosquito-coils.

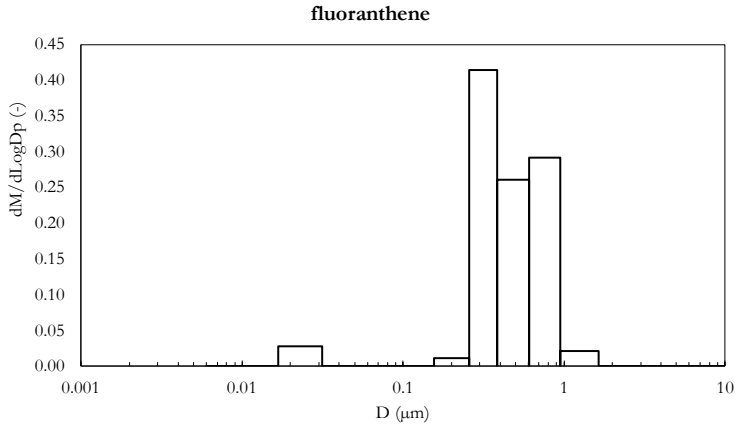

Figure 3-10. Relative mass size distribution of fluoranthene emitted by mosquito-coils.

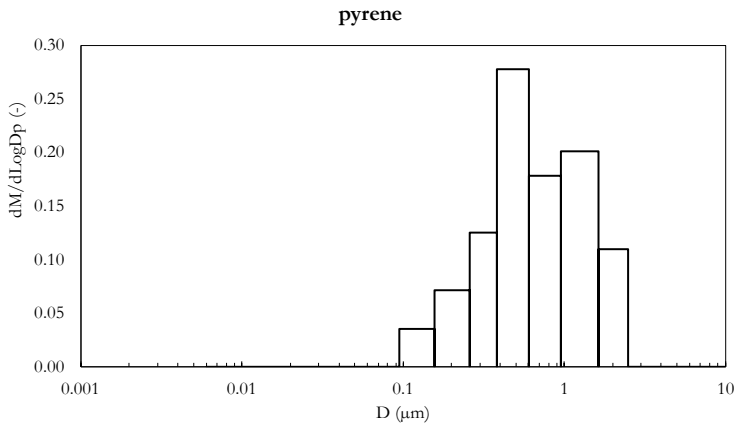

Figure 3-11. Relative mass size distribution of pyrene emitted by mosquito-coils.

All the relative particle mass distributions here reported present a main mode at maximum 1 μm. Similar size distribution patterns, but for different sources, were reported by [238]. They tested the crop residue burning in a typical rural stove founding that the main mode characterizing the size distribution of particulate phase PAHs emitted from crop residue burning was around 1 μm. Hays et al. [239] measured with ELPI+™ $PM_{2.5}$ PAHs size distributions due to the combustions of wood in residence appliances. They found that the mode of size distributions of selected PAH compounds on $PM_{2.5}$ was lower than 1 μm.

3.4 Conclusions

This study, for the very first time, aimed to characterize the size-resolved chemical airborne particles emitted by indoor combustion sources, i.e., incenses, candles and mosquito-coils, in terms

of size dependent HMs and PAHs contributions to the PM_{10}. An experimental analysis based on airborne particle collection through an electric low-pressure impactor (ELPI +™) and consequent gas chromatography–mass spectrometry (GC-MS) and atomic emission spectrometry (ICP-AES) analyses were adopted. The main findings that can be drawn from this study highlight:

- PM_{10} relative particle mass distributions averaged during the two samplings present a bimodal distribution, around the 9th (606-952 nm) and 13th (367-539 nm) stages for candles. Incenses are characterized by a main mode at the 11th stage (1.64-2.48 μm) and mosquito coils, similarly, present a main mode around the 9th stage (606-952 nm).
- ICP-AES analysis showed the presence of different HMs, including Group 1 (As, Cd, Cr, Ni), 2 (Pb, Sb) and 3 (Cu) carcinogens due to the combustion of candles, incenses, and mosquito coils. Candles and incenses under investigation presented only Group 2 and 3 carcinogens, while mosquito coils also Group 1. Even if in studies documenting the emissions of carcinogens by these sources are available in literature, their size-resolved chemical distribution is shown in this study for the first time. The distributions are characterized by a mode below 1 μm and 0.1 μm for As and this aspect is noteworthy because smaller particles recently recognized as most critical for human health and the related metrics (number and surface area) being more representative of the health effects with respect to particle mass (e.g., PM_{10}).
- GC-MS analysis revealed the presence of non-carcinogenic PAHs among the sources combusted. Fluorene, phenanthrene, fluoranthene and pyrene were detected among eleven PAHs. The relative particle mass distributions are characterized by a main mode below 1 μm.
- Regarding the mass fractions, the results related to HMs are similar with those calculated for particles emitted by biomass-burning heating systems and higher than those founded for outdoor sites.

In conclusion, a detailed size-segregated chemical compositions of particles emitted by indoor sources, is extremely important in order to avoid the oversimplifying assumptions considering chemical composition of the emitted particles invariant to the particle size.

Chapter 4 - CASE STUDY 2:
A SIMPLIFIED APPROACH TO EVALUATE THE LUNG CANCER RISK RELATED TO AIRBORNE PARTICLES EMITTED BY INDOOR SOURCES

Indoor particle sources are recognized as detrimental for indoor air quality. Indeed, the high emission rates of the different aerosol metrics and carcinogenic compounds can lead to a high lung cancer risk for people exposed in indoor environments. A-priori lung cancer risk assessments could be very helpful to identify critical environments and sources, but they need complex and site-specific experimental analyses in order to measure particle concentration levels and chemical compositions. Thus, simplified assessments for lung cancer risks are highly welcomed.

In the present study, a simplified approach aiming at evaluating the lung cancer risk related to airborne particles emitted is proposed and applied to different indoor sources. The approach is based on the combination of (i) a recently developed approach to estimate the "emitted risk" of indoor particle sources and (ii) an easy-to-use mass balance equation to calculate the indoor "risk concentration" due to such emitted risk in an indoor environment. Simulations considering different scenarios in terms of previously characterized sources, ventilation rates, and exposure mitigation solutions were performed. The results show that the "risk emitted" is mostly related to sub-micron particles (with respect to super-micron ones) and that the lung cancer risk received by people in indoor environments can be extremely high for different sources, e.g., cooking activities. The ventilation rates of residential environments are not able to appreciably reduce the risk, whereas extraction hoods and air purifiers can significantly decrease it.

4.1 Aims of the work

In the present work, a simplified approach to evaluate the lung cancer risk related to airborne particles emitted by indoor sources was proposed. It is based on the combination of the novel approach proposed by Stabile et al. [149], here applied to estimate the "emitted risk" of indoor particle sources, and of an easy-to-use mass balance equation to calculate the indoor "risk concentration" due to such emitted risk in an indoor environment. The proposed approach was here applied to different indoor sources (including cooking activities, biomass-burning heating

systems, etc.) and considering different scenarios in terms of ventilation and exposure mitigation solutions.

4.2 Materials and methods

4.2.1 Evaluation of the Emitted Risk

The emitted risk (ER) related to the airborne particles emitted by the indoor sources was evaluated applying the approach previously proposed by Stabile et al. [149] to estimate the lung cancer risk emitted in a city by residential, industrial and traffic sectors. Their approach is based on that proposed by Sze-To et al. [131], which evaluates the additional or extra risk of developing lung cancer risk (ELCR, excess lifetime cancer risk) of the people exposed to airborne particles carrying cancerogenic compounds. The risk emitted (ER), i.e., the risk "emitted" by a source, was calculated modifying the abovementioned ELCR model by replacing the received particle surface area and mass doses with the particle surface area and mass emission rates, then allowing an easier evaluation of the risk emitted as:

$$ER = \frac{1}{BW}\left(\sum_{i}^{n} SF_i \cdot \frac{er_{m\_i}}{er_{PM_{10}}}\right) \cdot \left[c_f \cdot er_{SA(Alv+TB)} + er_{PM_{10\_dep}}\right] \quad (\mathrm{h}^{-1}) \tag{10}$$

Here BW is the average body weight of the population (typically 70 kg is adopted), SF_i (kg day mg^{-1}) is the inhalation slope factor used to describe the lifetime cancer potency of the i-th pollutant (i.e. the percent increase in the risk of getting cancer associated with exposure to a unit mass concentration of a chemical every day for a lifetime), er_{m_i} (mg day^{-1}) is the emission rate, expressed in terms mass, of the i-th carcinogenic compound content in the PM_{10}, er_{PM10} (mg day^{-1}) is the PM_{10} emission rate, c_f is the conversion coefficient (6.6×10^{-13} mg nm^{-2}), obtained by Sze-To et al. [131], representing the equivalent toxicity of the particle surface area metric expressed as particle mass, $er_{SA(Alv+TB)}$ (nm^2 day^{-1}) is the emission rate of particle lung-deposited surface area (i.e. deposited in the alveolar and tracheobronchial regions of the lungs), er_{PM10_dep} (mg day^{-1}) is the emission rate of PM_{10} deposited in the lungs, which is calculated multiplying the er_{PM10} by the typical deposition fraction of super-micron particles (here assumed equal to 0.2).

The authors, once again, point out that, differently from the indoor concentrations, the particle and chemical compound emission rates (er_{m_i}, er_{PM10}, $er_{SA(Alv+TB)}$, er_{PM10_dep}) just depend on the type of the source and can be evaluated through *ad-hoc* experimental analyses [240]. In the present study

the chemical composition of the emitted particles was considered invariant to the particle size; this could represent an oversimplified approach since sub- and super-micron particles may present different chemical composition [241]–[243]; nonetheless size-segregated chemical analyses for particles emitted by indoor sources are not currently available in the scientific literature. When these detailed data became available, the model could be straightforwardly updated as discussed in the result section (section 4.3). Moreover, in view of the application of the calculation of the hereinafter reported "risk concentration", both the size and the chemical composition of the emitted particles were assumed to be constant from the emission to the inhalation. In other words, condensation and coagulation phenomena were considered negligible.

The emission rates in terms of lung-deposited particle surface area are neither explicitly reported in scientific studies nor in other technical documents. Therefore, $er_{SA(Alv+TB)}$ was evaluated on the basis of the emission rates in terms of particle number (er_N) and particle distribution data reported in research papers. In particular, the emission rate in terms of lung-deposited particle surface area ($er_{SA(Alv+TB)}$) was scaled from the er_N as

$$er_{SA(Alv+TB)} = er_N \cdot \frac{SA_{Alv+TB}}{N} = \frac{er_N}{N} \cdot \int \frac{dN(D)}{dlogD} dD \cdot \pi D^2 \cdot DF(D) \quad (\mathrm{nm^2 h^{-1}}) \qquad (11)$$

where $SA_{(Alv+TB)}$ and N represent the total lung-deposited surface area and number concentrations of the airborne particles emitted by the source under investigation. In particular, for each specific aerosol, the N and SA_{Alv+TB} concentrations were obtained from the particle number distribution ($dN(D)/dlogD$) considering spherical particles, and the deposition fractions ($DF(D)$) in the alveolar and tracheobronchial regions were adopted from the ICRP [244] for light exercise activity as average value between male and female ones.

The *SFs* of the cancerogenic chemicals investigated in the present study were obtained from the data provided by the Office of Environmental Health Hazard Assessment [245]: in particular *SF* values for B(a)P, As, Cd, Cr, Ni, and Tobacco-specific N-nitrosamines NNK and NNN are equal to 3.9, 15.1, 6.3, 4.2, 0.91, 22.1 and 1.4 kg day mg^{-1}, respectively. The overall toxicity of the emitted particles (in terms of lung cancer risk) is expressed as *SF* of the mixture of the *n* cancerogenic pollutants on PM_{10} (SF_m): it represents the weighted average of the SF_i, i.e. the term $\sum_i^n SF_i \cdot \frac{er_{m\_i}}{er_{PM10}}$ reported in Eq. (10).

The ER approach here presented was applied, by way of example, to different indoor sources typically adopted in indoor environments and recognized as highly emitting: cooking activities (data for frying were available and adopted), candles, incenses, second-hand aerosol due to a conventional (tobacco) cigarette smoker, second-hand aerosol due to an electronic cigarette (with nicotine) vaper, open and closed fireplaces (burning wood) and pellet stoves.

Particle emission rates of the indoor sources

In order to apply the model proposed by Stabile et al. [149] to estimate the lung cancer risk emitted (ER) by the selected indoor sources, the emissions of airborne particles and their carcinogenic compound contents were considered. To this end a literature review was conducted in order obtain data on chemical and dimensional characteristics of the emitted particles. As hereinafter reported, the review confirmed that limited data are available in the literature; this is not a major issue since the main focus of the work is describing a novel approach and showing a possible application, whereas a detailed scientific literature review is beyond the scope of this work and the readers should refer to further studies. In particular, particle number (er_N) and mass emission rate (er_{PM10}) (expressed as part. min^{-1} and mg min^{-1}, respectively) were mostly gathered from previous papers: Buonanno et al. [97] for cooking activities (frying), Stabile et al. [246] for candles and incenses, Avino et al. [108] for second-hand due to conventional and electronic cigarette (with nicotine) use. In regards to the biomass-burning heating systems here investigated, i.e. open/closed fireplaces and pellet stoves, the emission rates are not explicitly reported in the scientific literature, therefore, they were estimated through a steady-state particle mass balance equation on the basis of median concentrations measured by Stabile et al. [129]:

$$er_{(N;PM10)} = \left[C_{comb(N;PM10)} \cdot (AER + k) \cdot P_{in} - C_{comb(N;PM10)} \cdot AER \cdot P_{out}\right] \cdot V \quad (part.h^{-1}; mg\ h^{-1}) \tag{12}$$

where C_{comb} and C_{back} are the median indoor particle concentrations (in terms of number, N, and PM_{10}, i.e., expressed as part. m^{-3} and mg m^{-3}) during and before (background) the combustion, respectively, V is the median room volume of the rooms where was performed the experimental campaign (roughly 50 m^3), AER is the air exchange rate (here supposed equal to 0.2 h^{-1}, considering the natural ventilation conditions [247], [248]), P_{in} and P_{out} are the penetration efficiencies (here assumed equal to 1), k is the deposition rate, here assumed equal to 0.9 h^{-1} and 0.7 h^{-1} for PM_{10} and SA_{Alv+TB}, respectively [249], [250]. Particle emission rates for the different indoor sources under investigation are summarized in the result section (section 4.3.1, please see Table 4-2).

Concerning the chemical characterization of the particles, the following studies (reporting their own data or summarizing data reported in the scientific literature until then) were considered: See and Balasubramanian [251] for cooking activities (frying), Derudi et al., Yang et al., and Lin [235], [237], [252], [253] for candles and incenses, Stabile et al. [254] for conventional cigarettes, Scungio et al. [255] for electronic cigarettes with nicotine, and Stabile et al. [129] for biomasses. The authors point out that the chemical characterization, and then the mass fraction of carcinogenic compounds carried by the particles emitted by smokers and vapers was evaluated on the basis of scientific literature data summarized in previous papers where the ELCRs due to direct inhalation of mainstream cigarette and e-cigarette aerosols were calculated [254], [255] and already adopted in a previous paper on second-hand smoke [108]: in other words, the relative amount of carcinogenic compounds ($\frac{er_{m\_i}}{er_{PM_{10}}}$) carried by particles of second-hand smoke was considered equal to that typical of the mainstream aerosol, therefore the SF_m values characteristics of mainstream aerosols were adopted. Carcinogenic compound emission rates for the different indoor sources under investigation are summarized in the result section (section 4.3.1, please see Table 4-3).

4.2.2 Risk of the exposed population

The risk emitted by each indoor source (eq. (10)) is clearly not representative of the real individual risk of the population because it would imply that the exposed population inhaled directly at the emission of that source. On the contrary, just as the particle emission rate generates a certain particle concentration in a room, analogously, the ER determines a "risk concentration". Thus, the "risk concentration" as a function of the time in a confined space ($RC_{in}(t)$) can be evaluated, similarly to the particle concentration trend, through a simplified zero-dimensional well-mixed models (mass-balance equations), where, once again, the chemical composition of the emitted particles was assumed invariant to the particle size and over time and the risk is considered instantaneously and evenly distributed in the confined space under investigation. The risk concentration is a function of (i) the initial "background" risk concentration (if any), (ii) the risk penetrating from outdoor to the indoor environment, (iii) the risk emitted by the indoor sources, and (iv) the risk due to the resuspension phenomena. In particular, the mass balance equation of the risk is:

$$RC_{in}(t) = RC_{back} \cdot e^{-TRR \cdot t} + \left(\frac{RC_{out} \cdot AER \cdot P_{out}}{TRR} + \frac{ER}{V \cdot TRR} + \frac{Res}{V \cdot TRR}\right) \cdot (1 - e^{-TRR \cdot t}) \quad (m^{-3}) \qquad (13)$$

where RC_{back} is the background risk concentration (before using the source), RC_{out} is the contribution of the outdoor risk concentration, *Res* (h^{-1}) is the resuspension rate of the particles (and then of the risk) (i.e., the risk contribution due to the particle resuspension phenomena), and *TRR* (h^{-1}) is the total removal rate of particles (and then of the risk). The *TRR* is made up of the air exchange rate (AER, h^{-1}) of the confined space and of the particle deposition rate (k, h^{-1}). Through such simplified mass balance equation approach the emitted risk (ER) is handled as a pollutant emission rate and dispersed in the microenvironment; thus, the dynamics of the emitted risk is affected by the dynamics of both sub-micron particles (for particle surface area-related risk contribution) and super-micron particles (for particle mass-related risk contribution). Nonetheless, as hereinafter shown in the results section, the contribution of the surface area-related risk to the ER is highly prevalent with respect to the super-micron ones, thus the latter can be neglected, and the dynamics of the ER can be just related to that of sub-micron particles. This assumption allows to neglect the term referring to the particle resuspension phenomenon (*Res*) as it is mainly characteristic of super-micron particles [256], or, at least, sub-micron particle resuspension is negligible with respect to the emission due to combustion phenomena [257]; moreover, since the aim of the study was to investigate the "extra risk" due to indoor sources, the outdoor contribution (RC_{out}) can be neglected as well. Therefore the Eq. (13) can be simplified as:

$$RC_{in}(t) = RC_{back} \cdot e^{-(TRR)\cdot t} + \frac{ER}{V \cdot (TRR)} \cdot \left(1 - e^{-(TRR)\cdot t}\right) \quad (m^{-3}) \tag{14}$$

Starting from the RC, the risk of developing lung cancer, i.e., the excess cancer risk due to a single exposure event (ECR_{SE}), can be defined as:

$$ECR_{SE} = \int_0^{T_{SE}} RC_{in}(t) \cdot IR \cdot T_{SE} \cdot dt \qquad (-) \tag{15}$$

where T_{SE} is the single event exposure time and $IR_{activity}$ ($m^3\ h^{-1}$) is the inhalation rate of the exposed population which is related to age groups and the activity performed. In particular, in the present work adult people (aged >19) performing sedentary activity whose inhalation rate ranges from 0.45 $m^3\ h^{-1}$ to 0.54 $m^3\ h^{-1}$ [130] were considered.

Consequently, the excess lifetime cancer risk (ELCR) can be evaluated multiplying the ECR_{SE} by the number of single events occurring lifetime (i.e. in 70 years, according with the definition of ELCR) [131], [133].

Case studies: scenarios and mitigation solutions

The proposed approach was applied to different exposure scenarios considering a typical residential indoor microenvironment; to this end all the parameters of the eq. 4 have to be set. As regard the room size, an average volume of the Italian room, V=83 m^3 (ranging from 64-90 m^3), was chosen to perform the simulation of the risk concentration, such range was obtained considering typical floor areas (www.agenziaentrate.gov.it), number of rooms (www.istat.it), and height (DM 05.07.1975, www.gazzettaufficiale.it) of the Italian homes/dwellings.

The particle deposition rates, k, were chosen from the data provided by Howard-Reed et al. [258] and Wallace et al. [250] as a function of the particle diameter and summarized in Table 4-1. Actually, for the sake of simplicity, the particle number distribution mode of each source was adopted to determine the k values: for kitchen activities k was set equal 1 h^{-1} since a mode of the number distribution of about 50 nm was measured by Buonanno et al. [97], for candles and incenses k=1.6 h^{-1} and k=0.9 h^{-1} were adopted since modes of 35 and 200 nm, respectively, were measured by Stabile et al. [246], for conventional and electronic cigarettes k values equal to 0.7 h^{-1} and 1.6 h^{-1} were set since modes of 100 nm and 30 nm, respectively, were measured by Avino et al. [108], and for biomass heating systems k was set to 0.8 h^{-1} due to the mode at 120 nm resulting from Tiwari et al. [259].

Referring to the air exchange rate, AER, it should be pointed out that homes mostly do not present mechanical ventilation systems, thus the ventilation is due to natural infiltration and manual airing. In order to show the possible effect to the room ventilation on the risk received by exposed population, simulations were performed for different air exchange rates as representative of typical real-life situations: 0.2 h^{-1}, which is the typical data measured in homes poorly ventilated [138], [260], [261], 0.5 h^{-1}, which is the value suggested by the technical standard [262], and 1 h^{-1} representing a value suitably achievable using heat recovery single-room unit [263]. For cooking events, simulations with higher AERs were also carried out (up to 12 h^{-1}) (Table 4-1).

Regarding the exposure time, the single event exposure times (T_{SE}) were evaluated considering the duration of the emission of the indoor source, as reported in the scientific literature, and a further exposure time of 2 hours (120 min) during which the risk (and particle) concentration decays as soon as the source was turned off. The T_{SE} values adopted in the present study to evaluate

the ECR_{SE} are summarized in Table 4-1 for all the investigated sources. The single event exposure time related to the cooking activity was determined as average value between adult men and women living in North and South of Italy as reported in Buonanno et al. [130]. They reported that, on average, Italian people spend roughly one hour per day for cooking activities (including both lunch and dinner preparation), thus, in the present study, 27 min was adopted as median duration for a single cooking activity event. For candles and incenses, a median usage time of 130 min per day was considered as reported by Petry et al. [264] based on a survey carried out on a sample of Belgian population. The time exposure to the second-hand smoke was assumed equal to the use of cigarettes (conventional and electronic) themselves. To this end data on cigarette smoking pattern of Italian adults was considered as reported in previous papers [254], [265] then resulting in a median emission duration of "second-hand" aerosol for each cigarette/e-cigarette smoked equal to 5 minutes. Finally, for biomass-heating systems a median daily emission of 8 hours was considered.

Given the simulation conditions, for all the scenarios investigated, an exponential increase of particle and risk concentrations was expected, then reaching a peak occurring as long as the source is active. Subsequently, an exponential decay of the RC is expected as soon as the source is switched off. The increase rate, peak concentration, and decay rate, for a given emission rate, are affected, as clearly expressed by the eq. (14), by the room volume, ventilation rate, particle deposition rate. Further mitigation solutions aiming at reducing the emission rate (e.g., local extraction by hoods) and filtrating the particles in the room (air purifiers) can also help in reducing the risk of the exposed population and were also included in these simulations. Cooking activities, especially frying, represent one of the most impacting indoor sources [130], [133], [134] due to its high emission rate. In order to reduce the dispersion of cooking-generated particles in the indoor environment, a suitable solution could be installing hoods aiming at reducing the particles, and then, the risk, emitted by the such source through an on-the-spot local extraction. As an example, Buonanno et al. [134] observed up to a ten-fold reduction of the ELCR for exposed people when hoods were adopted. Indeed, as the hood exhaust flow increases, the particle removal increases as well [266]. In particular, Sun et al. [98] have reported kitchen hood efficiency ranging from 25% to 98%; in these analysis, in order to address the effect of hoods, simulations with hoods characterized by the maximum removal efficiency (98%) were performed (in the case of AER=0.2 h^{-1}). In particular, we have considered the hood in operation just during the emission period, then it was considered not in operation during the following decay period.

Table 4-1. Summary of the parameters adopted in the simulations performed to calculate the risk concentration in a typical room as a function of the indoor source investigated: single event exposure time (T_{SE}, including both the source usage time and the further 120-min exposure during the decay), deposition rate (k), air exchange rate (AER), room volume (V), and inhalation rate (IR). Where available, data are provided as median value and range (minimum-maximum).

Indoor source	**T_{SE}** (min)	***k*** (h^{-1})	**AER** (h^{-1})	**V** (m^3)	**IR** ($m^3\ h^{-1}$)
Cooking activities	27 (8.5-43.5) + 120	1.0	0.2, 0.5, 1.0 (and >1.0, up to 12)		
Candles	130 (114-144) + 120	1.6			
Incenses		0.9			
Second-hand - conventional cigarettes	5 (1.2-10.8) + 120	0.7		83 (64-90)	0.49 (0.45-0.54)
Second-hand - Electronic cigarettes (with nicotine)		1.6	0.2, 0.5, 1.0		
Open fireplaces (wood)	480 (420-540) + 120	0.8			
Closed fireplaces (wood)					
Pellet stoves					

Air purifiers, i.e. systems equipped with fans (or pumps) that purify the air through a series of filters, represent a further possible solution to reduce indoor particle and risk concentrations [267]. Indeed, air purifiers are typically equipped with HEPA (high-efficiency particulate air) filters that can also trap sub-micron particles. Air purifiers can be chosen according to the clean air delivery rate (CADR) declared by the manufacturer on the basis of standardized tests; it is defined by the product of the volumetric flow rate ($m^3\ h^{-1}$) and the particle removal efficiency ($\eta_{purifier}$). Thus, high CADRs can be achieved either by increasing the disposable flow rate of the purifier or by increasing the filter efficiency [268]. In the simulations we have considered an air purifier, currently on the market, characterized by a declared CADR for sub-micron particles of 390 $m^3\ h^{-1}$, an efficiency

(down to 20 nm particles) $\eta_{purifier}$=99%, and a recommended maximum floor area of 95 m². The effect of the air purifier on the risk concentration (eq. (14)) can be simply addressed by adding the corresponding contribution ($ACH \cdot \eta_{purifier}$ [267]) to the *TRR* (that will be modified in $AER+k+ACH \cdot \eta_{purifier}$, h^{-1}), where the $ACH \cdot \eta_{purifier}$ represents the ratio between the CADR and the room volume (V): thus, in this scenario, adopting the abovementioned median room volume, $ACH \cdot \eta_{purifier}$=4.73 h^{-1}. The use of air purifiers was simulated in the case of the worst ventilation scenario (i.e. AER=0.2 h^{-1}), here the air purifier was considered in operation throughout the exposure time (i.e. including both the emission period and the decay period).

4.2.3 Data post-processing

In order to include the variability of the input parameters, emitted risk (ER), risk concentration (RC), weighted average slope factor (SF_m), and excess cancer risk (ERC_{SE}) were calculated through the abovementioned eqs. (1)–(6) and applying a Monte Carlo method [269]. To this end probability distribution functions characteristics of each parameter were considered. In particular, due to the limited data available, uniform or constant probability distribution functions were just adopted. For uniform distribution functions the median value and the corresponding range between minimum and maximum values were reported. Data statistics on time of exposure, deposition rate, room volume and inhalation rates are summarized in Table 4-1, whereas data distributions concerning particle emission rates and carcinogenic compound emission rates are summarized in Table 4-2 and Table 4-3, respectively. In order to show the effect of the air exchange rate on the excess cancer risk, simulations were performed considering different (constant) AER values which are summarized in Table 4-1 as well. Results in terms of weighted average slope factor (SF_m), emitted risk (ER), risk concentration (RC), and excess cancer risk (ERC_{SE}) were checked for normality through the Shapiro-Wilk test; since they resulted, in general, not normally distributed, we have expressed them as median values and 5th - 95th percentile ranges.

4.3 Results and discussion

4.3.1 Lung cancer risk emitted

Summary of the emission rates of the indoor sources

In Table 4-2 the emission rates of each indoor source in terms of particle number (er_N, part. min^{-1}), deposited surface area ($er_{SA(Alv+TB)}$, nm² min^{-1}), and mass (er_{PM10}, mg min^{-1}) are reported as obtained from the literature review performed. The data collected clearly show that incenses and cooking activities (frying) are characterized by the highest emission rates in terms of number

(1.3×10^{13} and 1.7×10^{12} part. min^{-1}, respectively) and deposited surface area (9.4×10^{16} and 9.6×10^{16} nm^2 min^{-1}, respectively), whereas the highest PM_{10} emission rate is due to the second-hand aerosol produced by conventional cigarette smokers.

Table 4-2. Summary of the particle number distribution modes and emission rates in terms of number, deposited surface area and mass (PM_{10}) for the indoor sources under investigation. Data are reported as median values and ranges (minimum-maximum); corresponding references are also reported.

Indoor source	**mode** (nm)	er_N (part. min^{-1})	$er_{SA(Alv+TB)}$ (nm^2 min^{-1})	er_{PM10} (mg min^{-1})	**Ref.**
Cooking activities	54	1.7×10^{12} (1.1×10^{12}-2.3×10^{12})	9.6×10^{16} (4.5×10^{16}-14×10^{16})	2.0 (1.2-2.8)	[97]
Candles	35	7.4×10^{11} (6.8×10^{11}-8.1×10^{11})	1.1×10^{14} (1.0×10^{14}-1.2×10^{14})	7.8×10^{-3} (0.7×10^{-3}-15×10^{-2})	[246]
Incenses	200	1.3×10^{13} (0.8×10^{13}-1.8×10^{13})	9.4×10^{16} (2.1×10^{16}-17×10^{16})	1.1 (0.7-1.5)	
Second-hand - conventional cigarettes	100	4.3×10^{11} (3.2×10^{11}-5.4×10^{11})	5.7×10^{15} (4.2×10^{15}-7.0×10^{15})	4.9 (3.7-6.2)	[108]
Second-hand - electronic cigarettes (with nicotine)	30	9.6×10^{10} (7.2×10^{10}-1.2×10^{11})	5.9×10^{14} (4.4×10^{14}-7.3×10^{14})	< LOD	
Open fireplaces (wood)	130	5.0×10^{10} (2.9×10^{10}-7.2×10^{10})	1.7×10^{14} (1.1×10^{14}-2.2×10^{14})	1.7×10^{-1} (0.5×10^{-1}-2.9×10^{-1})	[129]
Closed fireplaces (wood)		1.6×10^{10} (0.6×10^{10}-2.6×10^{10})	6.1×10^{13} (2.5×10^{13}-9.7×10^{13})	8.0×10^{-2} (3.7×10^{-2}-12×10^{-2})	
Pellet stoves		6.4×10^{9} (4.1×10^{9}-8.6×10^{9})	2.3×10^{13} (1.5×10^{13}-3.2×10^{13})	2.5×10^{-2} (1.8×10^{-2}-3.2×10^{-2})	

In Table 4-3 the emission rates of the carcinogenic compounds, adopted to calculate the weighted average slope factors (SF_m) of each source, are summarized as obtained from the literature

review performed. The table clearly shows that each source is characterized by a different emission profile in terms of carcinogenic compounds, indeed, nitrosamines (NNN and NNK) were just measured in conventional and electronic cigarettes, Cr was only present in conventional cigarettes, As was not detected in candles and incenses, as well as no B[a]P was measured for electronic cigarettes. As mentioned in the section 0, the mass fraction of carcinogenic compounds carried by the particles emitted by smokers and vapers was considered equal to that typical of the mainstream aerosol as already adopted in a previous paper on second-hand smoke [108], indeed, both carcinogenic compound concentrations and PM_{10} concentrations for conventional cigarette smokers and electronic cigarette vapers were expressed as mg puff^{-1} as measured in the mainstream aerosol.

For detailed discussions regarding the dimensional and chemical characterization of the particles emitted by each source under investigation, the readers are suggested to refer to the mentioned papers where the experimental analyses are exhaustively described. On the contrary, the quantitative contribution of each compound to the overall toxicity of the source was reported in Table 4-4.

In Table 4-4 the overall carcinogenic effect related to the particles emitted by each source, expressed as weighted average slope factors (SF_m), is reported along with the relative contribution of each carcinogenic compound to the SF_m. Amongst the indoor sources investigated, pellet is characterized by the highest SF_m (median value of 1.5×10^{-2} kg day mg^{-1}), while the lowest is that of the electronic cigarettes (1.9×10^{-6} kg day mg^{-1}).

The contribution to SF_m varies significantly as a function of the source, as an example the main contributor for cooking activities is As (77%), lower contributions are due to Cd and Ni, whereas the effect of the other compounds is negligible. For candles and incenses the main contribution is due to the Ni (>50%); such contribution is even higher for biomasses (wood and pellet). NNK and NNN are only present in particles emitted by conventional cigarettes, whilst the main contributors to the SF_m for electronic cigarettes are As, Cd, and NNK.

Emitted risk of the indoor sources

In Table 4-5 the hourly Emitted Risk (ER) of the different indoor sources investigated is reported on the basis of the methodology shown in the section 4.2.1. Moreover, the contributions to the ER due to the different aerosol metrics, i.e. lung-deposited surface area and PM_{10}, are also highlighted. As expected, and already mentioned in the methodology section, the contribution of the super-micron particles to the ER (i.e. the ER_{PM10} contribution) is actually negligible for all the

sources investigated, indeed the sub-micron particle-related ER (i.e. $ER_{SA(Alv+TB)}$) is at least three orders of magnitude larger than the super-micron one. This result allows just considering the $ER_{SA(Alv+TB)}$ contribution when applying the mass balance equation of the risk in a confined space, as hypothesized in the methodology section.

Table 4-3. Summary of the emission rates of the carcinogenic compounds for the indoor sources under investigation. Data are reported as median values and ranges (minimum-maximum); corresponding references are also reported. Emission rates are expressed in mg min^{-1}, with the exception of conventional and electronic cigarette ones (expressed as mg $puff^{-1}$) as they were obtained from data on mainstream aerosol as reported in previous papers [108], [254], [255], PM_{10} emission rates per puff (mg $puff^{-1}$) for conventional and electronic cigarettes were also reported in order to calculate the mass fraction of carcinogenic compounds carried by the particles as described in section 2.1. Data converted were converted to mg $puff^{-1}$ on the basis of data on puff volume and number of puff per cigarette reported in Stabile et al. [254].

Indoor source	**B[a]P**	**As**	**Cd**	**Ni**	**Ref.**
			(mg min^{-1})		
Cooking activities	6.3×10^{-6} ($3.2\text{-}9.5)\times10^{-6}$	3.3×10^{-4} ($1.8\text{-}4.7)\times10^{-4}$)	1.3×10^{-4} ($0.61\text{-}2.0)\times10^{-4}$	6.8×10^{-4} ($3.0\text{-}11)\times10^{-4}$	[270]
Candles	2.9×10^{-7} ($1.8\text{-}4.0)\times10^{-7}$	< LOD	3.0×10^{-6} ($1.6\text{-}4.4)\times10^{-6}$	2.5×10^{-5} ($1.3\text{-}3.7)\times10^{-5}$	[235], [237], [252], [253]
Incenses	5.2×10^{-6} ($3.2\text{-}7.2)\times10^{-6}$	< LOD	8.0×10^{-6} ($4.3\text{-}12)\times10^{-6}$	1.9×10^{-4} ($1.0\text{-}2.7)\times10^{-4}$	
Open fireplaces (wood)	1.0×10^{-5} ($0.33\text{-}1.8)\times10^{-5}$	1.1×10^{-8} ($0.33\text{-}1.8)\times10^{-8}$	4.1×10^{-6} ($1.3\text{-}7.0)\times10^{-6}$	1.2×10^{-3} ($0.38\text{-}2.1)\times10^{-3}$	
Closed fireplaces (wood)	1.0×10^{-5} ($0.33\text{-}1.8)\times10^{-5}$	1.1×10^{-8} ($0.33\text{-}1.8)\times10^{-8}$	4.1×10^{-6} ($1.3\text{-}7.0)\times10^{-6}$	1.2×10^{-3} ($0.38\text{-}2.1)\times10^{-3}$	[129]
Pellet stoves	1.0×10^{-7} ($0.72\text{-}1.3)\times10^{-7}$	2.3×10^{-6} ($1.6\text{-}2.9)\times10^{-6}$	1.1×10^{-5} ($0.77\text{-}1.4)\times10^{-5}$	3.0×10^{-4} ($2.2\text{-}3.8)\times10^{-4}$	

Indoor source	**B[a]P**	**As**	**Cd**	**Cr**	**Ni**	**NNK**	**NNN**	**PM_{10}**	**Ref.**
				(mg $puff^{-1}$)					
Conv. cig.	1.1×10^{-6} ($0.088\text{-}1.2)\times10^{-6}$	5.3×10^{-7} ($2.6\text{-}7.9)\times10^{-7}$	7.1×10^{-6} ($3.5\text{-}11)\times10^{-6}$	1.3×10^{-6} ($0.026\text{-}2.6)\times10^{-6}$	2.4×10^{-8} ($0\text{-}4.7)\times10^{-8}$	9.9×10^{-5} ($8.1\text{-}1.2)\times10^{-5}$	1.7×10^{-5} ($1.2\text{-}2.1)\times10^{-5}$	2.8×10^{-1} ($1.3\text{-}4.8)\times10^{-1}$	[110], [249]
Elect. Cig. with nicotine	< LOD	0.1×10^{-6}	0.6×10^{-6}	< LOD	8.0×10^{-7} ($4.0\text{-}12)\times10^{-7}$	1.0×10^{-7} ($0.6\text{-}1.8)\times10^{-7}$	1.0×10^{-7} ($0.1\text{-}2.2)\times10^{-7}$	6.0 (3.0-8.1)	[108], [255]

Table 4-4. Weighted average slope factors (SF_m), expressed as median value and 5th -95th percentile range, and median relative contribution of the carcinogenic compounds for the indoor sources under investigation.

Indoor source	SF_m	contribution of each compound to the SF_m						
	(kg day mg^{-1})	B[a]P	As	Cd	Cr	Ni	NNK	NNN
Cooking activities	3.3 (2.1-5.2)×10^{-3}	<1%	77%	13%	<1%	10%	<1%	<1%
Candles	5.5 (2.7-28)×10^{-3}	3%	<1%	44%	<1%	53%	<1%	<1%
Incenses	2.1 (1.4-3.3)×10^{-4}	9%	<1%	21%	<1%	70%	<1%	<1%
Second-hand - conventional cigarettes	1.1 (0.8-1.5)×10^{-3}	1%	3%	15%	<1%	<1%	73%	8%
Second-hand - electronic cigarettes (with nicotine)	1.9 (1.2-2.9)×10^{-6}	<1%	20%	42%	<1%	8%	28%	2%
Open fireplaces (wood)	6.9 (2.7-19)×10^{-3}	4%	<1%	2%	<1%	94%	<1%	<1%
Closed fireplaces (wood)	6.9 (2.7-19)×10^{-3}	4%	<1%	2%	<1%	94%	<1%	<1%
Pellet stoves	1.5 (1.1-2.0)×10^{-2}	<1%	9%	18%	<1%	73%	<1%	<1%

Table 4-5. Emitted risk (ER) expressed as median value and 5th -95th percentile range, of the indoor sources investigated and relative contributions of deposited surface area ($ER_{SA(Alv+TB)}$) and PM_{10} particle metrics (ER_{PM10}).

Indoor source	ER(h^{-1})	$ER_{SA(Alv+TB)}$	ER_{PM10}
Cooking activities	6.6×10^{-3} (3.1-13)×10^{-3}	>99.99%	<0.01%
Candles	1.4×10^{-5} (0.6-7.6)×10^{-5}	>99.99%	<0.01%
Incenses	4.4×10^{-4} (1.3-9.0)×10^{-4}	>99.99%	<0.01%
Second-hand - conventional cigarettes	1.3×10^{-4} (0.9-2.0)×10^{-4}	99.97%	0.03%

Second-hand - electronic cigarettes (with nicotine)	2.3×10^{-8} $(1.4\text{-}4.0)\times10^{-8}$	>99.99%	negligible
Open fireplaces	2.7×10^{-5} $(1.0\text{-}7.6)\times10^{-5}$	99.99%	0.01%
Closed fireplaces	9.8×10^{-6} $(3.4\text{-}30\times10^{-6}$	99.96%	0.04%
Pellet stoves	9.9×10^{-6} $(6.0\text{-}150)\times10^{-6}$	99.97%	0.03%

The highest ER amongst the sources investigated is the cooking activities one. This is mainly due to the abovementioned high contributions of the lung-deposited surface area emission rate ($er_{SA(Alv+TB)}$) but also to the high slope factor (3.3×10^{-3} kg day mg^{-1}; Table 4-4). A very high $er_{SA(Alv+TB)}$ was also recognized for incense, nonetheless, the resulting ER is lower than the cooking activity one since the slope factor is lower (2.1×10^{-4} kg day mg^{-1}). On the contrary, pellet stoves, which are characterized by the most harmful chemical composition of the emitted particles amongst the source investigated in the present work, present a much lower $er_{SA(Alv+TB)}$ with respect to cooking activities. The lowest ER amongst the sources here considered is that characteristics of electronic cigarettes (ER=2.3×10^{-8} h^{-1}) due to the low particle emission rate and SF_m values.

With regard to biomass heating systems, the ER related to open fireplace is higher than closed one and pellet stoves. Such differences are due to the different particle emission rate, indeed the $er_{SA(Alv+TB)}$ resulted much higher for open fireplaces then leading to ER larger than pellet stove one even if the pellet slope factor is roughly two-fold than the wood one.

4.3.2 Risk of the exposed population

As mentioned in the previous paragraphs, the ER of the source leads to an increase of the risk concentration (RC) in an indoor microenvironment which can be described by a simplified zero-dimensional model (eq. (14)). By a way of example, in Figure 4-1, the RC_{in} trends when cooking activities are performed (also with mitigation solutions) are shown. In particular, as mentioned above, the activity was performed for 27 min (median duration), then, as soon as it is switched off, a concentration decay occurs. In figure, the trends for the three different AER values are graphed: in particular, as the AER increases (from 0.2 to 1 h^{-1}), the RC_{in} peak decreases and, when the source is switched off, the RC_{in} decays more rapidly to the initial (background) concentrations. Similar trends are obviously expected for the other sources; nonetheless different RC levels are reached due to the different ER and duration of the emission.

Such different RC levels clearly affect the risk of the exposed population as clearly highlighted in Table 4-6 where the ECR_{SE} of the exposed population to each source is reported on the basis of

the exposure times discussed and summarized in section 4.2.2 (i.e. considering a further 2 hour exposure during the concentration decay period). ECR_{SE} values for the three AERs considered in the simulations are shown. The data highlight that, for a given ventilation rate, the highest ECR_{SE} is due to cooking activities (1.3×10^{-5} for AER=0.2 h^{-1}), followed by open fireplaces and incenses ($>10^{-6}$), and closed fireplaces, pellet stoves and candles ($>10^{-7}$). Thus, a single cooking activity event (and further 120 min exposure) would lead to a risk higher than the lifetime lung cancer risk threshold suggested by the WHO (1×10^{-5}). The high ECR_{SE} due to the exposure to biomass heating systems are due to the very long exposure event adopted in the simulations; on the contrary, the very short emission duration of cigarettes leads to the lower ECR_{SE} values related to second-hand aerosols, especially for electronic cigarettes (5.2×10^{-12} for AER=0.2 h^{-1}).

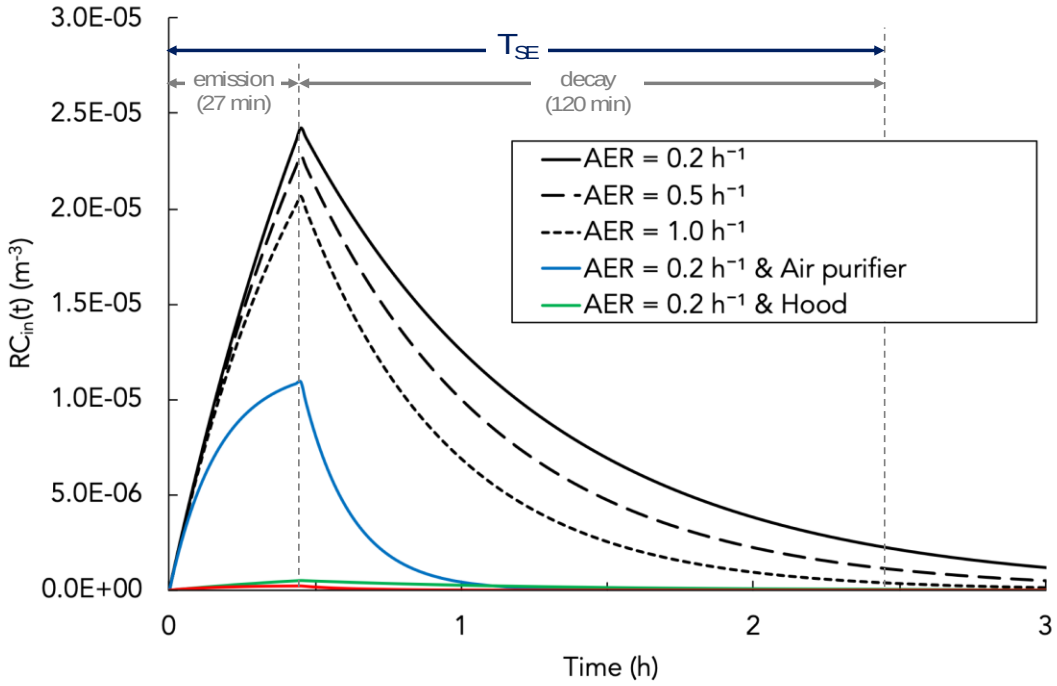

Figure 4-1. Median RC_{in} trends for cooking activities as a function of the AER and mitigation solutions (hood and air purifier).

Despite the absolute risk values, which are affected by the boundary conditions adopted in the simulations (e.g. room volume, exposure time, etc.) the relative reduction of the risk as a function of the ventilation rate need to be discussed. Indeed, from ECR_{SE} data of Table 4-6, it can be recognized that the typical AER values of residential environments are not able to reduce significantly the ECR_{SE}: from 0.2 to 1 h^{-1} the median ECR_{SE} was not even halved. In order to obtain

a significant reduction of the ECR_{SE} very high AERs would be required. As an example, in Figure 4-2 the ECR_{SE} for cooking activities as a function of the AER were reported also for ventilation rates much larger than those technically achievable in homes: the graph shows that a 10-fold reduction of the median ECR_{SE} (from 10^{-5} to 10^{-6}) would need an AER > 10 h^{-1}. Summarizing, the general ventilation can just partially reduce the lung cancer risk related to the exposure to indoor-generated particles.

Table 4-6. ECR_{SE} of the population exposed to the indoor sources as a function of the three AER values; results are expressed as median value and 5th -95th percentile range.

Indoor source	**AER** (h^{-1})		
	0.2 h^{-1}	0.5 h^{-1}	1 h^{-1}
Cooking activities	1.3×10^{-5} $(0.5\text{-}3.0)\times10^{-5}$	1.1×10^{-5} $(0.41\text{-}2.5)\times10^{-5}$	8.1×10^{-6} $(3.2\text{-}19)\times10^{-6}$
Candles	1.0×10^{-7} $(0.5\text{-}5.9)\times10^{-7}$	8.8×10^{-8} $(3.9\text{-}50)\times10^{-8}$	7.1×10^{-8} $(3.2\text{-}41)\times10^{-8}$
Incenses	4.8×10^{-6} $(1.4\text{-}9.5)\times10^{-6}$	3.9×10^{-6} $(1.1\text{-}7.6)\times10^{-6}$	2.9×10^{-6} $(0.8\text{-}5.6)\times10^{-6}$
Second-hand - conventional cigarettes	5.4×10^{-8} $(2.5\text{-}10)\times10^{-8}$	4.4×10^{-8} $(2.1\text{-}8.3)\times10^{-8}$	3.3×10^{-8} $(1.5\text{-}6.2)\times10^{-8}$
Second-hand - electronic cigarettes (with nicotine)	5.2×10^{-12} $(2.2\text{-}11)\times10^{-12}$	4.5×10^{-12} $(1.9\text{-}9.7)\times10^{-12}$	3.7×10^{-12} $(1.6\text{-}7.9)\times10^{-12}$
Open fireplace	1.2×10^{-6} $(0.4\text{-}3.5)\times10^{-6}$	9.2×10^{-7} $(3.3\text{-}27)\times10^{-7}$	6.7×10^{-7} $(2.4\text{-}20)\times10^{-7}$
Closed fireplace	4.3×10^{-7} $(1.5\text{-}15)\times10^{-7}$	3.4×10^{-7} $(1.2\text{-}12)\times10^{-7}$	2.4×10^{-7} $(0.8\text{-}8.7)\times10^{-7}$
Pellet stoves	4.6×10^{-7} $(2.6\text{-}7.4)\times10^{-7}$	3.6×10^{-7} $(2.1\text{-}5.8)\times10^{-7}$	2.6×10^{-7} $(1.5\text{-}4.2)\times10^{-7}$

Thus, adopting mitigation solutions could represent a key approach in reducing the lung cancer risk of the exposed population. Indeed, as shown in Figure 4-1 for cooking activities, the RC concentration levels when adopting hoods and/or air purifiers resulted much lower than those with no mitigation solutions. In particular, the kitchen hood is able to reduce the ER of the source and,

consequently, the risk concentration peak in the room is significantly reduced as well. When the emission period ends, the hood is switched off, thus the decay rate, i.e., the total removal rate, *TRR* (equal to $AER+k$) is exactly the same of the abovementioned scenarios with no mitigation solutions. The presence of the air purifier per se does not affect the risk emitted, but significantly increases the total removal rate (in this case equal to $AER+k+ACH\cdot\eta_{purifier}$), then reducing the sharpness of the concentration increase during the emission period and speeding up the risk decay process as soon as the emission ends. In Figure 4-3 the ERC_{SE} values with and without mitigation solutions for all the investigated sources and scenarios are reported. In the case of cooking activities, using a hood with a 98% efficiency would reduce the median ECR_{SE} to 2.5×10^{-7}. A local extraction can just be adopted for cooking activities whereas it is not suitable for other indoor sources. In that case the use of an air purifier would be helpful: adopting an air purifier providing an $ACH\cdot\eta_{purifier}$=4.73 h^{-1}, as that discussed in the methodology, would reduce the median ECR_{SE} due to the exposure to the different indoor sources by 70-80% with respect to the AER=0.2 h^{-1} scenario (in Figure 4-3). Thus, in the case of cooking activities, adopting both a high efficiency hood and an air purifier could reduce the median lung cancer risk of exposed population of roughly three orders of magnitude (i.e., down to 10^{-8}).

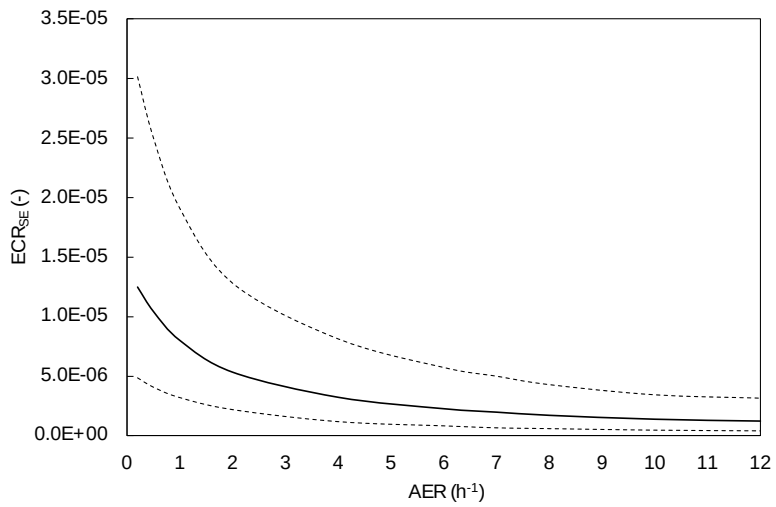

Figure 4-2. ECR_{SE} for cooking activities as a function of the AER. Data are reported as median (solid line), 5th and 95th percentile (dashed lines) trends.

As reported in the methodology section, from the ECR_{SE} the excess lifetime cancer risk (ELCR) can be estimated if the number of the single exposure events is known. As an example, for biomass-burning heating systems, to estimate the median ECR_{SE} we have considered a median emission

period for each exposure event of 8 hours and further 2 hours of exposure during the decay. A rough estimate of the ELCR for a person exposed daily during the heating period (e.g., from mid-November to mid-March, i.e., 136 days year^{-1}) for his/her entire life (70 years) would be roughly 10^{-2}-10^{-3} (i.e., 100-1000 new cases for 100000 exposed persons) depending on the heating system (fireplace, stove) and AER. Such ELCR agrees with the value estimated in a previous paper [133], [134]. Analogously, the lifetime lung cancer risk contribution of each source can be roughly estimated by summing up the ELCR of each source.

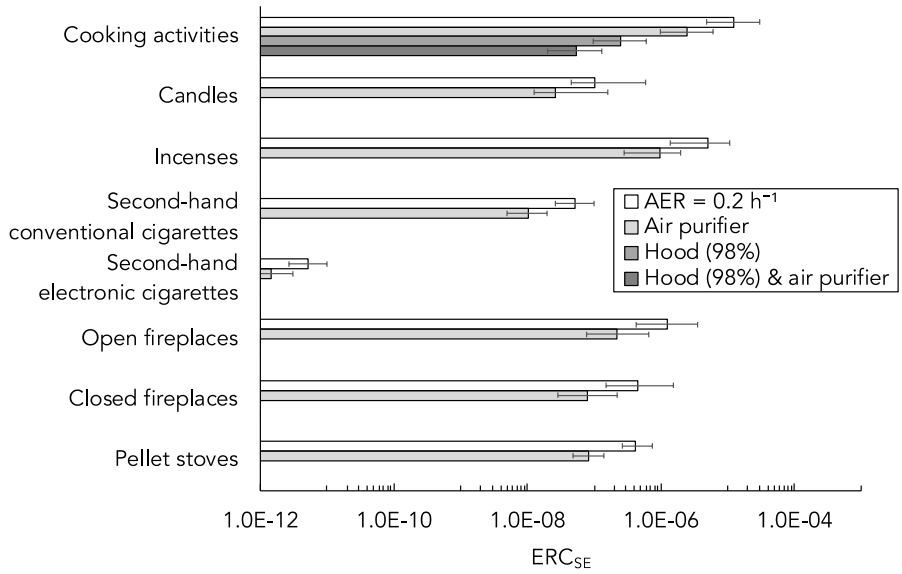

Figure 4-3. Effect of the mitigation solutions on ECR_{SE} for the different sources and scenarios: hood (with a 98% efficiency, only for cooking activities) and air purifier ($ACH \cdot \eta_{purifier}$=4.73 h^{-1}). Bars represent the median values, whereas the error bars represent 5th-95th range.

4.3.3 Strength, limitations, and research needs

The proposed simplified approach could be very helpful for air quality experts and engineers to estimate the lung cancer risk due to the exposure to airborne particles emitted by indoor sources just adopting peer-reviewed data available from the scientific literature on particle emission rates (both in terms of aerosol metrics and chemical composition). This is clearly a strength of the research as it provides an easy-to-use approach that could be applied through simplified zero-dimensional well-mixed models (mass-balance equations) allowing the estimate of the risk in each indoor exposure scenarios. The proposed approach presents assumptions and limitations that need to be checked when applied; as an example, considering the risk concentration homogeneous in

the confined space could be not adequate for large volumes or to evaluate the exposure of a person in the close proximity of the source, in that cases more complex (and site-specific) computational fluid-dynamic (CFD) solutions would be needed [271]. Similarly, when applying the simplified mass-balance equation to evaluate the risk of the exposed population, a further hypothesis is adopted, i.e., the chemical composition and the size of the emitted particles are invariant over time. Although the amount of the carcinogenic compounds does not vary once the particles are emitted, considering no variations in size implies that no condensation and coagulation phenomena are occurring as well. This can be quite acceptable for most of the indoor situation but, for very high emissions of very small particles (e.g. natural gas combustion, with modes <10 nm, [98]) in small rooms, it could be an unsound assumption. Thus, such simplified hypotheses adopted to simulate the emitted particles (and the related risk) can be, at a first glance, considered minor and somehow known and, hence, manageable.

On the contrary, the main limitation in terms of the applicability of the proposed approach are related to two aspects that have not been yet investigated by the scientific literature: a) adopting a chemical composition of the emitted particles invariant to the particle size, and b) adopting a fixed coefficient to convert the toxicity of the particle surface area metric in particle mass (ι_j) for all the indoor sources.

In regards to the chemical composition of the emitted particles as a function of the particle size, the authors are well aware that assuming constant concentrations of the chemical compounds for each particle size could be an oversimplified approach since particles may present different chemical compositions as a function of their sizes [241]–[243]. If a size-segregated chemical composition of the aerosol emitted by each source were available, the emitted risk model could be easily modified calculating and adopting different SF_m for each particle diameter (or at least for sub- and super-micron particle independently). Nonetheless, to date, such detailed size-segregated chemical composition of the particles emitted by the investigated sources are not available; on the contrary, the studies reporting the chemical analysis of the particles emitted by such sources, if any (as summarized in the section 0), just report an overall chemical concentration over the entire size range. This lack of information represents a huge opportunity for the scientific community involved in indoor aerosol studies; as an example, combined techniques made up of particle collection in cascade impactors and further chemical analyses (i.e. mass spectrometry, x-ray fluorescence, etc.) should be adopted in properly designed experimental campaigns allowing the collection of a detectable particle mass also for smaller diameters [272].

With regard to the coefficient to convert the toxicity of the particle surface area metric in particle mass (c_f), the authors highlight that the generalization of the c_f parameter to all sources is debatable. Sze-To et al. [131] defined (and back-calculated) this parameter using epidemiological data and size distribution data measured from a combination of gasoline and diesel vehicles; moreover, they assumed that c_f should vary with the physical size rather than the chemical constituent of the PM. Adopting the same c_f parameter for all the sources could be in principle not correct but, to date, this is the best available method to take into account for the toxicity of the sub-micron particle fraction. As an alternative, c_f values for each source should be carried out as reported by Sze-To et al. [131], anyway, this is not easy task since epidemiological data characteristics of people exposed only to one specific source should be provided too. We point out that the need for such a conversion parameter is due to the fact that the slope factor (i.e., cancer potency associated with exposure to a unit concentration of a chemical) are currently defined with respect to the particle mass concentration, and this is an inheritance of having considered mass-based aerosol metrics (e.g., PM_{10}) as the main metrics related to the health effect. In the next future, since the sub-micron particles are now considered a major threat for human health, toxicological and epidemiological studies attempting to evaluate the slope factors in terms of sub-micron particle metrics (likely surface area) are needed. This would avoid the use of general conversion parameters and could allow the simultaneous use of mass- and surface area-based slope factors for PM_{10} and surface area metrics, respectively.

All the critical aspects here discussed contribute to increase the uncertainty of the results provided in terms of emitted risk, weighted average slope factor, and excess cancer risk; indeed, the uncertainty represents a measure of how confident we are of the results, thus larger uncertainties on the input data and simplified hypotheses adopted could affect the uncertainty of the results. A proper uncertainty budget for the output data provided is quite complex (also for the limited data on input parameters) and beyond the aims of the current study as it would require an ad-hoc research; this is the reason why a stochastic approach (i.e. Monte Carlo method) was at least performed in order to take into account the possible variability of the input parameters. Nonetheless, the limitations here summarized do not undermine the approach proposed and its transferability, moreover, the availability of the abovementioned data in the future will reduce the uncertainty of the results it provides. The authors also highlight that a similar approach can be carried out for other airborne particle-related health effects too (e.g., cardiovascular, neurodegenerative diseases) if corresponding dose-response relationships are known.

4.4 Conclusions

In this study, a simplified approach to estimate the lung cancer risk of people exposed to airborne particle emitted by indoor sources was proposed and applied. The approach allows to perform estimates of the lung cancer risk for different indoor exposure scenarios as a function of the specific source, room volume, ventilation rate, and (possible) mitigation solutions. It is based on the straightforward application of a mass balance equation of the, here defined, "emitted risk" which is the parameter considering, simultaneously, the emission rates, the chemical composition (in terms of carcinogenic compounds), and the size distribution of sub- and super-micron particles emitted by the source. Thus, predictive assessments of the risk can be performed for previously characterized sources, without performing site specific and time-demanding experimental analyses.

The approach, here applied to different sources, allowed to draw the following general evidences:

- the "risk emitted", whatever the source, is dominated by the sub-micron particles (and by the corresponding aerosol metrics, e.g., deposited surface area) with respect to super-micron particle (i.e., PM_{10});
- the lung cancer risk received by people in indoor environments can be extremely high for different (very common) sources, such as cooking activities;
- the typical ventilation rates achievable in residential environments do not significantly reduce the risk, thus other mitigation solutions are needed;
- the reduction of the emission (e.g., using extraction hoods, when suitable) represents the more effective mitigation solution, as an example, for the indoor environment here considered, a 100-fold reduction of the risk due to cooking activities was estimated;
- air purifiers can also significantly decrease the lung cancer risk (roughly one order of magnitude for the proposed scenarios).

In conclusion, the proposed approach represents a very useful tool, but its applicability is obviously affected by the availability of source emission data. In this sense, the literature review here conducted showed a lack of data; therefore, studies trying to fill this gap of knowledge are highly welcomed.

Chapter 5 - CASE STUDY 3:
EFFECTIVENESS OF ECO-FEEDBACK IN IMPROVING THE INDOOR AIR QUALITY IN RESIDENTIAL BUILDINGS: MITIGATION OF THE EXPOSURE TO AIRBORNE PARTICLES

Indoor air quality, a major concern for human health, is strongly influenced by occupants' behavior but people are not aware about how their everyday behavior affects their exposure to pollutants. In the present study it was tried to cope with the gap of knowledge between lack of awareness and the understanding of how occupants' behaviors affect the environment. To this end we performed an evaluation of the IAQ awareness of 100 families through questionnaire surveys and an investigation of an "eco-feedback" strategy based on awareness-raising campaigns. In particular, information and experimental campaigns were conducted in 10 homes allowing the evaluation of its effectiveness in the short-term. Results showed that the occupants are not properly aware of the IAQ in their homes and of their exposure to airborne particles including the possible contribution of indoor sources. Anyway, the eco-feedback strategy adopted resulted successful both in terms of promoting behavioral changes of the occupants and reducing the concentration levels while airborne particle emitting sources (i.e., cooking) were in operation. Indeed, the exposure to airborne particles while cooking measured after the information campaign resulted lower than the baseline exposure with median relative reductions of 47% and 59% for PM_{10} and particle number concentration, respectively. The outcomes of the study could be of great interest for scientists involved in designing eco-feedback campaigns and indoor airborne particle monitoring since, for the first time, the potential effect of an eco-feedback strategy on indoor air quality was shown.

5.1 Aims of the work

In view of bridging the gap of knowledge concerning the IAQ awareness and the effectiveness of eco-feedback on IAQ and exposure to airborne particles, the scientific community should address the following questions: i) *are the occupants aware of their exposure to airborne particles in their homes?* ii) *is it possible to make them aware through trustworthy information?* and, in case, *are they able to mitigate their exposure to indoor-generated airborne particles?* iii) *how their mitigation strategies affect the different airborne particle metrics?* However, to date, there is a lack of data on eco-feedback strategy applied to IAQ

and airborne particles, and the few available studies are limited to particles >0.5 μm [273]–[275]. Moreover, no quantitative information on the effectiveness of eco-feedback approach on exposure to airborne particles and IAQ were provided by the scientific literature.

The novel aspect of the present work is the attempt to answer the abovementioned questions and quantifying, for the very first time, the effect of an eco-feedback strategy on different airborne particle metrics, including the ultrafine particles. To this end, in the present study we aimed at: i) investigating the IAQ awareness of occupants through questionnaire surveys; ii) applying an eco-feedback strategy, based on both a trustworthy information campaign and an experimental campaign, to evaluate, in the short-term, the possible behavioral changes of the occupants and their ability in reducing the concentration levels, while source emitting airborne particles were in operation. The research was carried out with specific regard to the heating season due to their typical highest exposure to airborne particles. The outcomes of the study could be of great interest for scientists engaged in citizen science researches [276].

5.2 Materials and methods

The methodology implemented in this work was divided in two main sections which will be detailed in the following paragraphs:

- the evaluation of the IAQ awareness of 100 families through the submission of questionnaire surveys in order to investigate their habits, perceptions, and intentions with respect to the management of indoor environments;
- the application of an "eco-feedback" strategy based on awareness-raising campaigns (an information campaign and an experimental campaign conducted in 10 homes), with the scope to increase IAQ awareness with respect to the baseline value. The evaluation of the eco-feedback effectiveness through qualitative (behavioral changes obtained from final surveys with respect to initial perception and habits) and quantitative results (reduction of the actual exposure to airborne particle metrics) was also carried out. In particular, the eco-feedback effectiveness was evaluated comparing quantitative and qualitative results collected for three days before and for three days after the information campaign, respectively, in order to obtain a short-term effect of the eco-feedback strategy.

5.2.1 Evaluation of the IAQ awareness

The evaluation of IAQ awareness was conducted by recruiting 100 volunteer families living in South-Central Italy, in an area including Lazio, Molise and Campania regions. The recruited homes

were located either in urban (42%), sub-urban (24%) and rural areas (34%). In Figure 5-1 the geographical location of the homes is shown along with a general indication of their outdoor air quality: indeed, the average number of exceedance days in the 2018-2021 period with respect to the 24-h average PM_{10} threshold value admitted by the current outdoor air quality standards (50 μg m^{-3}; [74]) was graphically reported. To this end, PM_{10} concentration level measured by the closest fixed monitoring stations of the Italian air quality agency were considered. The authors point out that the current legislation allows a maximum of 35 exceedance per year [74], but, several families involved in the survey live in areas with more than 35 exceedances. The families, on average, resulted composed by four people, had an average age of around 40 years; the homes are inhabited 16 to 20 hours daily, i.e., about 75% of the day.

Figure 5-1. Localization of the 100 volunteer families participating to the survey: the size of the points is proportional to the number of families participating, whereas the color represents the number of exceedance days with respect to the 24-h average PM_{10} threshold value admitted by the current outdoor air quality standards (50 μg m^{-3}) provided by the closest monitoring station of the Italian air quality agency. The number of exceedance days were retrieved from the air quality agency website and are reported as average values of the period 2018-2021. Please note that the maximum allowed exceedance days from the current regulation is 35. Points in grey were too far from monitoring stations and their outdoor air quality was not classified.

The questionnaire surveys were provided in the period January-March 2022 and people were asked to answer with specific regard to the period they filled out the questionnaire. This allowed to obtain information on the IAQ awareness specifically for the heating season, which is the season leading to the highest indoor exposure to airborne particles. The questionnaire surveys on the IAQ awareness were characterized by several parts in order to get information on: i) home localization, number and age of occupants, time spent at home, ii) characteristics of the building envelope (apartment or detached home, type of windows, building energy rating); iii) presence and type of possible pollutant sources (e.g. type of stoves, smoking persons, type of heating systems); iv)

presence of removal systems (e.g. mechanical ventilation, air purifiers, etc.); v) occupants' behavior referred to the use of possible pollutant sources (e.g. cooking and other combustion processes) and removal strategies (e.g. use of hoods, manual airing, etc.); vi) specific questions about occupants' IAQ awareness. The questionnaires mostly presented multiple-choice questions to which the occupants were asked to provide a "yes/not/unsure answer", a rating ("bad", "poor", "fair", "good" and "excellent"), or selecting an answer from a limited number of pre-defined options (here multiple-choice was also allowed). In order to conduct statistical analysis, numerical scores (from 1 to 5) were associated to these ratings. Open-ended questions and optional comment areas were also provided to allow people providing detailed answers for specific questions.

The surveys were performed through interviewer-administered questionnaires conducted as face-to-face interviews by a researcher. This method can better guarantee the validity and the reliability of the questionnaires since the researcher had the possibility to explain and clarify any doubts and concerns arising from the users. Nonetheless, we point out that the presence of the researchers hasn't "pressurized" the users to give "appropriate" rather than truthful answers [277].

To assess the awareness of the occupants and evaluate the effectiveness of the information campaign hereinafter described, amongst the several questions collected, the following ones were considered:

- *Have you ever looked for information on the IAQ in homes?*
- *If not, why? ("it is not an important issue", "I am not aware of the IAQ problems", other)*
- *How do you rate the outdoor air quality of your area? (from "bad" to "excellent")*
- *How do you rate the IAQ in your house? (from "bad" to "excellent")*
- *In order to guarantee a proper air exchange of your house, do you think is preferable to adopt manual airing, mechanical ventilation, nothing? (multiple choices allowed)*
- *When cooking, do you usually adopt the following mitigation strategies: kitchen hoods, manual airing, nothing? (multiple choices allowed)*
- *What is the reason why you adopt these mitigation strategies (if any)? ("reducing smells", "reducing relative humidity", "improving the indoor air quality", other; multiple choices allowed)*
- *Would you install a mechanical ventilation system to improve the IAQ of your house?*
- *Would you use a portable air purifier to improve the IAQ of your house?*

5.2.2 Design of the eco-feedback strategy

The eco-feedback strategy adopted in the present research is based on awareness-raising campaigns. To this end, both an information campaign and an experimental campaign were

performed, and their short-term effectiveness was evaluated through results gathered from qualitative and quantitative analyses carried out before and after the information campaign, namely during the "baseline" and "follow-up" periods. In particular, the investigation of the eco-feedback effectiveness was conducted considering 10 families of the abovementioned 100 volunteer families who accepted to be involved in the second part of the research. A scheme of the methodology adopted to evaluate the effectiveness of the eco-feedback is reported in Figure 5-2.

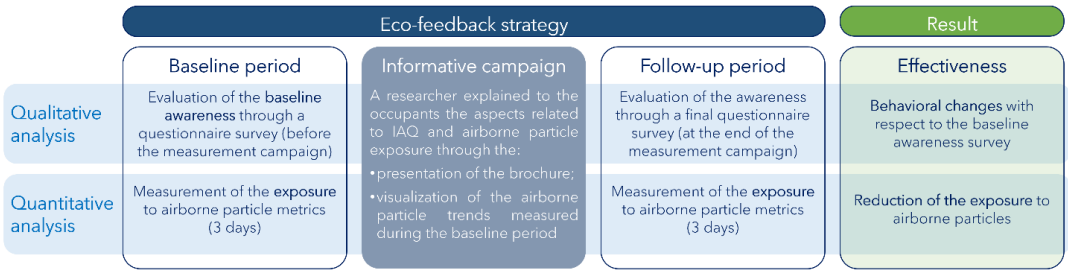

Figure 5-2. Scheme of the methodology adopted to evaluate the effectiveness of the eco-feedback strategy.

Quantitative analysis

The quantitative analysis was made up of two experimental analyses carried out during the baseline and follow-up periods for three consecutive days, respectively. In particular, real-time measurements of airborne particle metrics (particle number and mass concentrations), CO_2 concentrations, temperature and relative humidity were carried out. Both during the baseline and follow-up periods, the occupants were asked to fill out a daily diary of their activities related to the use of indoor sources (i.e., cooking activities, biomass burning, use of candles, smoking) as well as the implementation of possible mitigation strategies (i.e., opening windows or using kitchen hood).

The experimental analysis was performed through simultaneous measurements of the following environmental parameters: indoor and outdoor particle number concentrations (PNCs, part. cm^{-3}), indoor and outdoor PM_{10} ($\mu g\ m^{-3}$), indoor CO_2 concentration (ppm), indoor temperature (T, °C), and indoor relative humidity (RH, %). Measurements were performed through the following instruments:

- two diffusion-charger particle counters (Testo DiSCmini), based on the electrical charging of the aerosol, to measure particle number concentrations in the 10-700 nm size range with 1-s time resolution.

- two photometers, i.e., DustTrak™ DRX Aerosol Monitors (Model 8534, TSI Inc.), operating on the basis of a light scattering technique, to measure PM_{10} concentrations with 1-s time resolution.

- a non-dispersive infrared analyzer (Testo – Ambient CO_2 probe) to measure indoor temperature, humidity, and CO_2 concentration with 1-s time resolution.

A DustTrak photometer, a DiSCmini, and an Ambient CO_2 probe were placed indoor, whereas a further DustTrak photometer and DiSCmini were placed outdoor. The room where combustion sources were typically used, i.e., the kitchen, was chosen as indoor sampling site since cooking activities represent one of the most used indoor sources. Instruments were placed at > 2 m from the stoves so that they were not directly exposed to the sources thus allowing to measure the average concentration experienced by people in that room. The same indoor site, for each home, was adopted for baseline and follow-up periods in order to properly compare the exposure levels. As outdoor sampling sites balconies, terraces were mostly chosen. All the collected data were post-processed as 1-min average value.

In view of a proper quantitative evaluation of the eco-feedback effectiveness, particular attention was paid to the data quality assurance. In particular, the DustTrak photometers were calibrated by comparison with the gravimetric method (which represents the reference method for particle mass concentration measurements) at the beginning of the experimental campaign performing a simultaneous 4-h long sampling simultaneously in an indoor microenvironment where typical activities (including cooking, using heating systems) were carried out. The DiscMinis were compared (in terms of particle concentration) to a TSI 3068B Aerosol Electrometer, using NaCl particles generated through a Sub-micrometer Aerosol Generator (TSI 3940). Nonetheless, since the portable instruments considered in the experimental campaign could present artifacts [278], [279], both DustTraks photometers and Discminis were zeroed before each of the 3-day measurement period using a HEPA filter; moreover, 10-min parallel reading of the two DustTraks and the two Discminis (the ones placed indoor and outdoor) were carried before each of the 3-day measurement period at the outdoor site. Finally, the Testo – Ambient CO_2 probe was calibrated by the manufacturer before the campaign.

The comparison amongst the airborne particle and CO_2 concentrations as well as temperature and relative humidity values measured during baseline and follow-up periods allowed providing a quantitative evaluation of the eco-feedback effectiveness in the short-term ("right-now evaluation" [274]). Since indoor airborne particle concentrations (both PM_{10} and PNC) are also influenced by the outdoor values [280], [281], when comparing baseline and follow-up concentrations, indoor values were normalized to the simultaneous outdoor ones. We compared PM_{10} and PNC measured during all the emitting activities, as indicated by the occupants through the diaries, performed in

the baseline and follow-up periods, by decreasing the indoor concentration values measured at each cooking event of the simultaneous median outdoor concentration. On the contrary, indoor CO_2 data were not normalized to the outdoor values since the outdoor CO_2 concentration (for given geographical area and season) are quite constant and its effect on the indoor values can be considered negligible [282]. As hereinafter detailed, the evaluation of the effectiveness of the eco-feedback strategy was carried out just considering cooking events. Once again, we point out that the aim of the proposed research is measuring the effectiveness of the eco-feedback approach in terms of exposure reductions to the different airborne particle metrics resulting from the adoption of mitigation strategies, for this reason the occupants were not forced to adopt any mitigation strategies and that the experiments were not conducted under controlled conditions (e.g. specific cooking procedures, adoption of specific mitigation strategy, etc.): we measured the occupants' exposure as resulting from the way they run their homes (in terms of mitigation strategy, cooking activities, etc.). Thus, from the data we collected, it is not possible to evaluate the effect of a specific mitigation strategy on the exposure reduction.

Qualitative analysis

The qualitative analysis consists of: i) an evaluation of the baseline awareness of the occupants through a questionnaire survey (i.e. that described in the section 5.2.1) administrated before the experimental analysis by the researchers; ii) a final questionnaire survey administrated during the follow-up period after the experimental campaign. In particular, the final questionnaires were administrated by a researcher by means of face-to-face interviews as well as for baseline questionnaires (as described in section 5.2.1). The final questionnaire survey presented questions aimed at recognizing possible short-term variations of perceptions, habits, and intentions of the occupants as a consequence of the awareness-raising campaigns performed.

To evaluate the effectiveness of the information campaign hereinafter described, amongst the questions asked, the following ones were considered:

- *Did you find the information campaign useful?*

- *When cooking, during the follow-up period, did you adopt the following mitigation strategies: kitchen hoods, manual airing, manual airing & kitchen hoods, nothing (multiple choices allowed)?*

- *Do you think you could maintain the new habits (if any) in the long run?*

- *Would you buy a device to measure indoor air quality parameters in your house?*

- *In order to guarantee a proper air exchange of your house, do you think is preferable to adopt manual airing, mechanical ventilation, unsure? (multiple choices allowed)*

- *Would you install a mechanical ventilation system to improve the indoor air quality of your house?*
- *Would you use a portable air purifier to improve the indoor air quality of your house?*

Information campaign

The information campaign was provided by the researchers between the baseline and follow-up periods. In particular, the researchers provided trustworthy information by explaining to the occupants the aspects related to IAQ and airborne particle exposure. To this end, they used an illustrative brochure (Figure 5-3) where information explaining "why the houses are polluted" (e.g. outdoor-to-indoor penetration of outdoor-generated air quality parameters, indoor-generated pollutants), "what are the main indoor pollutants" (UFPs, PM_{10}, VOC, heavy metals, PAHs, etc.), "what are the risks related to indoor exposure", and "how the exposure can be reduced" (hood, air purifiers, mechanical ventilation, manual airing) were reported. The brochure was then given to the occupants so that they could check it during the follow-up period. Moreover, to reinforce the information provided, the researchers also showed to the occupants the airborne particle trends measured during the baseline period in order to make them aware of the effect of the indoor-generated particle sources (e.g., cooking) to their exposure. It is important to highlight that, despite the information provided, the occupants were not asked to apply any specific mitigation strategy or to actively interact with the instruments during the follow-up periods. Thus, the eco-feedback strategy we adopted cannot be considered as based on the use of in-home displays. The instruments we used were essentially adopted to perform the quantitative evaluation of the exposure reduction.

5.3 Results and discussions

5.3.1 IAQ awareness: perceptions, habits, and intentions

The investigation carried out through questionnaire surveys administrated to 100 families who volunteered to provided information regarding their IAQ perception, habits, and intention revealed that IAQ still represents an underestimated issue. Indeed, the general IAQ perception of the occupants was not in agreement with the actual exposure levels they experienced. Indeed, 76% of the investigated families had never looked for information on the IAQ in homes firstly because they were not aware of the IAQ-related problems (68%) and secondly because they did not consider it an important issue (32%). In fact, people resulted having a general positive (or at least non-negative) perception about the IAQ in their houses: they rated their IAQ as excellent (4%), good (53%), or, at most, fair (43%) whereas no "poor" or "bad" scores were detected.

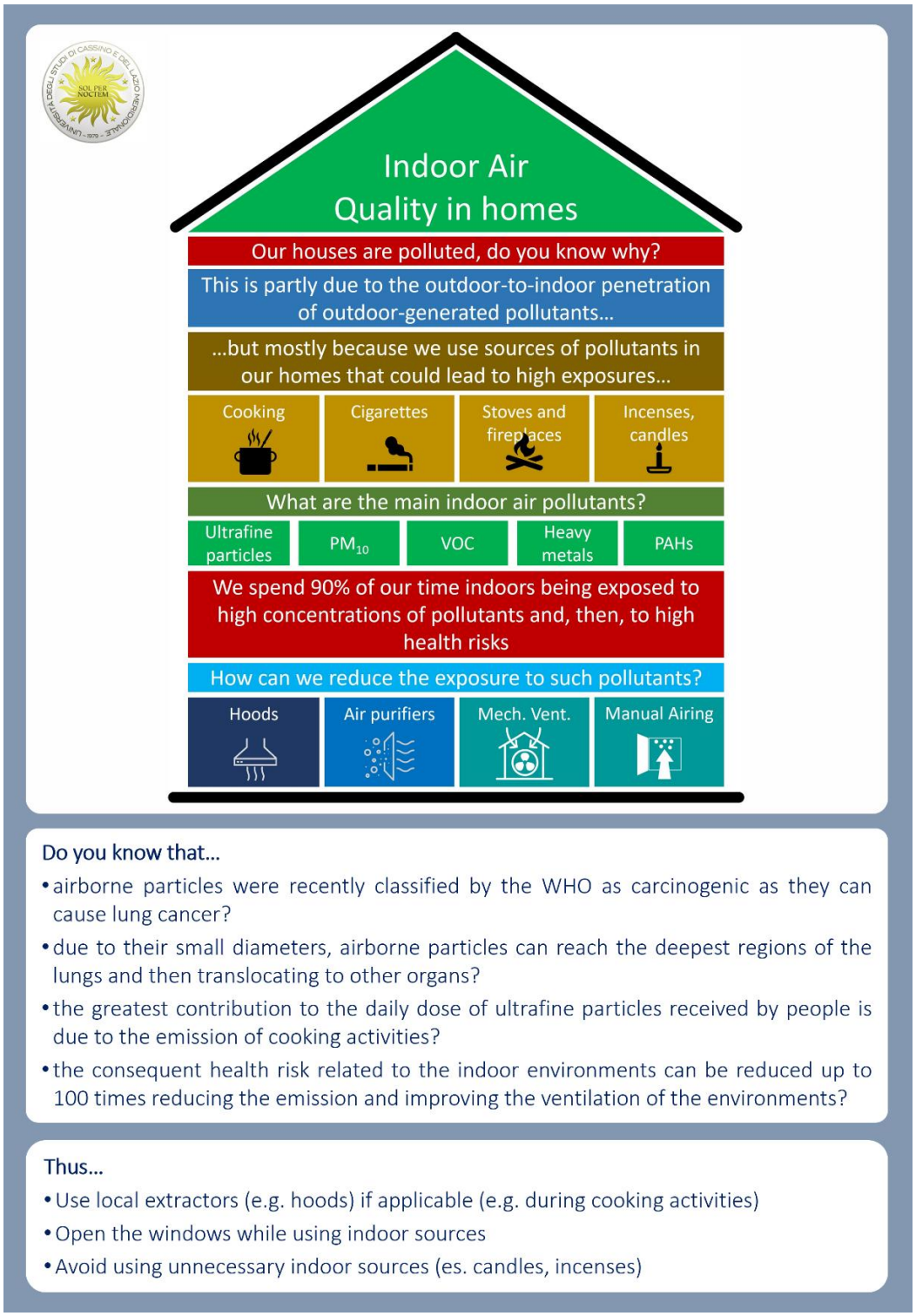

Figure 5-3. Illustrative brochure provided to the occupants to informed them about the indoor air quality in homes.

Actually, the outdoor air quality was perceived as positive too, with ratings mostly spanning from excellent (16%) to good (40%) and fair (30%), and limited negative evaluations (poor 6%, bad 8%). This is somehow surprising since 61% of the volunteer families live in areas with a bad outdoor air quality, i.e. characterized by more than the maximum allowed number of exceedance days with respect to the 24-h average PM10 threshold value admitted by the current outdoor air quality standards (50 μg m-3; [74]) (Figure 5 1). Thus, the results show a lack of awareness of the investigated population both in terms of indoor and outdoor air quality and suggest that the IAQ perception is mostly related to the outdoor one. Indeed, 86% of families simultaneously had a non-negative perception of indoor and outdoor air quality (Figure 5 4), moreover, indoor, and outdoor air quality ratings resulted positively correlated (global Pearson coefficient equal to + 0.458, p-value <0.001).

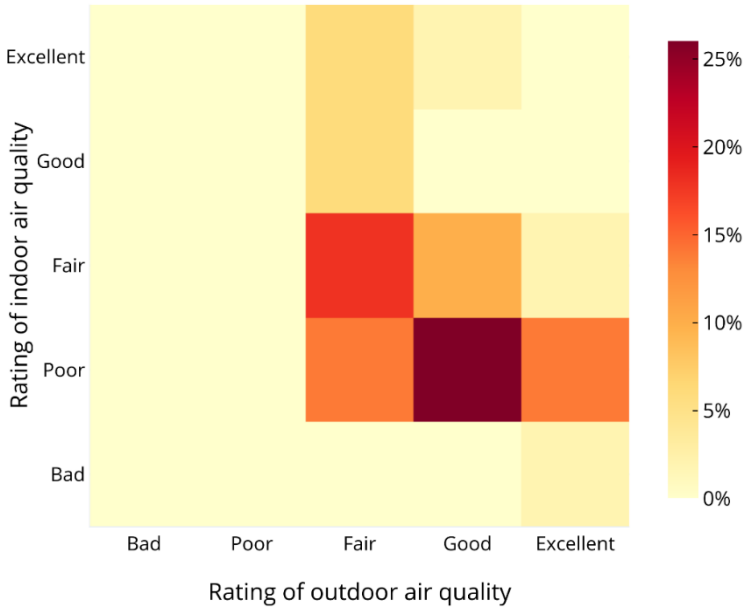

Figure 5-4. Relative frequencies of the ratings on indoor and outdoor air quality scores expressed by the 100 volunteers participating to the survey.

Such a mistaken perception of indoor air quality also affects the people habits and intentions in managing the indoor environment; indeed, just 48% of the people usually use kitchen hood while cooking and 72% open the windows. Nonetheless, the reasons why they adopt those mitigation strategies were mainly reducing smells (64%) and indoor relative humidity (32%), whereas just 24% of the interviewed selected the IAQ response. As regard the intentions, since the IAQ was not perceived as an issue, the non-propensity to install mechanical ventilation systems (67%) or purchase air purifiers (41%) resulted quite high.

5.3.2 Eco-feedback effectiveness

Results of the quantitative analysis

During the whole experimental campaign (i.e. including both baseline and follow-up periods), according to the diaries filled out by the volunteers, we detected 172 cooking activities (85 events during the baseline period and 87 during the follow-up period), 8 events of use of heating systems with an indoor combustion (e.g. fireplaces, biomass stoves), and no events due to other sources such as smoking, incenses, candles etc. (Table 5-1). The limited number of combustion events for heating purposes is due to the large use of heating system with hydronic distribution and radiator emission system (whose generator, i.e., boiler, is installed outdoor). Since the number of heating events with indoor sources were not statistically relevant, the analysis of the eco-feedback effectiveness was carried out just considering cooking events. Moreover, in order to avoid misinterpretation of the data, we have excluded from the statistical analysis all the cooking events occurring during or after the use of heating systems: e.g., if the heating system was run from the early afternoon to the evening, the cooking event occurring in that period (e.g., dinner) was excluded from the analysis.

Table 5-1. Information obtained from the diaries: number of events and adoption of mitigation strategies.

Type of combustion event	**Baseline period**	**Follow-up period**
Cooking activities and average duration	85 events 35 min event^{-1}	87 events 33 min event^{-1}
Use of heating systems with indoor combustion	5 events	3 events
Other combustion sources (smoking, candles, incenses)	No events	No events
Adoption of mitigation strategies during cooking events	**Baseline period**	**Follow-up period**
Use of hood (average duration and frequency of occurrence)	6 min event^{-1} 24% of events	15 min event^{-1} 41% of events
Manual airing (average duration and frequency of occurrence)	14 min event^{-1} 29% of events	21 min event^{-1} 65% of events

In Figure 5-5 an illustrative example of PNC (part. cm^{-3}), PM_{10} (μg m^{-3}) and CO_2 (ppm) trends (both indoor and outdoor) measured for 24 h in one of the homes under investigation is reported. In the graph the cooking events and the manual airing periods, as resulting from the diaries filled

out by the occupants, are also highlighted. The trends clearly show peaks during the cooking activities, in particular, PNCs reached values 2 or 3 orders of magnitude larger than those measured before the event (i.e., when no sources are present). After the peak, i.e., after the cooking activity, a concentration decay is clearly recognizable, but the concentrations remain still higher than the outdoor values for hours. Please note that the concentration decay is a function of air exchange rate, particle deposition rate, and further removal rates due to other removal mechanisms (e.g. hoods, air purifiers) [124], [283], [284]. Thus, faster decays can be obtained if hoods are turned on and windows are kept open. When the effect of the source disappears (e.g. during the night), the indoor concentrations are typically lower than the outdoor ones as the building envelope reduce the penetration of outdoor-generated pollutants [281]. CO_2 peaks were also detected during cooking activities, nonetheless, the effect of the cooking events on the indoor CO_2 concentration is less evident likely due to the high contribution of the CO_2 exhaled by the occupants [285]–[287].

In Table 5-2 the concentration levels measured during the experimental campaigns, both during baseline and follow-up periods, are reported. Indoor concentrations measured during the cooking events and those measured during the remaining periods of the days are separately reported. Median PNCs during cooking events resulted extremely high (1.12×10^5 and 8.55×10^4 part. cm^{-3} for baseline period and follow-up periods, respectively), and, specifically, much larger than those measured when no sources are in operation as well as at outdoor site. For PM_{10} and CO_2 similar behaviors were recognized but the absolute differences resulted much lower, this is likely because PNC represents the airborne particle metric better related to combustion sources [288]–[290].

Data also show that median concentrations of PNC, PM_{10} and CO_2 measured while cooking during follow-up periods resulted lower than baseline periods. Nonetheless, to properly evaluate the effectiveness of the eco-feedback strategy here adopted, more detailed home-by-home analyses need to be performed as hereinafter reported.

As an example, in Figure 5-6 the statistics of the PNCs, PM_{10}, and CO_2 measured during cooking events for baseline and follow-up periods in one of the homes under investigation are reported. Here, PNC and PM_{10} data represent the difference between indoor values while cooking and simultaneous outdoor values, whereas CO_2 data are reported as indoor values (outdoor data are not available and its variation can be considered negligible). PNC, PM_{10}, and CO_2 measured during cooking events after the information campaign (i.e. during the follow-up period) resulted statistically lower (Kruskal-Wallis test, $p<0.01$ [291]) than baseline values: the occupants of this home were able to obtain a relative reduction of median values equal to 50%, 35% and 28% for

PNC, PM_{10}, and CO_2, respectively. These relative reductions in this specific home were obtained just applying the easiest mitigation strategies suggested through the information campaign, i.e., opening the windows and using the hood during cooking activities, whereas neither air-purifiers nor mechanical ventilation systems were installed.

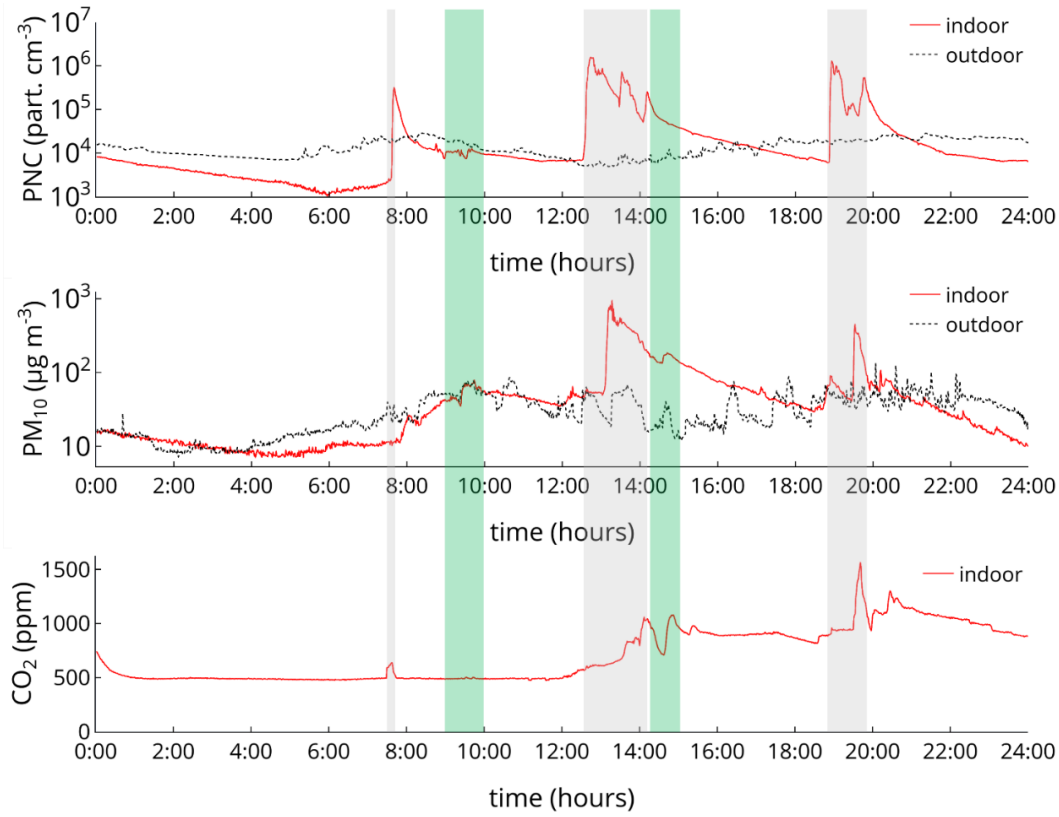

Figure 5-5. Illustrative example of PNC (part. cm^{-3}), PM_{10} (µg m^{-3}) and CO_2 (ppm) 24-h trends measured in one of the homes under investigation: indoor (solid line) and outdoor (dashed line) concentrations are reported as well as cooking periods (grey-shaded areas) and manual airing periods (green-shaded areas), as resulting from the diaries filled out by the occupants, are highlighted.

Similar results were obtained for all the homes considered in the experimental analysis, to this end in Figure 5-7 home-by-home relative reduction of median values (follow-up vs. baseline period) in terms of CO_2, RH, T, PM_{10} and PNCs measured while cooking are reported for all the homes investigated. Due to the mitigation strategies adopted by the occupants, i.e., manual airing, the indoor temperature while cooking during follow-up periods resulted slightly lower than the baseline period one: we detected a median reduction of 6%, spanning from 16% down to an increase of 4%. Thus, in terms of energy saving, on average, the effect of the mitigation strategies adopted can be considered sustainable. As expected, the effect of the mitigation strategies on the indoor relative

humidity is variegated as it spans from an increase of roughly 40% to a reduction of 36%. Indeed, the effect of the type of food on the generated water vapor as well as the possible large variation of outdoor absolute humidity values can strongly affect the indoor RH levels then undermining the mitigation solution adopted. On the contrary, as shown in the specific case study of Figure 5-6, significant reductions were recognized for CO_2, PM_{10}, and PNC: indeed, median reductions of the 10 homes resulted equal to 28% (range of 23%-39%), 47% (range of 8%-70%), and 59% (range of 49%-77%), respectively. Such quantitative data demonstrate the effectiveness of the eco-feedback strategy here adopted in mitigating the exposure to airborne particle metrics.

Table 5-2. Median particle concentrations (and corresponding 5^{th}-95^{th} range) measured in the 10 homes considered in the experimental analysis (both indoor and outdoor) during both cooking events and remaining periods of the day (no cooking events).

	Baseline period			**Follow-up period**		
Metrics	Indoor - no cooking events	Indoor - cooking events	Outdoor	Indoor - no cooking events	Indoor - cooking events	Outdoor
PNC (part. cm^{-3})	1.31×10^4 (3.44×10^3 - 1.10×10^5)	1.12×10^5 (1.66×10^4 - 6.07×10^5)	3.04×10^4 (8.71×10^3 - 9.31×10^4)	1.07×10^4 (2.68×10^3 - 1.66×10^5)	8.55×10^4 (1.22×10^4 - 7.12×10^5)	2.78×10^4 (2.32×10^3 - 1.35×10^5)
PM_{10} ($\mu g\ m^{-3}$)	58 (15 - 162)	83 (34 - 525)	47 (10 - 246)	61 (20 - 304)	57 (20 - 248)	36 (3 - 175)
CO_2 (ppm)	692 (365-1473)	769 (363-1826)	-	588 (362-1296)	693 (394-1580)	-

As mentioned above, the occupants were able to improve their IAQ just adopting manual airing and using hoods while cooking (once again, we point out that the occupants were not forced to apply any of these mitigation strategies; they did it if, how and when they want to). From the diaries they filled out quantitative information on their change of habits were available: in particular, as summarized in Table 5-1, before the information campaign (baseline period) hoods were used, on average, only 24% of the cooking events and for 6 min $event^{-1}$ (i.e., on average, 17% of the entire duration of the cooking event) whereas during the follow-up periods these values increased to 41% and 19 min $event^{-1}$ (i.e. 44% of the cooking event duration). Similarly, manual airing increased from

29% of the cooking events and 14 min event^{-1} (41% of the cooking event duration) to 65% and 21 min event^{-1} (64% of the cooking event duration).

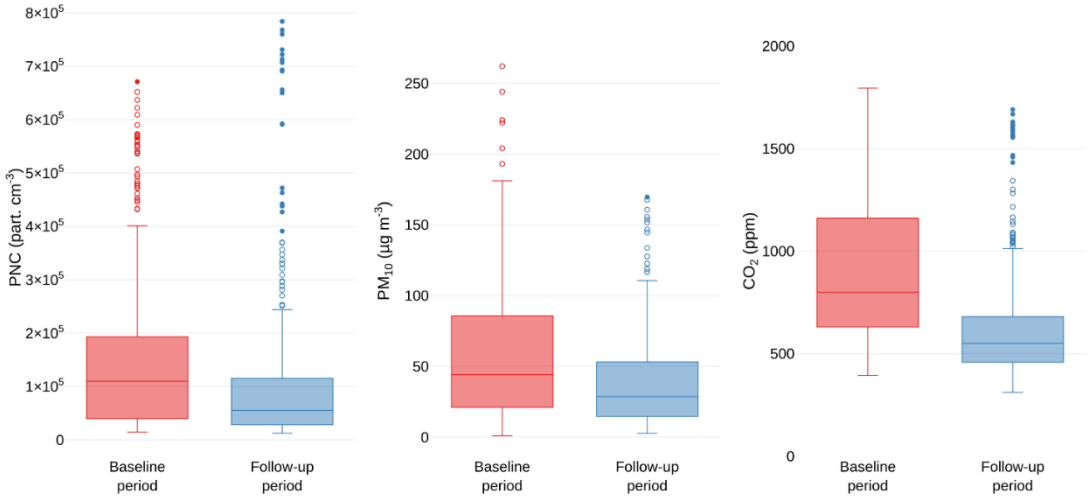

Figure 5-6. Statistics of the PNC (part. cm^{-3}), PM_{10} (µg m^{-3}) and CO_2 (ppm) (reported as box-plots) measured during cooking events for baseline and follow-up periods in one of the homes under investigation. PNC and PM_{10} data represent the difference between indoor values while cooking and simultaneous median outdoor values, whereas CO_2 data are reported as indoor values.

The effectiveness of the eco-feedback strategy, revealed from quantitative results, raised the question if the reduction obtained for airborne particle metrics can be somehow predicted measuring other parameters easily detectable through low-cost sensors (e.g., CO_2). In this case, reductions amongst the different metrics should be well correlated. Nonetheless, this is not the case since extremely weak correlations were detected amongst reductions of CO_2, PM_{10}, and PNC (Figure 5-7). Moreover, the information gathered from a specific metrics cannot be extended to other ones also for a further reason: the increase in concentrations detected for a specific metrics could not occur for other metrics. Indeed, during the 6-day experimental campaign 172 cooking events were performed and all of them caused an increase in terms of PNC (frequency of occurrence of 100%, Figure 5-7) confirming that such metrics is the one better related to combustion processes, whereas just 75% and 66% of the cooking events generated a visible increase in terms of CO_2 and PM_{10} concentration, respectively. This is likely due to the effect of influence parameters: as an example, type of food, cooking temperature, type of stove strongly influence the quantity and the size of the particle emitted and in some cases negligible emissions of super-micron particles occur [97], [292]–[294]. Similarly, CO_2 exhaled by the occupants can hide the contribution of the cooking-related CO_2 emissions [285]–[287]. When it comes to temperature and relative

humidity, increases (or decreases) were even less detectable, as an example, cooking events caused an increase in temperature only for 3% of the cases.

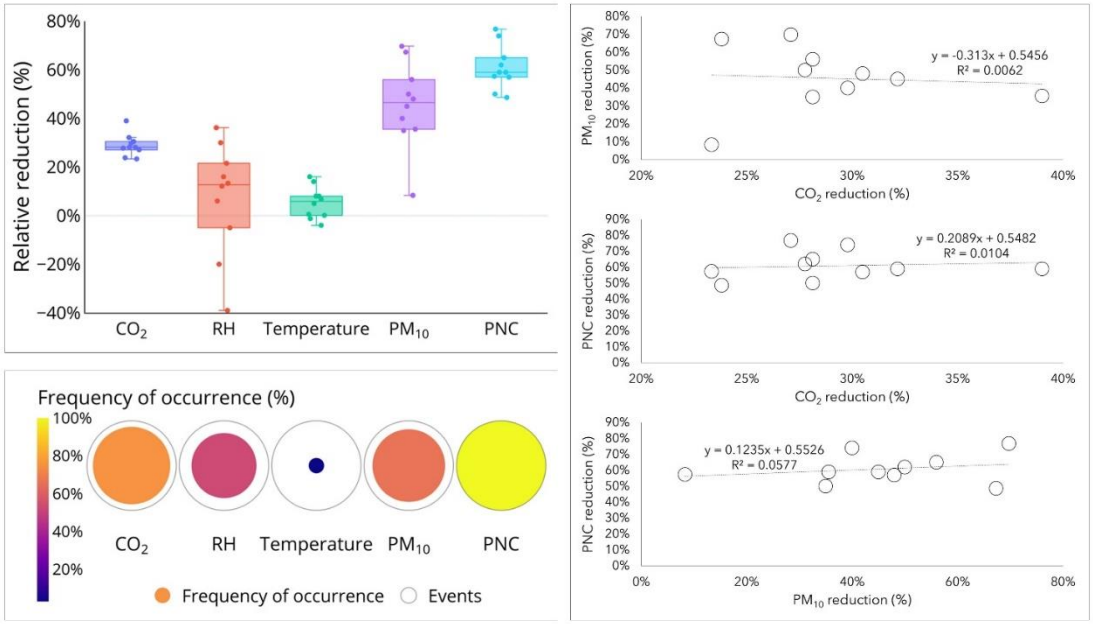

Figure 5-7. Relative reductions amongst median values measured during cooking activities performed within baseline and follow-up periods in the 10 homes as resulting from the quantitative analysis and correlations amongst reductions of the different metrics. Frequencies of occurrence of the increase for each parameter with respect to the number of cooking events are also graphed.

Results of the qualitative analysis

The effectiveness of the eco-feedback strategy was also confirmed by the results of the qualitative analysis; indeed, the information campaign produced an immediate change in habits, perceptions, and intentions at least during cooking activities, as summarized in Figure 5-8. Despite 90% of ten volunteer families in the first questionnaire survey reported that they had never looked for information on the IAQ in homes, they have found the information campaign useful (100%) and 90% of them would buy a device to measure IAQ parameters in their house. Moreover, to guarantee a proper air exchange of the house, before the information campaign, the volunteers consider preferable just adopting manual opening of windows (90%), whereas only 10% of the families selected both mechanical ventilation and manual airing. In contrast, after the campaign, 80% of the families would prefer adopting both manual opening of windows and mechanical ventilation. All these answers confirm a short-term change in IAQ perception.

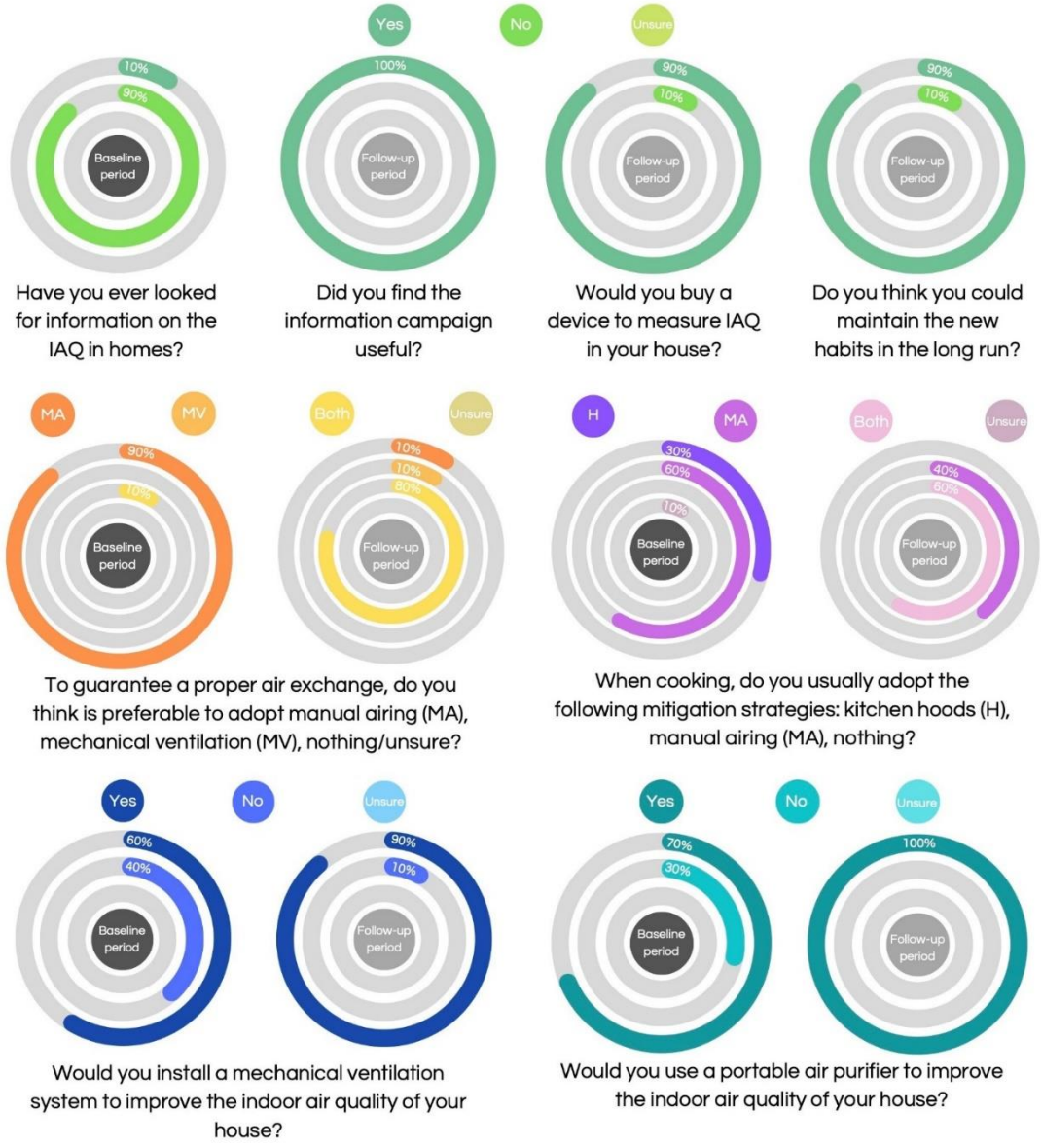

Figure 5-8. Change in perceptions, habits, and intentions of the IAQ of the ten families involved in the eco-feedback strategy.

A behavioral change also in terms of habits was recognized; indeed, in the baseline questionnaire survey, just 30% and 60% of the people reported that they usually used hoods and opened the windows while cooking, respectively, none of them adopted these two mitigation strategies simultaneously, and one family usually didn't apply any mitigation strategy. On the contrary, after the information campaign, all the families implemented mitigation strategies, in particular, 60% of

the families simultaneously performed manual airing and used kitchen hoods, whereas the remaining 40% performed only manual airing.

Finally, also the intentions referred to the IAQ problems improved: the percentage of families willing to install a mechanical ventilation or use an air purifier increased to 90% and 100%, respectively.

Once again, we point out that evaluation of the eco-feedback strategy effectiveness we conducted is a short-term evaluation, thus behavioral changes should be checked on the long-run. Nonetheless, from the answers we collected, the investigated families reported to be mostly inclined to maintain the new habits in the long run (90%).

Significance, applicability, and limitations

The quali-quantitative analysis has revealed that a simple eco-feedback strategy based on awareness-raising campaigns (i.e., trustworthy information campaign and experimental campaign) is able to increase the IAQ awareness of the occupants and reduce their exposure to different airborne particle metrics even during heating seasons (i.e., when the highest exposures are expected in homes). The performance of the eco-feedback strategy here adopted represents a short-term performance, since the comparison of qualitative and quantitative results amongst baseline and follow-up periods was performed within few days. This can be considered a limitation of the study, since the durability of the behavior-changing effect represents a critical aspects of eco-feedback approaches [295]. Nonetheless, a long-lasting effect of the eco-feedback would be extremely expensive and time demanding since measurement campaigns of several months (including different seasons) would have been performed. The use of cheap and easy-to-use IAQ monitors (e.g. in-home displays, low-cost sensors) continuously reporting the actual concentrations of selected pollutants [151], [296] could be a valuable support to consolidate occupants' habits and intentions aiming at improving the indoor air quality. Nonetheless, the use of in-home displays is quite straightforward for energy or water consumptions (also for non-expert people), indeed, scientific studies reported that occupants are able to understand information provided and to act accordingly [162], [163]. On the contrary, the measurement and interpretation of IAQ parameters is more complex since i) no threshold values are available for residential buildings (e.g., for PM_{10}, PNC and CO_2), ii) the concentrations are affected by several influence parameters (e.g., source, room volume, air exchange rate, etc.), iii) low-cost sensors are not currently available for all the pollutants and their metrological performances are questionable. The latter aspect is currently of great concern since low-cost sensors are more and more often used as an alternative for air quality

monitoring assessment also involving non-expert people (i.e. citizen science [297], [298]) and smart home applications ([120]). Nonetheless, despite CO_2 low-cost sensors are currently available and reliable for indoor monitoring, PM_{10} low-cost sensors present serious concerns in terms of calibration, accuracy and long-term variation problems [175], [299]–[301] and PNC low-cost sensors are barely not yet available [302]. If we add that PNC, PM_{10} and CO_2 concentration increases and relative reductions are poorly correlated (as we demonstrated), we can conclude that eco-feedback strategies willing to reduce the exposure to all the airborne particle metrics (including ultrafine particles) cannot yet properly supported by the interaction of the occupants with instruments or displays. This is the reason why, in this study, we did not force or suggest the occupants interacting with the instruments. Indeed, the instruments we adopted cannot be classified as low-cost sensors (the cost PM_{10} and PNC instruments is roughly 10 k€ each) thus they will not be routinely used unless than for research reasons. Moreover, although they are not low-cost sensors, their data quality assurance can be guaranteed only by expert people through the methodology described [278], [279], [303], [304].

The non-availability of low-cost sensors for eco-feedback purposes makes it hard to overcome a further limitation of the present study, i.e., the limited number of people involved in the evaluation of the eco-feedback strategies. Indeed, the present study just involved 10 volunteer families which were analyzed during the heating period: increasing the sample would require years even considering short-term assessments (i.e., roughly one week per home as in the present study). On the contrary, in research studies involving low-cost sensors and in-home displays (e.g. to increase the awareness on energy consumption) a larger sample (>100 homes) can be easily achieved [162], [176].

A further aspect that should be improved in future studies concerning the effect of the eco-feedback on the IAQ is the questionnaire design. In the present work we aimed at guaranteeing their validity and reliability adopting face-to-face interviews performed by researchers involved in the study. This approach can be here accepted since it represents the very first study where a quantitative evaluation of the eco-feedback effectiveness on IAQ is shown. Nonetheless, in future studies, sociologists should be involved also in order to get more in-depth information from the questionnaires and perform more detailed correlations amongst the eco-feedback results and the population characteristics.

We want to highlight that these limitations do not undermine the significance of the study since, for the very first time, it provided useful data to design IAQ eco-feedback strategies and assess how occupants' behavior influence their exposure to airborne particles.

5.4 Conclusions

The work aims at investigating the indoor air quality awareness of residential building occupants and a possible solution to increase it in order to reduce the exposure of people to different airborne particle metrics during the heating period.

To this end we i) investigated the IAQ awareness of 100 volunteer families through questionnaire surveys and ii) applied an eco-feedback strategy, based on both a trustworthy information campaign and an experimental campaign, to evaluate the possible short-term behavioral changes of the occupants (10 families) and their ability in reducing the concentration levels while airborne particle emitting sources (i.e., cooking) were in operation (quali-quantitative analysis).

The study allowed to quantify for the very first time the effectiveness of an eco-feedback strategy in terms of exposure to different airborne particle metrics (including particle number concentration) then addressing the abovementioned scientific questions raised from the analysis of the state-of-art:

i) are the occupants aware of their exposure to airborne particles in their homes?

- the investigated population is not properly aware of the IAQ in their homes and of their exposure to airborne particles; indeed, from the questionnaire survey it turned out a good correlation amongst the occupants' rating of indoor and outdoor air quality (86% of families simultaneously has a non-negative perception of indoor and outdoor air quality), thus suggesting that they perceive the indoor air quality mostly affected by the outdoor rather than possible indoor sources;

- the misperception of the IAQ also affects occupants' habits and intentions, in fact, they do not routinely use mitigation strategies while indoor sources are in operation, and, in case, their use is mainly governed by other reasons (i.e. reducing smells and relative humidity) than air quality (just 24% of the interviewed); moreover, they are poorly inclined to install *ad-hoc* engineering solutions such as mechanical ventilation systems or air purifiers;

ii) is it possible to make them aware through trustworthy information? and, in case, are they able to mitigate their exposure to indoor-generated airborne particles?

- the eco-feedback strategy adopted resulted successful both in terms of promoting behavioral changes of the occupants and reducing the concentration levels while airborne particle emitting sources (i.e., cooking) were in operation;

- in particular, the qualitative analysis demonstrated that IAQ-related perceptions, habits and intentions resulted improved after the information campaign, as an example all the families found the information campaign useful and, after the information campaign, 60% of the families simultaneously performed manual airing and used kitchen hoods while cooking;

iii) how their mitigation strategies affect the different airborne particle metrics?

- the exposure to airborne particle metrics while cooking events measured during the experimental campaign carried out after the information campaign (follow-up period) resulted lower than the baseline exposure; relative reductions of 47% (range of 8%-70%) and 59% (range of 49%-77%) were obtained for PM_{10} and PNC, respectively;

- such reductions were due to more frequent and longer manual airing and hood use as resulting from diaries filled out by the occupants; in fact, manual airing and hood use during the follow-up period increased to 64% and 44% of the entire duration of the cooking event, respectively (during the baseline periods they were used 17% and 41% of the cooking event duration, respectively);

- the relative reductions in terms of CO_2, PM_{10} and PNC resulted poorly correlated, moreover, despite PNC, cooking events do not always cause "detectable" increases in CO_2 and PM_{10} concentrations; thus, the exposure levels to airborne particles cannot be related to other parameters whose measurement could be performed through easy-to-use low-cost sensors (e.g., CO_2).

The outcomes of the study could be of great interest for scientists and air quality experts involved in indoor assessment, citizen science-based monitoring, and assessment of eco-feedback strategies, indeed, besides, showing the potential effect of an eco-feedback strategy on indoor air quality improvement, it also points out state-of-art criticalities that should be considered to properly designing eco-feedback campaigns and indoor airborne particle monitoring.

Chapter 6 - CASE STUDY 4:
RESPIRATORY PARTICLES EMISSION RATES FROM CHILDREN DURING SPEAKING

The number of respiratory particles emitted during different respiratory activities is one of the main parameters affecting the airborne transmission of respiratory pathogens. Information on respiratory particle emission rates is mostly available for adults (few studies have investigated adolescents and children) and generally involves a limited number of subjects.

In the present study we attempted to reduce this knowledge gap by conducting an extensive experimental campaign to measure the emission of respiratory particles of more than 400 children aged 6 to 12 years while they pronounced a phonetically balanced word list at two different voice intensity levels ("speaking" and "loudly speaking"). Respiratory particle concentrations, particle distributions, and exhaled air flow rates were measured to estimate the respiratory particle emission rate. Sound pressure levels were also simultaneously measured.

We found out that median respiratory particle emission rates for speaking and loudly speaking were 26 particles s^{-1} (range 7.1–93 particles s^{-1}) and 41 particles s^{-1} (range 10–146 particles s^{-1}), respectively. Children sex was significant for emission rates, with higher emission rates for males during both speaking and loudly speaking. No effect of age on the emission rates was identified.

Concerning particle size distributions, for both respiratory activities, a main mode at approximately 0.6 μm and a second minor mode at <2 μm were observed, and no differences were found between males and females. This information provides important input parameters in predictive models adopted to estimate the transmission risk of airborne pathogens in indoor spaces.

6.1 Aims of the work

In the present study, more than 400 children attending primary and secondary schools (aged 6 to 12) were involved in an experimental study aimed at providing emission rates of respiratory particles while speaking at two different intensity levels – "speaking" and "loudly speaking". To this purpose experimental apparatus and testing protocol were optimized and, indeed, respiratory

particle emission rates were obtained by directly measuring respiratory particle concentration and exhaled flow rate while subjects pronounced a phonetically balanced word list.

6.2 Materials and methods

To provide respiratory particle emission rates (i.e., respiratory particles emitted per unit time), two different tests were performed: a) measurement of the air flow velocity exhaled by children while speaking and loudly speaking (to estimate the exhaled air flow rate) and b) measurement of the respiratory particle concentration while speaking and loudly speaking. Tests were performed on more than 400 children aged 6 to 12 years attending primary and secondary schools in Cassino (FR), Central Italy. After the collected data were carefully examined, 371 measurements/children were considered valid for data post-processing. In particular, the data/children for whom instrument issues (e.g., missing data not recorded by the instruments) and/or test issues (children performing one of the tests improperly) occurred were excluded from the analysis. Details of the investigated population of children who provided valid measurements are provided in Figure 6-3.

Table 6-1. Details (sex and age) of the investigated population (only children whose data were considered valid).

Entire population		371
Sex	Male	49.9%
	Female	50.1%
Age (years)	6	11.1%
	7	11.3%
	8	14.8%
	9	10.2%
	10	9.4%
	11	27.5%
	12	15.6%

Air velocity and particle concentration measurement tests were performed while children read the phonetically balanced word list typically adopted for word recognition testing in Italian. The word list is as follows: "*papà, babbo, tetto, dado, cocco, lago, ciccio, Gigi, mamma, nonna, fifa, viva, sasso, rosa, sciocco, zia, zanzara, Lulù, ramarro, rana, giugno, luglio, strada, spruzzo, completo, taxi, cosmopolita, sardanapalo, Nabucodonosor, Afghanistan*".

6.2.1 Human subjects

The ethical committee of the University of Cassino and Southern Lazio approved this study; indeed, the research was performed in accordance with relevant guidelines and regulations of the committee. Informed consent from the parents of the recruited children was obtained prior to study participation.

6.2.2 Evaluation of the exhaled air flow rate

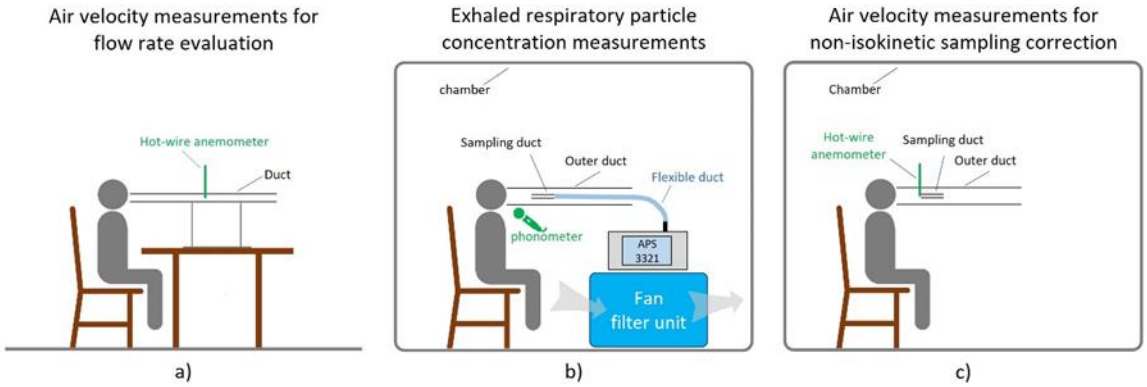

Figure 6-1. Experimental set up adopted to measure (a) air velocity to estimate the air flow rates, (b) respiratory particle concentrations and, (c) air velocity for non-isokinetic sampling correction while speaking and loudly speaking.

The velocity of the exhaled air while speaking at two different intensities (test a) was measured with a Testo 405i Smart Probe hot-wire anemometer (measurement range 0–30 m s^{-1}; resolution 0.01 m s^{-1}) recently calibrated by the manufacturer. The children were asked to read the word list twice consecutively at their normal intensity level (referred to as "speaking") and twice at a higher intensity level (referred to as "loudly speaking"). The children were not asked to speak at a specific sound pressure level but just to read the list at their own speaking and loudly speaking sound pressure level. During the test they had to speak as close as possible to the inlet of a duct (diameter 0.0465 m; length 1 m) as illustrated in Figure 6-1a; the air velocity sampling point was placed at the center of the section (i.e., maximum velocity) and at a distance of 40 cm from the inlet to guarantee fully developed flow in the duct. The air flow rates for speaking and loudly speaking were evaluated by multiplying the average velocity at the center of the duct during the test by the cross-sectional area of the duct and by the average-to-maximum velocity correction factor (which is 0.5 because the flow through the duct was laminar).

6.2.3 Measurement of the respiratory particle concentration

The respiratory particle concentration exhaled by children while speaking (test b) was measured by an aerodynamic particle sizer spectrometer (APS 3321, TSI Inc.) which measures particle number distribution and total concentration in the 0.5–20 μm diameter range, with a sampling flow rate of 5 L min^{-1}, on the basis of a time-of-flight technique. The APS was recently calibrated by the manufacturer to guarantee the quality of the data. To avoid miscounting due to the presence of environmental airborne particles, the test was conducted in a 1.80 m × 1.20 m × 2.20 m plexiglass chamber with a fan filter unit (FFU) to reduce the background particle concentration level. The FFU is a 55 cm × 74 cm × 60 cm parallel pipe equipped with a HEPA H14 filter plus an F7 pre-filtration stage and characterized by an adjustable flow rate (up to 850 m^3 h^{-1}). To guarantee accurate particle sampling, the apparatus shown in Figure 6-3b was set up. In particular, children were asked to speak as close as possible to a 15-cm diameter duct (the outer duct). A further sampling duct was placed inside the outer duct at 10 cm from the outer duct inlet section and connected to the APS through a 40-cm flexible duct. The sampling duct was printed by a 3D printer using a biodegradable thermoplastic aliphatic polyester. The 4-cm diameter duct was designed to carry out isokinetic sampling; indeed, the air velocity resulting from the APS flow rate (about 0.07 m s^{-1}) was the average air velocity typically produced by children while speaking as determined from preliminary tests previously performed on 10 children.

The following procedure was adopted for the test: i) the FFU was run at the maximum flow rate for 3 min to reduce the airborne particle background concentration in the chamber; ii) the FFU was switched off and a 30-s background concentration measurement (with a 1-s sampling frequency) was carried out; iii) particle concentrations and distributions were measured with a 1-s sampling frequency while the child being tested read the word list twice consecutively at his/her normal intensity level (speaking); iv) the FFU was run at the maximum flow rate for 3 min to reduce the airborne particle background concentration in the chamber; v) the FFU was switched off and a 30-s background concentration measurement (with a 1-s sampling frequency) was carried out; vi) particle concentrations and distributions were measured with a 1-s sampling frequency while the child read the word list twice at a higher intensity level (loudly speaking). The children were asked to speak and loudly speak with the same sound pressure level as during test a. The voice intensity level during the tests was also measured with a Delta Ohm HD2110 (Geass) phonometer placed 10 cm from the child's mouth. Average intensity levels while speaking and loudly speaking were

obtained to normalize to the average background intensity level inside the chamber; indeed, the phonometer was switched on during the entire procedure (steps i-to-vi).

The respiratory particle emission rates for speaking and loudly speaking were evaluated by multiplying the estimated air flow rates by the respiratory particle concentrations. The estimated air flow rates were corrected for possible non-isokinetic sampling as described below on the basis of actual air velocity measurements. The respiratory particle concentrations while speaking (step iii of the measurement procedure) and loudly speaking (step iv of the measurement procedure) were provided as average values and were normalized to the corresponding background concentration measured during steps ii and v of the measurement procedure, respectively. The resulting average particle concentrations were corrected for particle losses as described below.

6.2.4 Correction for non-isokinetic sampling and particle losses

As mentioned above, isokinetic sampling is a critical aspect to be considered when sampling air flow in ducts. This is why we designed a sampling duct with a cross-sectional area that could guarantee nominal isokinetic sampling. Nonetheless, the air velocity while speaking can vary significantly amongst children, so corrections for non-isokinetic sampling need to be considered. This is why we also measured the air velocity while speaking at the inlet section of the sampling duct for each child, and for both speaking and loudly speaking while using the hot-wire anemometer as depicted in Figure 6-3c. In particular, air velocity measurements were performed while the child being tested read the word list twice consecutively. The average velocities resulting from the test were adopted to perform the isokinetic correction. Thus, the correction factor of the particle concentration due to possible non-isokinetic sampling was evaluated according to the formulation proposed by Xu [305], which is a function of the difference between the actual speaking velocity and the sampling velocity and the Stokes number. Every measured concentration was corrected on the basis of the measured air velocity for both speaking and loudly speaking; corrections applied ranged between 0.8% and 4.0%.

Sampling and particle losses during transport through the inlet system were considered and corrected through a recently developed particle loss calculator multifunctional software tool [306]. The tool takes into account the different particle loss mechanisms (diffusion, sedimentation, turbulent inertial deposition, inertial deposition due to bend and contraction) occurring in the entire sampling line. The corrections calculated (and applied) were all <1%.

6.2.5 Statistical analysis

All the data (sound pressure level, air velocity, respiratory particle concentrations, emission rates) were tested through a preliminary normality test (Shapiro-Wilk test with a 95% confidence level; i.e., *p*-value <0.05) to check if they followed a Gaussian distribution. Sound pressure level data followed a Gaussian distribution; therefore statistical analyses were carried out using analysis of variance (ANOVA) and a post-hoc Tukey–Kramer test [307] with a 95% confidence level (i.e., *p*-value <0.05). Other parameters that did not follow a Gaussian distribution were analyzed using a non-parametric test and a further post-hoc test (Kruskal-Wallis test) [291]**,** adopting a 95% confidence level (i.e., *p*-value <0.05).

6.3 Results and discussions

6.3.1 Air flow rate and sound pressure level

The exhaled air flow rates and sound pressure levels produced by children while speaking and loudly speaking are presented in Table 6-2 for females and males. The median exhaled air flow rate values for speaking activities were 0.28 and 0.31 $m^3 h^{-1}$ for females and males, respectively, and were not significantly different. Similarly, there were no significant differences between females and males in the exhaled air flow rate values for loudly speaking (median values of 0.31 and 0.34 $m^3 h^{-1}$). Median exhaled air flow rates were also the same for speaking and loudly speaking for females and males. In contrast, a slight age effect was recognized: older children (11 and 12 years old) recorded statistically higher flow rates than younger children (6 years old) as reported in Table 6-2. Sound pressure levels were significantly different between females and males for both speaking (median values 79.4 and 80.9 dB, respectively) and loudly speaking (85.5 and 88.1 dB, respectively). Moreover, sound pressure levels were statistically different (for both females and males) between speaking and loudly speaking. No age effect was detected as the sound pressure levels were the same for children in all age groups (for speaking and loudly speaking separately).

Table 6-2. Median (and 5^{th}–95^{th} percentile) values of sound pressure level, exhaled flow rate, particle concentration, and particle emission rate while speaking and loudly speaking for the entire investigated population and as a function of sex and age.

Population	**Sound pressure level (dB)**		**Particle concentration (particles cm^{-3})**		**Emission rate (particles s^{-1})**	
	Speaking	Loudly speaking	Speaking	Loudly speaking	Speaking	Loudly speaking

Entire population		80.0 (73.1-87.4) *	86.3 (79.5-95.1) *	0.30 (0.11-0.94) *	0.43 (0.15-1.37) *	26 (7.1-93) *	41 (10-146) *
Sex	Female	79.4 (72.5-86.3) *+	85.5 (79.4-92.8) *●	0.29 (0.10-0.72) Δ	0.37 (0.15-1.14) +	23 (7.0-62) *+	33 (8.9-98) *●
	Male	80.9 (74.3-88.3) Δ+	88.1 (79.6-95.8) Δ●	0.33 (0.11-1.09)*Δ	0.53 (0.18-1.40) *+	28 (7.7-105) Δ+	51 (13-162)Δ●
Age	6	78.9 (72.4-87.3)	84.6 (77.0-91.0)	0.32 (0.16-1.92)	0.56 (0.24-2.53) *Δ	24 (7.1-165)	43 (11-164)
	7	81.6 (76.4-87.3)	86.6 (81.3-95.4)	0.37 (0.12-0.90)	0.61 (0.20-1.58)	23 (8.8-106)	48 (12-148)
	8	81.1 (73.4-89.0)	87.4 (81.4-94.1)	0.37 (0.14-0.83) *	0.60 (0.18-1.41) Δ	30 (12-82)	54 (14-129)
	9	79.6 (75.1-88.6)	86.3 (81.0-94.8)	0.26 (0.11-0.92)	0.40 (0.18-1.02)	22 (6.7-77)	33 (12 -126)
	10	79.2 (72.9-88.2)	84.8 (78.7-95.4)	0.27 (0.11-0.69)	0.53 (0.13-1.35)	22 (5.8-71)	41 (7.3-148)
	11	79.7 (73.2-86.0)	86.8 (79.9-96.0)	0.29 (0.10-0.73)	0.39 (0.15-1.37)	28 (7.5-86)	41 (11-154)
	12	80.0 (74.0-86.3)	85.8 (79.1-94.6)	0.24 (0.10-0.68) *	0.32 (0.16-0.97) *	20 (7.7-81)	31 (13-112)

6.3.2 Respiratory particle concentrations and size distributions

The respiratory particle concentrations (normalized with respect to the background concentrations) as a function of sex and speaking activity are shown in Table 6-1. Values for females and males were significantly different for loudly speaking (median values 0.37 and 0.53 particles cm^{-3}, respectively) but not for speaking (median values 0.29 and 0.33 particles cm^{-3}, respectively). The respiratory particle concentrations were statistically different (for both females and males) between speaking and loudly speaking (please see the "entire population" data in Table 6-1). Such differences as a function of the speaking activity were also recognized in previous studies [200], [201], [206], [207]. However, an accurate comparison of the measured concentrations between this

study and previous studies cannot be easily achieved because of the different methodologies applied in the experimental studies in terms of experimental apparatus, respiratory activity, and type of volunteers. Nonetheless, a rough comparison with previous studies reveals that the particle concentrations we measured for children were within the ranges measured for similar speaking activities performed by adolescents and adults [200], [201], [204]–[206], [209] as shown in Table 6-2.

Table 6-3. Comparison of respiratory particle concentrations and/or emission rates with previous studies (for speaking activities only).

Author	**Respiratory activity**	**Participants**	**Particle concentration or emission rate**
This study	Speaking, i.e., reading a text at normal and higher intensity level	371 children	Concentrations: • Speaking = 0.11-0.94 particles cm^{-3} (median 0.30 particles cm^{-3}) • Loudly speaking = 0.15-1.37 particles cm^{-3} (0.43 particles cm^{-3}) Emission rates: • Speaking = 7.1-92.5 particles s^{-1} (median 25.6 particles s^{-1}) • Loudly speaking = 10.4-146.2 particles s^{-1} (median 40.6 particles s^{-1})
Mürbe et al. [202]	Speaking, i.e., reading a text	8 adolescents	Emission rate: 16-267 particles s^{-1} (median 80 particles s^{-1})
Ahmed et al. [205]	Phonation (specific frequencies and different vocal intensity levels)	40 adults	Emission rate: 2.1-22 particles s^{-1} (median 9.1 particles s^{-1})

Bagheri et al. [207]	Speaking, i.e., reading a text at normal and higher intensity level	132 subjects including 21 children aged 5-9 years old and 24 children aged 10-14 years	Concentrations: • Speaking 5-9 yrs = geometric mean±deviation 0.041±1.654 particles cm^{-3} • Speaking 10-14 yrs = geometric mean±deviation 0.077±2.324 particles cm^{-3} • Loudly speaking 5-9 yrs = geometric mean±deviation 0.072±1.859 particles cm^{-3} • Loudly speaking 10-14 yrs = geometric mean±deviation 0.120±2.187 particles cm^{-3} Concentration increases with age (e.g., adults)
Asadi et al. [206]	Speaking, i.e., reading a text	48 adults	Concentrations: 0.06-3 particles cm^{-3} Emission rates: 1-50 particles s^{-1}
Archer et al. [209]	Speaking at a controlled sound pressure level	Adolescents aged 12-14 years and adults aged19-72 years	Concentrations: • Adolescents = 0.10 – 0.36 particles cm^{-3} (median 0.21 particles cm^{-3}) • Adults = 0.02-1.70 particles cm^{-3} (median 0.18 particles cm^{-3}) Emission rates: • Adolescents = 19.7-74.5 particles s^{-1} (median 40.7 particles s^{-1}) • Adults = 11.4-306 particles s^{-1} (median 60.1 particles s^{-1})

Fleischer et al. [203]	Speaking, i.e., reading a text	15 children aged 8-10 years	Emission rates: 8-86 particles s^{-1} (median 24 particles s^{-1})
Morawska et al. [201]	Speaking, i.e., voiced counting	15 adults	Concentrations: median 0.3 particles cm^{-3}
Gregson et al. [204]	Speaking at different volumes	25 adults	Concentrations: 0.016-3.7 particles cm^{-3} (median, at 70-80 dB, 0.22 particles cm^{-3})

These results also showed a slight age effect on the respiratory particle concentrations. Indeed, 12-year-old children had significantly lower concentrations than 8-year-old children for speaking, and also 6- and 8-year-old children for loudly speaking (Table 6-1). This is a novel finding that should be explored in future research because the few previous studies involving children [203], [207] reported a respiratory particle concentration increase as a function of age, although this was not adequately justified. However, these studies involved a small number of volunteers that limited statistical comparisons. Tavares et al. (2012) reported that the efficiency of the respiratory mechanism during phonation in children aged >10 years was different from that of children aged <10 years [308]. In addition, children aged 6–8 years typically lose their central incisors [309], reducing the physical barrier for respiratory particle emission. Nonetheless, the larynx and pulmonary system grow and mature through puberty, and this may also affect aerosol formation [310], [311]. Thus, further studies should be carried out to evaluate if these or other phenomena actually affect respiratory particle emission.

Figure 6-1 shows the median (and corresponding 5th–95th percentile range) respiratory particle size distributions measured for the entire population investigated for speaking and loudly speaking activities. Both distributions present a main mode at approximately 0.6 μm and a second minor mode at <2 μm. Similar distributions were obtained in previous studies, independent of frequency and loudness [202], [205]–[207]. In particular, the main mode is characteristic of the respiratory particles generated in the bronchioles (and it is present also in breathing activities), whereas the second mode is generally associated with the generation occurring in the larynx and pharynx which are more typical of speaking and singing activities [207]. In Figure 6-1, median distributions for females and males are also reported. These distributions were similar for the activities of boys and

girls; thus, sex was not a factor affecting particle generation. In contrast, a slight age effect was observed in younger children, in whom the second mode (at <2 μm) was more pronounced than in older children. This is clearly detectable in Figure 6-1 where, for example, median distributions for 6-year-old and 12-year-old children (those characterized by statistically different concentrations) are also reported. This aspect is worthy of further investigation as it was not previously discovered in the few papers reporting particle size distributions for children. In fact, an increase of the second mode was previously shown only in adults as a function of sound pressure levels (speaking at higher intensity or singing seems to increase respiratory particle generation in the larynx) [204], [206].

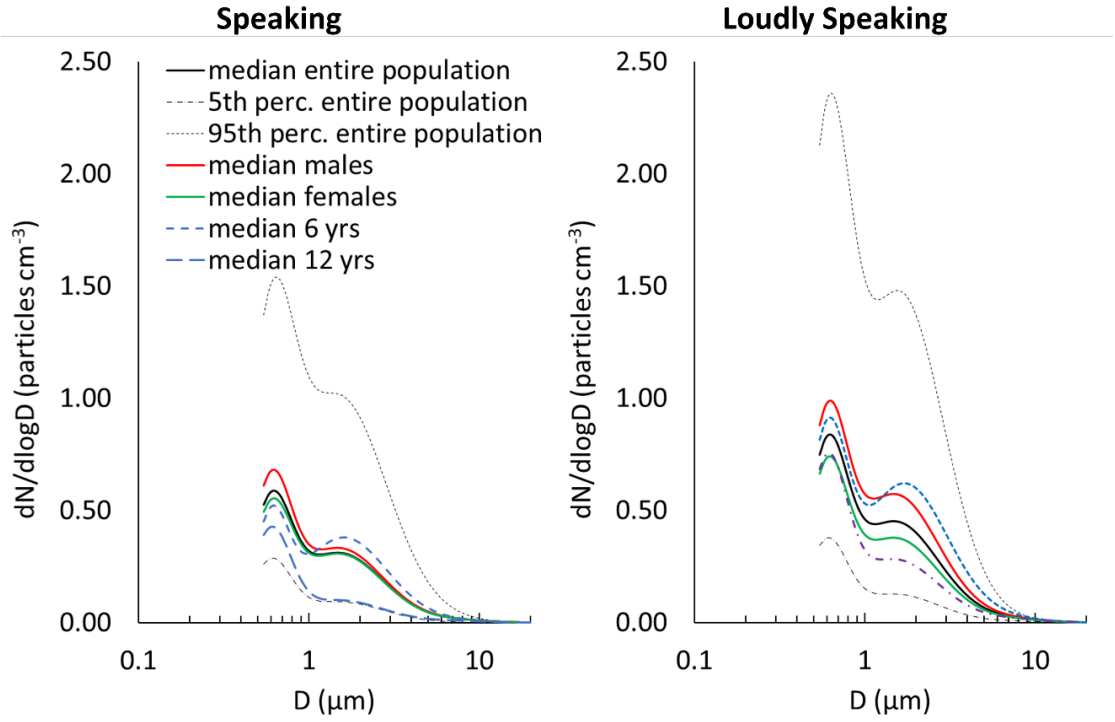

Figure 6-2. Median respiratory particle size distributions for speaking (left) and loudly speaking (right) activities for the entire population, males, females, 6-year-old children, and 12-year-old children. 5th and 95th percentile distributions for the entire population are also shown.

6.3.3 Emission rates

Table 6-1 shows the respiratory particle emission rates for speaking and loudly speaking tests. The emission rates for speaking and loudly speaking for the entire investigated population were significantly different, with median values of 26 and 41 particles s^{-1}, respectively. The emission rates span a wide range, with 5th–95th percentile ranges of 7.1–93 and 10–146 particles s^{-1} for speaking and loudly speaking, respectively. A wide range of respiratory particle emissions was also reported

in previous papers for adults and adolescents [202], [205], [206]. In Table 6-2, the existing data on respiratory particle concentrations and emission rates are summarized and compared with those obtained by this study. The emission rates for children for the present study were slightly lower or comparable to those obtained for children and adolescents by Fleischer et al. [203] and Mürbe et al. [202], respectively. Fleischer et al. [203] also reported a higher emission rate for adults, and similar behavior was reported by Bagheri et al. [207] in terms of particle concentrations. These two studies are of great relevance because they compare (adopting the same methodology) adults with children/adolescents. Other studies reported lower values for adults, but again, a proper comparison cannot really be performed due to the methodological differences amongst the studies. For example, Ahmed et al. [205] found a median emission rate amongst adults of 9.1 particles s^{-1}, but they performed a different phonation exercise, which may not be comparable with speaking activities.

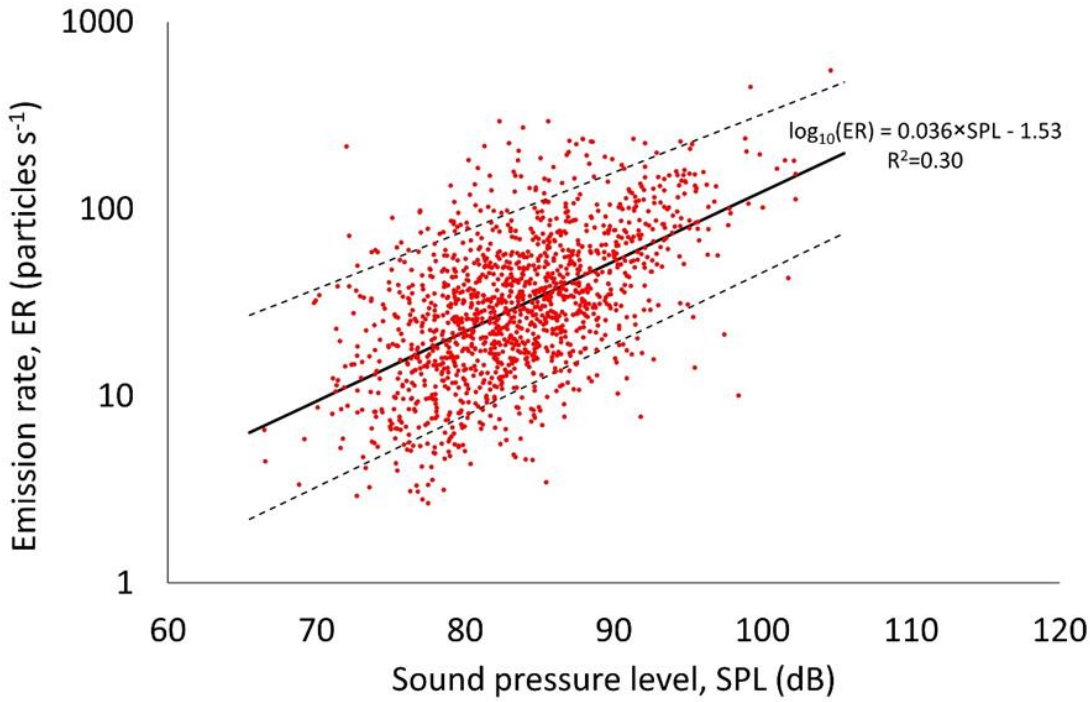

Figure 6-3. Respiratory particle emission rate (ER) as a function of the sound pressure level (SPL) including both speaking and loudly speaking. The black solid line represents the linear regression; the black dashed lines represent the 5th–95th percentile range.

Differences in emission rates between males and females are also reported in Table 6-1. In particular, males had significantly higher emissions than females both while speaking (median values of 28 and 23 part s^{-1}, respectively) and loudly speaking (51 and 33 part s^{-1}, respectively),

consistent with the differences in particle concentrations (Table 6-1). In contrast, differences in emission rates due to the age of the child (Table 6-3) were not significant for either speaking or loudly speaking activities, even for age groups with different particle concentrations (e.g., 6-year-olds vs 12-year-olds). This result is likely due to the balancing of two opposite effects: the slight increase in the flow rate as a function of age (older children recorded statistically higher flow rates than younger children, Table 6-1) and the slight reduction in respiratory particle concentration with age (older children recorded statistically lower particle concentrations than younger children, Table 6-1). These emission characteristics clearly highlight an effect of the vocal loudness on the concentrations and emission rates. To quantify the vocal loudness effect, respiratory particle emission rates (ERs) are plotted against the sound pressure levels in Figure 6-2. Here, the results for the entire population and both the speaking activities are plotted together. Figure 6-2 clearly shows an increase in the emission rates with the vocal loudness, which was also reported in previous studies [202], [206], [207]. In particular, an increase of 0.036 units of $\log_{10}(ER)$ (R^2=0.30) was found for a unit increase of the sound pressure level. Such an increase was slightly lower than that detected by Mürbe et al. [202] for adolescents and by Archer et al. [209] for a population mostly composed of adults (0.05 units of $\log_{10}(ER)$).

6.4 Conclusions

In the present study the emission of respiratory particles of more than 400 children aged 6 to 12 years while they pronounced a phonetically balanced word list at two different voice intensity levels ("speaking" and "loudly speaking") was measured.

The study allowed to find the following results: i) the median exhaled air flow rate values for speaking activities were 0.28 and 0.31 $m^3\ h^{-1}$ for females and males, respectively, and were not significantly different; ii) sound pressure levels were significantly different between females and males for both speaking (median values 79.4 and 80.9 dB, respectively) and loudly speaking (85.5 and 88.1 dB, respectively; iii) particle concentrations values for females and males were significantly different for loudly speaking (median values 0.37 and 0.53 particles cm^{-3}, respectively) but not for speaking (median values 0.29 and 0.33 particles cm^{-3}, respectively); iv) particle size distributions, for both respiratory activities, present a main mode at approximately 0.6 μm and a second minor mode at <2 μm, and no differences were found between males and females; v) the emission rates for speaking and loudly speaking for the entire investigated population were significantly different,

with median values of 26 (range 7.1–93 particles s^{-1}) and 41 particles s^{-1} (range 10–146 particles s^{-1}), respectively.

The findings of this study are of great significance as they could be applied to existing models to provide predictive estimates of the risk of infection in indoor environments and/or in close-proximity configurations [185], [186], [192], [193]. Indeed, such models are strongly dependent on the viral emission of the infected subject which is, in turn, influenced by the viral load carried by the respiratory particles (that can be obtained from PCR tests) and by the number of emitted particles. Thus, these findings are an important input for an effective simulation of the viral emission of children.

CONCLUSIONS

Air quality and public health in indoor environments represent major modern-day challenges of technical and scientific communities involved in designing and managing built environments where people is highly exposed to airborne and respiratory particle sources. Airborne and respiratory particle dynamics (from their emission to risk of exposed people) have been partly addressed by the scientific community, but some missing aspects need to be deepened. The thesis here presented try to provide new knowledge related to airborne and respiratory particles, in terms of *emission*, *risk* and *eco-feedback* strategy, by performing advanced experimental analyses and proving useful approaches for risk estimates. The main findings that can be drawn highlight that:

- The size-resolved chemical composition related to particle emission due to combustion of incenses, candles and mosquito-coils reveal a preponderance of chemical compounds (e.g., heavy metals and PAHs) in the sub-micrometric particle range, responsible of the most impactful health effects. Among the sources under investigation, mosquito coils present carcinogenic Group 1 with a relative distribution mode below 1 μm and the size fraction is comparable with those found in biomass burning studies. The source emission data here reported allows the applicability of health risk models because the literature review showed a lack of data; therefore, this study trying to fill this gap of knowledge.
- Confirming the previous findings, the predictive assessments of the "risk emitted" performed for different sources, is dominated by the sub-micron particles and can be extremely high for different (very common) sources, such as cooking activities. The approach allows to perform estimates of the lung cancer risk for different indoor exposure scenarios as a function of the specific source, room volume, ventilation rate, and (possible) mitigation solutions. The typical ventilation rates achievable in residential environments do not significantly reduce the risk, thus other mitigation solutions are needed; as an example, the employment of hoods in the indoor environment here considered has resulted in a 100-fold reduction of the risk due to cooking activities, even more by using it simultaneously with a purifier.

- Acknowledged that the exposure to indoor sources (especially cooking activities) are impactful for human health, the criticality is that people are not properly aware of the IAQ in their homes. Indeed, 86% of families simultaneously has a non-negative perception of indoor and outdoor air quality, thus suggesting that they perceive the indoor air quality mostly affected by the outdoor rather than possible indoor sources. The misperception of the IAQ also affects habits and intentions, in fact, occupants do not routinely use mitigation strategies while indoor sources are in operation, and, in case, their use is mainly governed by other reasons (i.e. reducing smells and relative humidity) than air quality (just 24% of the interviewed); moreover, they are poorly inclined to install ad-hoc engineering solutions such as mechanical ventilation systems or air purifiers. Nevertheless, a trustworthy information resulted successful both in terms of promoting behavioral changes of the occupants and reducing the concentration levels while airborne particle emitting sources (i.e., cooking) were in operation. Indeed, more than half (60%) of the families simultaneously performed manual airing and used kitchen hoods while cooking and relative reductions were obtained for PM_{10} and PNC concentration levels, equal to 47% (range of 8%-70%) and 59% (range of 49%-77%), respectively. It is important to highlight that the non-correlation of reduction between CO_2, PM_{10} and PNC doesn't allow the measurement of the exposure levels to airborne particles through easy-to-use low-cost sensors (e.g., CO_2).
- From a management perspective of indoor environments and risk of infection due to other types of sources (e.g., respiratory particles), the particle concentrations values measured among 400 children (6 - 12 years old) for females and males were significantly different for loudly speaking but not for speaking, both for males/females, whose median values equal to 0.37/0.53 particles cm^{-3} 0.29 and 0.33 particles cm^{-3}, respectively. Particle size distributions, for both respiratory activities, present a main mode at approximately 0.6 μm and a second minor mode at <2 μm, and no differences were found between males and females were observed; the emission rates for speaking and loudly speaking for the entire investigated population were significantly different, with median values of 26 (range 7.1–93 particles s^{-1}) and 41 particles s^{-1} (range 10–146 particles s^{-1}), respectively. The findings of this study are of great significance as they could be applied to existing models to provide predictive estimates of the risk of infection in indoor environments and/or in close-proximity configurations. Indeed, such models are strongly dependent on the viral emission of the infected subject which is, in turn, influenced by the viral load carried by the respiratory particles (that can be obtained from PCR tests) and by the number of emitted particles.

It is hoped that the research results reported in this thesis will be helpful for IAQ experts and could be a driving force to raise awareness about the issues that characterize indoor environments.

BIBLIOGRAPHY

[1] C. Anastasio Martin, S. T., «Atmospheric nanoparticles», in *Nanoparticles and the Environment*, vol. 44, Washington D.C.: Mineralogical Society of America, 2001, pp. 293–349.

[2] P. Kulkarni Baron, P. A. ,. Willeke, K., *Aerosol measurement: principles, techniques, and applications (3rd edition)*. 2011.

[3] W. Li e L. Shao, «Transmission electron microscopy study of aerosol particles from the brown hazes in northern China», *J. Geophys. Res. Atmospheres*, vol. 114, fasc. D9, 2009.

[4] J. H. Seinfeld e S. N. Pandis, *Atmospheric chemistry and physics: from air pollution to climate change*. John Wiley & Sons, 2016.

[5] M. Koçak, N. Mihalopoulos, e N. Kubilay, «Contributions of natural sources to high PM10 and PM2. 5 events in the eastern Mediterranean», *Atmos. Environ.*, vol. 41, fasc. 18, pp. 3806–3818, 2007.

[6] M. Millán-Martínez, D. Sánchez-Rodas, A. M. S. de la Campa, e J. de la Rosa, «Contribution of anthropogenic and natural sources in PM10 during North African dust events in Southern Europe», *Environ. Pollut.*, vol. 290, p. 118065, 2021.

[7] B. Brunekreef, «Session 2: What properties of particulate matter are responsible for health effects?», *Inhal. Toxicol.*, vol. 12, fasc. SUPPL. 1, Art. fasc. SUPPL. 1, 2000.

[8] E. Vo, M. Horvatin, M. Bergman, B. Wu, e Z. Zhuang, «A technique to measure respirator protection factors against aerosol particles in simulated workplace settings using portable instruments», *J. Occup. Environ. Hyg.*, vol. 17, fasc. 5, pp. 231–242, 2020.

[9] R. Gunn, «The statistical electrification of aerosols by ionic diffusion», *J. Colloid Sci.*, vol. 10, fasc. 1, pp. 107–119, 1955.

[10] N. A. Fuchs, «On the stationary charge distribution on aerosol particles in a bipolar ionic atmosphere», *Geofis. Pura E Appl.*, vol. 56, pp. 185–193, 1963.

[11] W. A. Hoppel, «Ion-aerosol attachment coefficients, ion depletion, and charge distribution on aerosols», *J. Geophys. Res.*, vol. 90, fasc. D4, Art. fasc. D4, 1985.

[12] W. A. Hoppel e G. M. Frick, «The nonequilibrium character of the aerosol charge distributions produced by neutralizes», *Aerosol Sci. Technol.*, vol. 12, fasc. 3, pp. 471–496, 1990.

[13] A. Wiedensohler, «An approximation of the bipolar charge distribution for particles in the submicron size range», *J. Aerosol Sci.*, vol. 19, pp. 387–389, 1988.

[14] S. Mertes, F. Schroder, e A. Wiedensohler, «The particle detection efficiency curve of the TSI-3010 CPC as a function of the temperature difference between saturator and condenser», *Aerosol Sci. Technol.*, vol. 23, fasc. 2, Art. fasc. 2, 1995.

[15] M. R. Stolzenburg e P. H. McMurry, «An ultrafine aerosol condensation nucleus counter», *Aerosol Sci. Technol.*, vol. 14, fasc. 1, Art. fasc. 1, 1991.

[16] D. F. Banse, K. Esfeld, M. Hermann, B. Sierau, e A. Wiedensohler, «Particle counting efficiency of the TSI CPC 3762 for different operating parameters», *J. Aerosol Sci.*, vol. 32, fasc. 1, Art. fasc. 1, 2001.

[17] W. Liu, S. L. Kaufman, B. L. Osmondson, G. J. Sem, F. R. Quant, e D. R. Oberreit, «Water-based condensation particle counters for environmental monitoring of ultrafine particles», *J. Air Waste Manag. Assoc.*, vol. 56, fasc. 4, Art. fasc. 4, 2006.
[18] M. Hermann *et al.*, «Particle counting efficiencies of new TSI condensation particle counters», *J. Aerosol Sci.*, vol. 38, fasc. 6, Art. fasc. 6, 2007.
[19] P. R. Bevington, D. K. Robinson, J. M. Blair, A. J. Mallinckrodt, e S. McKay, «Data reduction and error analysis for the physical sciences», *Comput. Phys.*, vol. 7, fasc. 4, pp. 415–416, 1993.
[20] E. O. Knutson e K. T. Whitby, «Aerosol classification by electric mobility: apparatus, theory, and applications», *J. Aerosol Sci.*, vol. 6, fasc. 6, Art. fasc. 6, 1975.
[21] J. K. Agarwal e G. J. Sem, «Continuous flow, single-particle-counting condensation nucleus counter», *J. Aerosol Sci.*, vol. 11, fasc. 4, Art. fasc. 4, 1980, doi: 10.1016/0021-8502(80)90042-7.
[22] S. C. Wang e R. C. Flagan, «Scanning electrical mobility spectrometer», *Aerosol Sci. Technol.*, vol. 13, fasc. 2, Art. fasc. 2, 1990.
[23] Y. S. Cheng, «Aerosol deposition in the extrathoracic region», *Aerosol Sci. Technol.*, vol. 37, fasc. 8, Art. fasc. 8, 2003.
[24] Y. S. Cheng, Y. Zhou, e B. T. Chen, «Particle deposition in a cast of human oral airways», *Aerosol Sci. Technol.*, vol. 31, fasc. 4, Art. fasc. 4, 1999.
[25] M. Fierz, C. Houle, P. Steigmeier, e H. Burtscher, «Design, Calibration, and Field Performance of a Miniature Diffusion Size Classifier», *Aerosol Sci. Technol.*, vol. 45, fasc. 1, Art. fasc. 1, gen. 2011, doi: 10.1080/02786826.2010.516283.
[26] M. Fierz, H. Burtscher, P. Steigmeier, e M. Kasper, «Field Measurement of Particle Size and Number Concentration with the Diffusion Size Classifier (Disc)», SAE International, 2008. doi: 10.4271/2008-01-1179.
[27] L.-J. S. Liu, J. C. Slaughter, e T. V. Larson, «Comparison of light scattering devices and impactors for particulate measurements in indoor, outdoor, and personal environments», *Environ. Sci. Technol.*, vol. 36, fasc. 13, pp. 2977–2986, 2002.
[28] H.-S. Kwon, M. H. Ryu, e C. Carlsten, «Ultrafine particles: unique physicochemical properties relevant to health and disease», *Exp. Mol. Med.*, vol. 52, fasc. 3, pp. 318–328, 2020.
[29] S. Lin *et al.*, «Particle surface area, ultrafine particle number concentration, and cardiovascular hospitalizations», *Environ. Pollut.*, vol. 310, p. 119795, ott. 2022, doi: 10.1016/j.envpol.2022.119795.
[30] T. M. Sager e V. Castranova, «Surface area of particle administered versus mass in determining the pulmonary toxicity of ultrafine and fine carbon black: comparison to ultrafine titanium dioxide», *Part. Fibre Toxicol.*, vol. 6, pp. 15–15, 2009, doi: 10.1186/1743-8977-6-15.
[31] O. Schmid e T. Stoeger, «Surface area is the biologically most effective dose metric for acute nanoparticle toxicity in the lung», *Inhaled Part. Dosim.*, vol. 99, pp. 133–143, set. 2016, doi: 10.1016/j.jaerosci.2015.12.006.
[32] A. Jiries, «Vehicular contamination of dust in Amman, Jordan», *Environmentalist*, vol. 23, pp. 205–210, 2003.
[33] S. Kumari, M. K. Jain, e S. P. Elumalai, «Assessment of Pollution and Health Risks of Heavy Metals in Particulate Matter and Road Dust Along the Road Network of Dhanbad, India.», *J. Health Pollut.*, vol. 11, fasc. 29, p. 210305, mar. 2021, doi: 10.5696/2156-9614-11.29.210305.
[34] M. Saeedi, L. Y. Li, e M. Salmanzadeh, «Heavy metals and polycyclic aromatic hydrocarbons: pollution and ecological risk assessment in street dust of Tehran», *J. Hazard. Mater.*, vol. 227, pp. 9–17, 2012.
[35] P. Sakunkoo *et al.*, «Human health risk assessment of PM(2.5)-bound heavy metal of anthropogenic sources in the Khon Kaen Province of Northeast Thailand.», *Heliyon*, vol. 8, fasc. 6, p. e09572, giu. 2022, doi: 10.1016/j.heliyon.2022.e09572.

[36] R. Castel, R. Bertoldo, S. Lebarillier, Y. Noack, T. Orsière, e L. Malleret, «Toward an interdisciplinary approach to assess the adverse health effects of dust-containing polycyclic aromatic hydrocarbons (PAHs) and metal (loid) s on preschool children», *Environ. Pollut.*, p. 122372, 2023.
[37] M. Låg, J. Øvrevik, M. Refsnes, e J. A. Holme, «Potential role of polycyclic aromatic hydrocarbons in air pollution-induced non-malignant respiratory diseases», *Respir. Res.*, vol. 21, fasc. 1, p. 299, nov. 2020, doi: 10.1186/s12931-020-01563-1.
[38] G. Safo-Adu, F. Attiogbe, I. Emahi, e F. G. Ofosu, «A review of the sources, distribution sequences, and health risks associated with exposure to atmospheric polycyclic aromatic hydrocarbons», *Cogent Eng.*, vol. 10, fasc. 1, p. 2199511, dic. 2023, doi: 10.1080/23311916.2023.2199511.
[39] International Agency for Research on Cancer, «IARC: Outdoor air pollution a leading environmental cause of cancer deaths», Lyon/Geneva, 17 October 2013, ott. 2013.
[40] P. Smichowski e D. R. Gómez, «An overview of natural and anthropogenic sources of ultrafine airborne particles: analytical determination to assess the multielemental profiles», *Appl. Spectrosc. Rev.*, pp. 1–27, 2023.
[41] X. Li, R. Cai, J. Hao, J. N. Smith, e J. Jiang, «Online detection of airborne nanoparticle composition with mass spectrometry: Recent advances, challenges, and opportunities», *TrAC Trends Anal. Chem.*, p. 117195, 2023.
[42] M. López *et al.*, «Size-resolved chemical composition and toxicity of particles released from refit operations in shipyards», *Sci. Total Environ.*, vol. 880, p. 163072, 2023.
[43] G. Buonanno, G. Giovinco, L. Morawska, e L. Stabile, «Lung cancer risk of airborne particles for Italian population», *Env. Res*, vol. 142, pp. 443–451, ago. 2015, doi: 10.1016/j.envres.2015.07.019.
[44] E. Caracci, L. Stabile, e G. Buonanno, «A simplified approach to evaluate the lung cancer risk related to airborne particles emitted by indoor sources», *Build. Environ.*, vol. 204, 2021, doi: 10.1016/j.buildenv.2021.108143.
[45] G. N. Sze-To, C. L. Wu, C. Y. H. Chao, M. P. Wan, e T. C. Chan, «Exposure and cancer risk toward cooking-generated ultrafine and coarse particles in Hong Kong homes», *HVACR Res.*, vol. 18, fasc. 1–2, Art. fasc. 1–2, feb. 2012, doi: 10.1080/10789669.2011.598443.
[46] M. Derudi *et al.*, «Emissions of air pollutants from scented candles burning in a test chamber», *Atmos. Environ.*, vol. 55, pp. 257–262, 2012.
[47] G. C. Fang *et al.*, «Fine (PM2.5), coarse (PM2.5-10), and metallic elements of suspended particulates for incense burning at Tzu Yun Yen temple in central Taiwan», *Chemosphere*, vol. 51, fasc. 9, Art. fasc. 9, 2003.
[48] M. T. Hu *et al.*, «Characteritization of, and health risks from, polychlorinated dibenzo-p-dioxins/dibenzofurans from incense burned in a temple», *Sci. Total Environ.*, vol. 407, fasc. 17, Art. fasc. 17, 2009.
[49] X. Ji *et al.*, «Characterization of particles emitted by incense burning in an experimental house», *Indoor Air*, vol. 20, fasc. 2, Art. fasc. 2, 2010.
[50] S. Orecchio, «Polycyclic aromatic hydrocarbons (PAHs) in indoor emission from decorative candles», *Atmos. Environ.*, vol. 45, fasc. 10, pp. 1888–1895, 2011.
[51] J. Pagels *et al.*, «Chemical composition and mass emission factors of candle smoke particles», *J. Aerosol Sci.*, vol. 40, fasc. 3, Art. fasc. 3, 2009.
[52] A. A. Roy, S. P. Baxla, T. Gupta, R. Bandyopadhyaya, e S. N. Tripathi, «Particles emitted from indoor combustion sources: Size distribution measurement and chemical analysis», *Inhal. Toxicol.*, vol. 21, fasc. 10, Art. fasc. 10, 2009.

[53] S. W. See e R. Balasubramanian, «Physical characteristics of ultrafine particles emitted from different gas cooking methods», *Aerosol Air Qual. Res.*, vol. 6, fasc. 1, pp. 82–92, 2006.
[54] T.-T. Yang, S.-T. Lin, T.-S. Lin, e H.-Y. Chung, «Characterization of polycyclic aromatic hydrocarbon emissions in the particulate and gas phase from smoldering mosquito coils containing various atomic hydrogen/carbon ratios», *Sci. Total Environ.*, vol. 506, pp. 391–400, 2015.
[55] T.-T. Yang, S.-T. Lin, T.-S. Lin, e H.-Y. Chung, «Characterization of polycyclic aromatic hydrocarbon emissions in the particulate and gas phase from smoldering mosquito coils containing various atomic hydrogen/carbon ratios.», *Sci. Total Environ.*, vol. 506–507, pp. 391–400, feb. 2015, doi: 10.1016/j.scitotenv.2014.11.029.
[56] T. T. Yang, S. T. Lin, H. F. Hung, R. H. Shie, e J. J. Wu, «Effect of Relative Humidity on Polycyclic Aromatic Hydrocarbon Emissions from Smoldering Incense», *Aerosol Air Qual. Res.*, vol. 13, fasc. 2, Art. fasc. 2, 2013, doi: 10.4209/aaqr.2012.07.0182.
[57] L. Zhang, Z. Jiang, J. Tong, Z. Wang, Z. Han, e J. Zhang, «Using charcoal as base material reduces mosquito coil emissions of toxins», *Indoor Air*, vol. 20, fasc. 2, Art. fasc. 2, 2010.
[58] W. Zhou *et al.*, «Metals, PAHs and oxidative potential of size-segregated particulate matter and inhalational carcinogenic risk of cooking at a typical university canteen in Shanghai, China», *Atmos. Environ.*, vol. 287, p. 119250, ott. 2022, doi: 10.1016/j.atmosenv.2022.119250.
[59] A. K. Thakur, B. Kaundle, e I. Singh, «Mucoadhesive drug delivery systems in respiratory diseases», in *Targeting chronic inflammatory lung diseases using advanced drug delivery systems*, Elsevier, 2020, pp. 475–491.
[60] International Commission on Radiological Protection, «Human respiratory tract model for radiological protection. A report of a Task Group of the International Commission on Radiological Protection.», *Ann. ICRP*, vol. 24, fasc. 1–3, Art. fasc. 1–3, 1994, doi: 10.1016/0146-6453(94)90029-9.
[61] X.-Q. Jiang, X.-D. Mei, e D. Feng, «Air pollution and chronic airway diseases: what should people know and do?», *J. Thorac. Dis.*, vol. 8, fasc. 1, p. E31, 2016.
[62] A. Heinzerling, J. Hsu, e F. Yip, «Respiratory health effects of ultrafine particles in children: a literature review», *Water. Air. Soil Pollut.*, vol. 227, pp. 1–14, 2016.
[63] E. H. van den Hooven *et al.*, «Air pollution exposure during pregnancy, ultrasound measures of fetal growth, and adverse birth outcomes: a prospective cohort study», *Environ. Health Perspect.*, vol. 120, fasc. 1, pp. 150–156, 2012.
[64] M. Leung *et al.*, «Traffic-Related Air Pollution and Ultrasound Parameters of Fetal Growth in Eastern Massachusetts», *Am. J. Epidemiol.*, p. kwad072, 2023.
[65] C. A. Pope III, J. B. Muhlestein, H. T. May, D. G. Renlund, J. L. Anderson, e B. D. Horne, «Ischemic heart disease events triggered by short-term exposure to fine particulate air pollution», *Circulation*, vol. 114, fasc. 23, pp. 2443–2448, 2006.
[66] G. Hoek *et al.*, «Long-term air pollution exposure and cardio-respiratory mortality: a review», *Environ. Health*, vol. 12, fasc. 1, pp. 1–16, 2013.
[67] H. Liang *et al.*, «Association of outdoor air pollution, lifestyle, genetic factors with the risk of lung cancer: A prospective cohort study», *Environ. Res.*, vol. 218, p. 114996, 2023.
[68] C. D. Berg *et al.*, «AIR POLLUTION AND LUNG CANCER A Review by International Association for the Study of Lung Cancer Early Detection and Screening Committee», *J. Thorac. Oncol.*, 2023.
[69] W. Hill *et al.*, «Lung adenocarcinoma promotion by air pollutants», *Nature*, vol. 616, fasc. 7955, pp. 159–167, 2023.
[70] R. Chen *et al.*, «Beyond PM2. 5: The role of ultrafine particles on adverse health effects of air pollution», *Biochim. Biophys. Acta BBA-Gen. Subj.*, vol. 1860, fasc. 12, pp. 2844–2855, 2016.

[71] V. Shalini, G. Gadag, e P. V. Kalburgi, «Atmospheric Aerosols and their Effect on Human Health: A Review», 2023.
[72] M. Hussain, P. Madl, e A. Khan, «Lung deposition predictions of airborne particles and the emergence of contemporary diseases, Part-I», *Health (N. Y.)*, vol. 2, fasc. 2, pp. 51–59, 2011.
[73] M. U. Ali *et al.*, «Pollution characteristics, mechanism of toxicity and health effects of the ultrafine particles in the indoor environment: Current status and future perspectives», *Crit. Rev. Environ. Sci. Technol.*, vol. 52, fasc. 3, Art. fasc. 3, 2022.
[74] European Parliament and Council of the European Union, *EU Directive 2008/50/EC of the European Parliament and of the Council of 21 May 2008 on ambient air quality and cleaner air for Europe, 2008*, vol. L 152/1. 2008, pp. 1–44.
[75] S. S. Amaral, J. A. de Carvalho Jr, M. A. M. Costa, e C. Pinheiro, «An overview of particulate matter measurement instruments», *Atmosphere*, vol. 6, fasc. 9, pp. 1327–1345, 2015.
[76] R. N. Colvile, E. J. Hutchinson, J. S. Mindell, e R. F. Warren, «The transport sector as a source of air pollution», *Atmos. Environ.*, vol. 35, fasc. 9, pp. 1537–1565, 2001.
[77] K. Zhang e S. Batterman, «Air pollution and health risks due to vehicle traffic», *Sci. Total Environ.*, vol. 450, pp. 307–316, 2013.
[78] N. Künzli *et al.*, «Public-health impact of outdoor and traffic-related air pollution: a European assessment», *The Lancet*, vol. 356, fasc. 9232, pp. 795–801, 2000.
[79] C. Berggren e T. Magnusson, «Reducing automotive emissions—The potentials of combustion engine technologies and the power of policy», *Energy Policy*, vol. 41, pp. 636–643, 2012.
[80] G. Buonanno e L. Morawska, «Ultrafine particle emission of waste incinerators and comparison to the exposure of urban citizens», *Waste Manag.*, vol. 37, pp. 75–81, 2015.
[81] G. Buonanno, M. Scungio, L. Stabile, e W. Tirler, «Ultrafine particle emission from incinerators: the role of the fabric filter», *J Air Waste Manag Assoc*, vol. 62, fasc. 1, Art. fasc. 1, gen. 2012.
[82] M. I. Mitova, C. Cluse, C. G. Goujon-Ginglinger, S. Kleinhans, M. Rotach, e M. Tharin, «Human chemical signature: Investigation on the influence of human presence and selected activities on concentrations of airborne constituents», *Environ. Pollut.*, vol. 257, p. 113518, 2020.
[83] A. Sekar, G. K. Varghese, e M. R. Varma, «Analysis of benzene air quality standards, monitoring methods and concentrations in indoor and outdoor environment», *Heliyon*, vol. 5, fasc. 11, 2019.
[84] M. Bentayeb *et al.*, «Indoor air quality, ventilation and respiratory health in elderly residents living in nursing homes in Europe», *Eur. Respir. J.*, vol. 45, fasc. 5, pp. 1228–1238, 2015.
[85] S. Komae, K. Sekiguchi, M. Suzuki, R. Nakayama, N. Namiki, e N. Kagi, «Secondary organic aerosol formation from p-dichlorobenzene under indoor environmental conditions», *Build. Environ.*, vol. 174, p. 106758, mag. 2020, doi: 10.1016/j.buildenv.2020.106758.
[86] L. Morawska *et al.*, «Airborne particles in indoor environment of homes, schools, offices and aged care facilities: The main routes of exposure», *Env. Int*, vol. 108, pp. 75–83, nov. 2017, doi: 10.1016/j.envint.2017.07.025.
[87] H. Salonen, T. Salthammer, e L. Morawska, «Human exposure to ozone in school and office indoor environments», *Environ. Int.*, vol. 119, pp. 503–514, ott. 2018, doi: 10.1016/j.envint.2018.07.012.
[88] T. Salthammer, T. Schripp, S. Wientzek, e M. Wensing, «Impact of operating wood-burning fireplace ovens on indoor air quality», *Chemosphere*, vol. 103, pp. 205–11, mag. 2014, doi: 10.1016/j.chemosphere.2013.11.067.
[89] L. Stabile, G. De Luca, A. Pacitto, L. Morawska, P. Avino, e G. Buonanno, «Ultrafine particle emission from floor cleaning products», *Indoor Air*, vol. 31, fasc. 1, pp. 63–73, gen. 2021, doi: 10.1111/ina.12713.

[90] L. Morawska *et al.*, «Indoor aerosols: from personal exposure to risk assessment», *Indoor Air*, vol. 23, fasc. 6, pp. 462–87, dic. 2013, doi: 10.1111/ina.12044.
[91] L. Morawska *et al.*, «Airborne particles in indoor environment of homes, schools, offices and aged care facilities: The main routes of exposure», *Env. Int*, vol. 108, pp. 75–83, nov. 2017, doi: 10.1016/j.envint.2017.07.025.
[92] A. Pacitto *et al.*, «Daily submicron particle doses received by populations living in different low- and middle-income countries», *Environ. Pollut.*, vol. 269, p. 116229, gen. 2021, doi: 10.1016/j.envpol.2020.116229.
[93] C. Protano, M. Manigrasso, e P. Avino, «Second-hand smoke generated by combustion and electronic smoking devices used in real scenarios: Ultrafine particle pollution and age-related dose assessment.», *Environ. Int.*, vol. 107, pp. 190–195, 2017, doi: 10.1016/j.envint.2017.07.014.
[94] S. W. See e R. Balasubramanian, «Characterization of fine particle emissions from incense burning», *Build. Environ.*, vol. 46, fasc. 5, pp. 1074–1080, 2011.
[95] L. Stabile, G. Buonanno, P. Avino, A. Frattolillo, e E. Guerriero, «Indoor exposure to particles emitted by biomass-burning heating systems and evaluation of dose and lung cancer risk received by population», *Environ. Pollut.*, vol. 235, pp. 65–73, 2018, doi: 10.1016/j.envpol.2017.12.055.
[96] L. Stabile, F. C. Fuoco, e G. Buonanno, «Characteristics of particles and black carbon emitted by combustion of incenses, candles and anti-mosquito products», *Build. Environ.*, vol. 56, fasc. 0, pp. 184–191, 2012, doi: 10.1016/j.buildenv.2012.03.005.
[97] G. Buonanno, L. Morawska, e L. Stabile, «Particle emission factors during cooking activities», *Atmos. Environ.*, vol. 43, fasc. 20, pp. 3235–3242, 2009.
[98] L. Sun *et al.*, «Effect of venting range hood flow rate on size-resolved ultrafine particle concentrations from gas stove cooking», *Aerosol Sci. Technol.*, vol. 52, fasc. 12, pp. 1370–1381, 2018.
[99] L. Wallace, F. Wang, C. Howard-Reed, e A. Persily, «Contribution of gas and electric stoves to residential ultrafine particle concentrations between 2 and 64 nm: Size distributions and emission and coagulation rates», *Environ. Sci. Technol.*, vol. 42, fasc. 23, pp. 8641–8647, 2008.
[100] Y. Xiao, L. Wang, M. Yu, H. Liu, e J. Liu, «Effects of source emission and window opening on winter indoor particle concentrations in the severe cold region of China», *Build. Environ.*, vol. 144, pp. 23–33, ott. 2018, doi: 10.1016/j.buildenv.2018.08.001.
[101] S. Zhu *et al.*, «Investigating particles, VOCs, ROS produced from mosquito-repellent incense emissions and implications in SOA formation and human health», *Build. Environ.*, vol. 143, pp. 645–651, ott. 2018, doi: 10.1016/j.buildenv.2018.07.053.
[102] S. W. See e R. Balasubramanian, «Risk assessment of exposure to indoor aerosols associated with Chinese cooking», *Environ. Res.*, vol. 102, fasc. 2, pp. 197–204, 2006.
[103] Z. Zhang *et al.*, «Effects of cooking and window opening behaviors on indoor ultrafine particle concentrations in urban residences: A field study in Yangtze River Delta region of China», *Build. Environ.*, vol. 207, p. 108488, 2022.
[104] A. G. Schwartz e M. L. Cote, «Epidemiology of lung cancer», *Lung Cancer Pers. Med. Curr. Knowl. Ther.*, pp. 21–41, 2016.
[105] I. W. G. on the E. of C. R. to Humans, W. H. Organization, e I. A. for R. on Cancer, *Tobacco smoke and involuntary smoking*, vol. 83. Iarc, 2004.
[106] K. E. Farsalinos, G. Gillman, K. Poulas, e V. Voudris, «Tobacco-Specific Nitrosamines in Electronic Cigarettes: Comparison between Liquid and Aerosol Levels», *Int. J. Environ. Res. Public. Health*, vol. 12, fasc. 8, Art. fasc. 8, 2015, doi: 10.3390/ijerph120809046.
[107] M. L. Goniewicz *et al.*, «Levels of selected carcinogens and toxicants in vapour from electronic cigarettes», *Tob. Control*, mar. 2013, doi: 10.1136/tobaccocontrol-2012-050859.

[108] P. Avino, M. Scungio, L. Stabile, G. Cortellessa, G. Buonanno, e M. Manigrasso, «Second-hand aerosol from tobacco and electronic cigarettes: Evaluation of the smoker emission rates and doses and lung cancer risk of passive smokers and vapers», *Sci. Total Environ.*, vol. 642, pp. 137–147, nov. 2018, doi: 10.1016/j.scitotenv.2018.06.059.

[109] B. K. Coleman, M. M. Lunden, H. Destaillats, e W. W. Nazaroff, «Secondary organic aerosol from ozone-initiated reactions with terpene-rich household products», *Atmos. Environ.*, vol. 42, fasc. 35, Art. fasc. 35, nov. 2008, doi: 10.1016/j.atmosenv.2008.07.031.

[110] J. S. Hansen *et al.*, «Limonene and its ozone-initiated reaction products attenuate allergic lung inflammation in mice», *J. Immunotoxicol.*, vol. 13, fasc. 6, Art. fasc. 6, nov. 2016, doi: 10.1080/1547691X.2016.1195462.

[111] W. W. Nazaroff e C. J. Weschler, «Cleaning products and air fresheners: exposure to primary and secondary air pollutants», *Atmos. Environ.*, vol. 38, fasc. 18, Art. fasc. 18, giu. 2004, doi: 10.1016/j.atmosenv.2004.02.040.

[112] A. W. Nørgaard *et al.*, «Ozone-initiated Terpene Reaction Products in Five European Offices: Replacement of a Floor Cleaning Agent», *Environ. Sci. Technol.*, vol. 48, fasc. 22, Art. fasc. 22, nov. 2014, doi: 10.1021/es504106j.

[113] B. C. Singer, H. Destaillats, A. T. Hodgson, e W. W. Nazaroff, «Cleaning products and air fresheners: emissions and resulting concentrations of glycol ethers and terpenoids.», *Indoor Air*, vol. 16, fasc. 3, Art. fasc. 3, giu. 2006, doi: 10.1111/j.1600-0668.2005.00414.x.

[114] M. Waring e J. Siegel, «Indoor Secondary Organic Aerosol Formation Initiated from Reactions between Ozone and Surface-Sorbed D-Limonene», *Environ. Sci. Technol.*, vol. 47, fasc. 12, Art. fasc. 12, 2013, doi: 10.1021/es400846d.

[115] L. Li e D. R. Cocker, «Molecular structure impacts on secondary organic aerosol formation from glycol ethers», *Atmos. Environ.*, vol. 180, pp. 206–215, mag. 2018, doi: 10.1016/j.atmosenv.2017.12.025.

[116] P. Koutrakis, S. L. K. Briggs, e B. P. Leaderer, «Source apportionment of indoor aerosols in suffolk and onondaga counties, New York», *Environ. Sci. Technol.*, vol. 26, fasc. 3, Art. fasc. 3, 1992.

[117] Y. C. Chen, Z. Yuanhui, e E. M. Barber, «A dynamic method to estimate indoor dust sink and source», *Build. Environ.*, vol. 35, fasc. 3, Art. fasc. 3, 2000.

[118] T. L. Thatcher e D. W. Layton, «Deposition, resuspensiion, and penetration of particles within a residence», *Atmos. Environ.*, vol. 29, fasc. 13, Art. fasc. 13, 1995.

[119] C. He, L. Morawska, J. Hitchins, e D. Gilbert, «Contribution from indoor sources to particle number and mass concentrations in residential houses», *Atmos. Environ.*, vol. 38, fasc. 21, Art. fasc. 21, 2004.

[120] A. Schieweck *et al.*, «Smart homes and the control of indoor air quality», *Renew. Sustain. Energy Rev.*, vol. 94, pp. 705–718, 2018.

[121] A. Wierzbicka *et al.*, «Quantification of differences between occupancy and total monitoring periods for better assessment of exposure to particles in indoor environments», *Atmos. Environ.*, vol. 106, pp. 419–428, 2015, doi: 10.1016/j.atmosenv.2014.08.011.

[122] Y. Omelekhina *et al.*, «Effect of energy renovation and occupants' activities on airborne particle concentrations in Swedish rental apartments», *Sci. Total Environ.*, vol. 806, p. 149995, 2022.

[123] M. M. Abdel-Salam, «Seasonal variation in indoor concentrations of air pollutants in residential buildings», *J. Air Waste Manag. Assoc.*, vol. 71, fasc. 6, pp. 761–777, 2021.

[124] L. Stabile, G. Buonanno, A. Frattolillo, e M. Dell'Isola, «The effect of the ventilation retrofit in a school on CO2, airborne particles, and energy consumptions», *Build. Environ.*, vol. 156, pp. 1–11, 2019, doi: 10.1016/j.buildenv.2019.04.001.

[125] A. M. Coggins *et al.*, «Indoor air quality, thermal comfort and ventilation in deep energy retrofitted Irish dwellings», *Build. Environ.*, vol. 219, p. 109236, lug. 2022, doi: 10.1016/j.buildenv.2022.109236.
[126] D. D'Agostino e L. Mazzarella, «What is a Nearly zero energy building? Overview, implementation and comparison of definitions», *J. Build. Eng.*, vol. 21, pp. 200–212, gen. 2019, doi: 10.1016/j.jobe.2018.10.019.
[127] Á. Broderick, M. Byrne, S. Armstrong, J. Sheahan, e A. M. Coggins, «A pre and post evaluation of indoor air quality, ventilation, and thermal comfort in retrofitted co-operative social housing», *Build. Environ.*, vol. 122, pp. 126–133, 2017, doi: 10.1016/j.buildenv.2017.05.020.
[128] A. Pacitto *et al.*, «The influence of lifestyle on airborne particle surface area doses received by different Western populations», *Environ. Pollut.*, vol. 232, January 2018, Pages 113-122, pp. 113–122, 2018, doi: 10.1016/j.envpol.2017.09.023.
[129] L. Stabile, G. Buonanno, P. Avino, A. Frattolillo, e E. Guerriero, «Indoor exposure to particles emitted by biomass-burning heating systems and evaluation of dose and lung cancer risk received by population», *Environ. Pollut.*, vol. 235, pp. 65–73, 2018, doi: 10.1016/j.envpol.2017.12.055.
[130] G. Buonanno, G. Giovinco, L. Morawska, e L. Stabile, «Tracheobronchial and alveolar dose of submicrometer particles for different population age groups in Italy», *Atmos. Environ.*, vol. 45, fasc. 34, pp. 6216–6224, 2011.
[131] G. N. Sze-To, C. L. Wu, C. Y. H. Chao, M. P. Wan, e T. C. Chan, «Exposure and cancer risk toward cooking-generated ultrafine and coarse particles in Hong Kong homes», *HVACR Res.*, vol. 18, fasc. 1–2, pp. 204–216, feb. 2012, doi: 10.1080/10789669.2011.598443.
[132] World Health Organization, «Review of evidence on health aspects of air pollution – REVIHAAP Project, Technical Report», WHO Regional Office for Europe, Copenhagen, 2013. [Online]. Disponibile su: http://www.who.int/iris/handle/10665/75261#sthash.99r0pJWZ.dpuf
[133] G. Buonanno, G. Giovinco, L. Morawska, e L. Stabile, «Lung cancer risk of airborne particles for Italian population», *Env. Res*, vol. 142, pp. 443–451, ago. 2015, doi: 10.1016/j.envres.2015.07.019.
[134] G. Buonanno, L. Stabile, L. Morawska, G. Giovinco, e X. Querol, «Do air quality targets really represent safe limits for lung cancer risk?», *Sci. Total Environ.*, vol. 580, pp. 74–82, 2017, doi: 10.1016/j.scitotenv.2016.11.216.
[135] R. Sharma e R. Balasubramanian, «Indoor human exposure to size-fractionated aerosols during the 2015 Southeast Asian smoke haze and assessment of exposure mitigation strategies», *Environ. Res. Lett.*, vol. 12, fasc. 11, p. 114026, 2017.
[136] A. J. Koivisto *et al.*, «Source specific exposure and risk assessment for indoor aerosols», *Sci. Total Environ.*, vol. 668, pp. 13–24, 2019.
[137] L. Canale, M. Dell'Isola, G. Ficco, B. Di Pietra, e A. Frattolillo, «Estimating the impact of heat accounting on Italian residential energy consumption in different scenarios», *Energy Build.*, vol. 168, pp. 385–398, giu. 2018, doi: 10.1016/j.enbuild.2018.03.040.
[138] A. Frattolillo, L. Stabile, e M. Dell'Isola, «Natural ventilation measurements in a multi-room dwelling: Critical aspects and comparability of pressurization and tracer gas decay tests», *J. Build. Eng.*, vol. 42, p. 102478, ott. 2021, doi: 10.1016/j.jobe.2021.102478.
[139] T. Hussein, A. Wierzbicka, J. Löndahl, M. Lazaridis, e O. Hänninen, «Indoor aerosol modeling for assessment of exposure and respiratory tract deposited dose», *Atmos. Environ.*, vol. 106, pp. 402–411, apr. 2015, doi: 10.1016/j.atmosenv.2014.07.034.

[140] A. Pacitto *et al.*, «Daily submicron particle doses received by populations living in different low- and middle-income countries», *Environ. Pollut.*, vol. 269, p. 116229, gen. 2021, doi: 10.1016/j.envpol.2020.116229.
[141] L. Stabile, M. Dell'Isola, A. Russi, A. Massimo, e G. Buonanno, «The effect of natural ventilation strategy on indoor air quality in schools», *Sci. Total Environ.*, vol. 595, pp. 894–902, 2017, doi: 10.1016/j.scitotenv.2017.02.030.
[142] L. Stabile, A. Massimo, L. Canale, A. Russi, A. Andrade, e M. Dell'Isola, «The Effect of Ventilation Strategies on Indoor Air Quality and Energy Consumptions in Classrooms», *Buildings*, vol. 9, fasc. 5, 2019, doi: 10.3390/buildings9050110.
[143] L. Canale, M. Dell'Isola, G. Ficco, T. Cholewa, S. Siggelsten, e I. Balen, «A comprehensive review on heat accounting and cost allocation in residential buildings in EU», *Energy Build.*, vol. 202, p. 109398, nov. 2019, doi: 10.1016/j.enbuild.2019.109398.
[144] M. Dell'Isola, G. Ficco, F. Arpino, G. Cortellessa, e L. Canale, «A novel model for the evaluation of heat accounting systems reliability in residential buildings», *Energy Build.*, vol. 150, pp. 281–293, set. 2017, doi: 10.1016/j.enbuild.2017.06.007.
[145] M. Dell'Isola, G. Ficco, L. Canale, B. I. Palella, e G. Puglisi, «An IoT Integrated Tool to Enhance User Awareness on Energy Consumption in Residential Buildings», *Atmosphere*, vol. 10, fasc. 12, 2019, doi: 10.3390/atmos10120743.
[146] G. Buonanno, G. Johnson, L. Morawska, e L. Stabile, «Volatility characterization of cooking-generated aerosol particles», *Aerosol Sci. Technol.*, vol. 45, fasc. 9, pp. 1069–1077, 2011.
[147] T. Hussein *et al.*, «Particle size characterization and emission rates during indoor activities in a house», *Atmos. Environ.*, vol. 40, fasc. 23, pp. 4285–4307, 2006.
[148] J. Zhao, W. Birmili, T. Hussein, B. Wehner, e A. Wiedensohler, «Particle number emission rates of aerosol sources in 40 German households and their contributions to ultrafine and fine particle exposure», *Indoor Air*, vol. 31, fasc. 3, pp. 818–831, mag. 2021, doi: 10.1111/ina.12773.
[149] L. Stabile *et al.*, «A novel approach to evaluate the lung cancer risk of airborne particles emitted in a city», *Sci. Total Environ.*, vol. 656, pp. 1032–1042, mar. 2019, doi: 10.1016/j.scitotenv.2018.11.432.
[150] N. Luo, W. Weng, X. Xu, T. Hong, M. Fu, e K. Sun, «Assessment of occupant-behavior-based indoor air quality and its impacts on human exposure risk: A case study based on the wildfires in Northern California», *Sci. Total Environ.*, vol. 686, pp. 1251–1261, 2019.
[151] S. Kim e M. Li, «Awareness, understanding, and action: a conceptual framework of user experiences and expectations about indoor air quality visualizations», in *Proceedings of the 2020 CHI Conference on Human Factors in Computing Systems*, 2020, pp. 1–12.
[152] S. Höfner e A. Schütze, «Air Quality Measurements and Education: Improving Environmental Awareness of High School Students», *Front. Sens.*, vol. 2, p. 657920, 2021.
[153] G. Buonanno, L. Stabile, L. Morawska, G. Giovinco, e X. Querol, «Do air quality targets really represent safe limits for lung cancer risk?», *Sci. Total Environ.*, vol. 580, pp. 74–82, 2017, doi: 10.1016/j.scitotenv.2016.11.216.
[154] J. Froehlich, L. Findlater, e J. Landay, «The design of eco-feedback technology», in *Proceedings of the SIGCHI conference on human factors in computing systems*, 2010, pp. 1999–2008.
[155] I. Tsoulou, J. Senick, G. Mainelis, e S. Kim, «Residential indoor air quality interventions through a social-ecological systems lens: A systematic review», *Indoor Air*, vol. 31, fasc. 4, pp. 958–976, 2021.
[156] G. Grilli e J. Curtis, «Encouraging pro-environmental behaviours: A review of methods and approaches», *Renew. Sustain. Energy Rev.*, vol. 135, p. 110039, gen. 2021, doi: 10.1016/j.rser.2020.110039.

[157] K. E. Wallen e E. Daut, «The challenge and opportunity of behaviour change methods and frameworks to reduce demand for illegal wildlife», *Nat. Conserv.*, vol. 26, pp. 55–75, apr. 2018, doi: 10.3897/natureconservation.26.22725.
[158] A. P. Calitz, M. D. M. Cullen, e F. Odendaal, «Creating Environmental Awareness using an Eco-Feedback Application at a Higher Education Institution», *South. Afr. J. Environ. Educ.*, vol. 36, 2020.
[159] A. Francisco, H. Truong, A. Khosrowpour, J. E. Taylor, e N. Mohammadi, «Occupant perceptions of building information model-based energy visualizations in eco-feedback systems», *Appl. Energy*, vol. 221, pp. 220–228, 2018.
[160] L. Serna-Mansoux, A. Popoff, e D. Millet, «Eco-feedback performance exploration for Eco-feedback design», in *CFM 2013-21ème Congrès Français de Mécanique*, AFM, Maison de la Mécanique, 39/41 rue Louis Blanc-92400 Courbevoie, 2013.
[161] L. T. McCalley e C. J. H. Midden, «Computer based systems in household appliances: the study of eco-feedback as a tool for increasing conservation behavior», *Proc. 3rd Asia Pac. Comput. Hum. Interact. Cat No98EX110*, pp. 344–349, 1998.
[162] L. Canale, B. P. Slott, S. Finsdóttir, L. R. Kildemoes, e R. K. Andersen, «Do in-home displays affect end-user consumptions? A mixed method analysis of electricity, heating and water use in Danish apartments», *Energy Build.*, vol. 246, p. 111094, 2021.
[163] M. L. Chalal, B. Medjdoub, N. Bezai, R. Bull, e M. Zune, «Visualisation in energy eco-feedback systems: A systematic review of good practice», *Renew. Sustain. Energy Rev.*, vol. 162, p. 112447, 2022.
[164] J. E. Fontecha, A. Nikolaev, J. L. Walteros, e Z. Zhu, «Scientists wanted? A literature review on incentive programs that promote pro-environmental consumer behavior: Energy, waste, and water», *Socioecon. Plann. Sci.*, p. 101251, 2022.
[165] P. Petkov, S. Goswami, F. Köbler, e H. Krcmar, «Personalised eco-feedback as a design technique for motivating energy saving behaviour at home», in *Proceedings of the 7th Nordic Conference on Human-Computer Interaction: Making Sense Through Design*, 2012, pp. 587–596.
[166] G. Peschiera e J. E. Taylor, «The impact of peer network position on electricity consumption in building occupant networks utilizing energy feedback systems», *Energy Build.*, vol. 49, pp. 584–590, 2012.
[167] I. Vassileva, M. Odlare, F. Wallin, e E. Dahlquist, «The impact of consumers' feedback preferences on domestic electricity consumption», *Appl. Energy*, vol. 93, pp. 575–582, 2012.
[168] L. M. J. Geelen *et al.*, «Comparing the effectiveness of interventions to improve ventilation behavior in primary schools», *Indoor Air*, vol. 18, fasc. 5, p. 416, 2008.
[169] S. Semple *et al.*, «Using air-quality feedback to encourage disadvantaged parents to create a smoke-free home: Results from a randomised controlled trial», *Environ. Int.*, vol. 120, pp. 104–110, 2018.
[170] D. Sheikh Khan, J. Kolarik, e P. Weitzmann, «Design and application of occupant voting systems for collecting occupant feedback on indoor environmental quality of buildings – A review», *Build. Environ.*, vol. 183, p. 107192, ott. 2020, doi: 10.1016/j.buildenv.2020.107192.
[171] K. S. Tomsho *et al.*, «A Mixed methods evaluation of sharing air pollution results with study participants via report-back communication», *Int. J. Environ. Res. Public. Health*, vol. 16, fasc. 21, p. 4183, 2019.
[172] M. Kong, H. Kim, e T. Hong, «An effect of numerical data through monitoring device on perception of indoor air quality», *Build. Environ.*, vol. 216, p. 109044, mag. 2022, doi: 10.1016/j.buildenv.2022.109044.

[173] E. Pedersen, J. Borell, Y. Li, e K. Stålne, «Good indoor environmental quality (IEQ) and high energy efficiency in multifamily dwellings: How do tenants view the conditions needed to achieve both?», *Build. Environ.*, vol. 191, p. 107581, mar. 2021, doi: 10.1016/j.buildenv.2020.107581.

[174] S. Kim, J. A. Senick, e G. Mainelis, «Sensing the invisible: Understanding the perception of indoor air quality among children in low-income families», *Int. J. Child-Comput. Interact.*, vol. 19, pp. 79–88, mar. 2019, doi: 10.1016/j.ijcci.2018.12.002.

[175] M. R. Giordano *et al.*, «From low-cost sensors to high-quality data: A summary of challenges and best practices for effectively calibrating low-cost particulate matter mass sensors», *J. Aerosol Sci.*, vol. 158, p. 105833, 2021, doi: 10.1016/j.jaerosci.2021.105833.

[176] J. Du, W. Pan, e C. Yu, «In-situ monitoring of occupant behavior in residential buildings–a timely review», *Energy Build.*, vol. 212, p. 109811, 2020.

[177] M. Frontczak, R. V. Andersen, e P. Wargocki, «Questionnaire survey on factors influencing comfort with indoor environmental quality in Danish housing», *Build. Environ.*, vol. 50, pp. 56–64, 2012.

[178] D. Havens, H. R. Jary, L. B. Patel, M. E. Chiume-Chiphaliwali, e K. J. Mortimer, «Strategies for reducing exposure to indoor air pollution from household burning of solid fuels: Effects on acute lower respiratory infections in children under the age of 15 years», *Cochrane Database Syst. Rev.*, vol. 2017, fasc. 1, 2017, doi: 10.1002/14651858.CD011870.pub2.

[179] L. Morawska *et al.*, «A paradigm shift to combat indoor respiratory infection», *Science*, vol. 372, fasc. 6543, pp. 689–691, 2021, doi: 10.1126/science.abg2025.

[180] W. W. Nazaroff, «Indoor aerosol science aspects of SARS-CoV-2 transmission.», *Indoor Air*, vol. 32, fasc. 1, p. e12970, gen. 2022, doi: 10.1111/ina.12970.

[181] L. Bourouiba, «The Fluid Dynamics of Disease Transmission», *Annu. Rev. Fluid Mech.*, vol. 53, fasc. 1, pp. 473–508, gen. 2021, doi: 10.1146/annurev-fluid-060220-113712.

[182] J. Jimenez *et al.*, «What Were the Historical Reasons for the Resistance to Recognizing Airborne Transmission during the COVID-19 Pandemic?», *SSRN*, 2021.

[183] T. Greenhalgh, J. L. Jimenez, K. A. Prather, Z. Tufekci, D. Fisman, e R. Schooley, «Ten scientific reasons in support of airborne transmission of SARS-CoV-2.», *Lancet Lond. Engl.*, vol. 397, fasc. 10285, pp. 1603–1605, mag. 2021, doi: 10.1016/S0140-6736(21)00869-2.

[184] J. Sills *et al.*, «Airborne transmission of SARS-CoV-2», *Science*, vol. 370, fasc. 6514, pp. 303–304, ott. 2020, doi: 10.1126/science.abf0521.

[185] G. Buonanno, L. Morawska, e L. Stabile, «Quantitative assessment of the risk of airborne transmission of SARS-CoV-2 infection: Prospective and retrospective applications», *Environ. Int.*, vol. 145, p. 106112, dic. 2020, doi: 10.1016/j.envint.2020.106112.

[186] G. Buonanno, L. Stabile, e L. Morawska, «Estimation of airborne viral emission: Quanta emission rate of SARS-CoV-2 for infection risk assessment», *Environ. Int.*, vol. 141, p. 105794, ago. 2020, doi: 10.1016/j.envint.2020.105794.

[187] B. Schumm *et al.*, «Respiratory aerosol particle emission and simulated infection risk is greater during indoor endurance than resistance exercise», *Proc. Natl. Acad. Sci.*, vol. 120, fasc. 9, p. e2220882120, feb. 2023, doi: 10.1073/pnas.2220882120.

[188] L. Stabile, A. Pacitto, A. Mikszewski, L. Morawska, e G. Buonanno, «Ventilation procedures to minimize the airborne transmission of viruses in classrooms.», *Build. Environ.*, vol. 202, p. 108042, set. 2021, doi: 10.1016/j.buildenv.2021.108042.

[189] G. Buonanno, L. Ricolfi, L. Morawska, e L. Stabile, «Increasing ventilation reduces SARS-CoV-2 airborne transmission in schools: A retrospective cohort study in Italy's Marche region», *Front. Public Health*, vol. 10, 2022, [Online]. Disponibile su: https://www.frontiersin.org/articles/10.3389/fpubh.2022.1087087

[190] P. Azimi, Z. Keshavarz, J. G. Cedeno Laurent, e J. G. Allen, «Estimating the nationwide transmission risk of measles in US schools and impacts of vaccination and supplemental infection control strategies», *BMC Infect. Dis.*, vol. 20, fasc. 1, pp. 497–497, lug. 2020, doi: 10.1186/s12879-020-05200-6.

[191] L. D. Knibbs, L. Morawska, e S. C. Bell, «The risk of airborne influenza transmission in passenger cars», *Epidemiol. Infect.*, vol. 140, fasc. 3, pp. 474–478, 2012, doi: 10.1017/S0950268811000835.

[192] G. Cortellessa *et al.*, «Close proximity risk assessment for SARS-CoV-2 infection», *Sci. Total Environ.*, vol. 794, p. 148749, nov. 2021, doi: 10.1016/j.scitotenv.2021.148749.

[193] A. Henriques *et al.*, «Modelling airborne transmission of SARS-CoV-2 using CARA: Risk assessment for enclosed spaces», *medRxiv*, p. 2021.10.14.21264988, gen. 2021, doi: 10.1101/2021.10.14.21264988.

[194] L. Morawska, G. Buonanno, A. Mikszewski, e L. Stabile, «The physics of respiratory particle generation, fate in the air, and inhalation», *Nat. Rev. Phys.*, vol. 4, fasc. 11, pp. 723–734, 2022, doi: 10.1038/s42254-022-00506-7.

[195] G. Bagheri *et al.*, «Size, concentration, and origin of human exhaled particles and their dependence on human factors with implications on infection transmission», *J. Aerosol Sci.*, vol. 168, p. 106102, 2023.

[196] S. Balachandar, S. Zaleski, A. Soldati, G. Ahmadi, e L. Bourouiba, «Host-to-host airborne transmission as a multiphase flow problem for science-based social distance guidelines», *Int. J. Multiph. Flow*, vol. 132, p. 103439, nov. 2020, doi: 10.1016/j.ijmultiphaseflow.2020.103439.

[197] M. Abbas e D. Pittet, «Surfing the COVID-19 scientific wave», *Lancet Infect. Dis.*, pp. S1473-3099(20)30558–2, giu. 2020, doi: 10.1016/S1473-3099(20)30558-2.

[198] V. Stadnytskyi, C. E. Bax, A. Bax, e P. Anfinrud, «The airborne lifetime of small speech droplets and their potential importance in SARS-CoV-2 transmission», *Proc. Natl. Acad. Sci.*, vol. 117, fasc. 22, p. 11875, giu. 2020, doi: 10.1073/pnas.2006874117.

[199] B. E. Scharfman, A. H. Techet, J. W. M. Bush, e L. Bourouiba, «Visualization of sneeze ejecta: steps of fluid fragmentation leading to respiratory droplets», *Exp. Fluids*, vol. 57, fasc. 2, p. 24, gen. 2016, doi: 10.1007/s00348-015-2078-4.

[200] G. R. Johnson *et al.*, «Modality of human expired aerosol size distributions», *J. Aerosol Sci.*, vol. 42, fasc. 12, pp. 839–851, dic. 2011, doi: 10.1016/j.jaerosci.2011.07.009.

[201] L. Morawska *et al.*, «Size distribution and sites of origin of droplets expelled from the human respiratory tract during expiratory activities», *J. Aerosol Sci.*, vol. 40, fasc. 3, pp. 256–269, mar. 2009, doi: 10.1016/j.jaerosci.2008.11.002.

[202] D. Mürbe, M. Kriegel, J. Lange, L. Schumann, A. Hartmann, e M. Fleischer, «Aerosol emission of adolescents voices during speaking, singing and shouting», *PLOS ONE*, vol. 16, fasc. 2, p. e0246819, feb. 2021, doi: 10.1371/journal.pone.0246819.

[203] M. Fleischer *et al.*, «Pre-adolescent children exhibit lower aerosol particle volume emissions than adults for breathing, speaking, singing and shouting», *J. R. Soc. Interface*, vol. 19, fasc. 187, p. 20210833, feb. 2022, doi: 10.1098/rsif.2021.0833.

[204] F. K. A. Gregson *et al.*, «Comparing aerosol concentrations and particle size distributions generated by singing, speaking and breathing», *Aerosol Sci. Technol.*, vol. 55, fasc. 6, pp. 681–691, giu. 2021, doi: 10.1080/02786826.2021.1883544.

[205] T. Ahmed *et al.*, «Characterizing respiratory aerosol emissions during sustained phonation», *J. Expo. Sci. Environ. Epidemiol.*, vol. 32, fasc. 5, pp. 689–696, set. 2022, doi: 10.1038/s41370-022-00430-z.

[206] S. Asadi, A. S. Wexler, C. D. Cappa, S. Barreda, N. M. Bouvier, e W. D. Ristenpart, «Aerosol emission and superemission during human speech increase with voice loudness», *Sci. Rep.*, vol. 9, fasc. 1, p. 2348, feb. 2019, doi: 10.1038/s41598-019-38808-z.
[207] G. Bagheri *et al.*, «Size, concentration, and origin of human exhaled particles and their dependence on human factors with implications on infection transmission», *J. Aerosol Sci.*, vol. 168, p. 106102, feb. 2023, doi: 10.1016/j.jaerosci.2022.106102.
[208] S. Asadi, A. S. Wexler, C. D. Cappa, S. Barreda, N. M. Bouvier, e W. D. Ristenpart, «Effect of voicing and articulation manner on aerosol particle emission during human speech», *PloS One*, vol. 15, fasc. 1, p. e0227699, 2020.
[209] J. Archer *et al.*, «Comparing aerosol number and mass exhalation rates from children and adults during breathing, speaking and singing», *Interface Focus*, vol. 12, fasc. 2, p. 20210078, 2022.
[210] X. Xie, Y. Li, H. Sun, e L. Liu, «Exhaled droplets due to talking and coughing», *J. R. Soc. Interface*, vol. 6, fasc. suppl_6, pp. S703–S714, 2009.
[211] M. Riediker e L. Morawska, «Low Exhaled Breath Droplet Formation May Explain Why Children are Poor SARS-CoV-2 Transmitters», *Aerosol Air Qual. Res.*, vol. 20, fasc. 7, pp. 1513–1515, 2020, doi: 10.4209/aaqr.2020.06.0304.
[212] L. Gammaitoni e M. C. Nucci, «Using a mathematical model to evaluate the efficacy of TB control measures», *Emerg. Infect. Dis.*, pp. 335–342, 1997.
[213] C. Riley, G. Murphy, e R. L. Riley, «Airborne spread of measles in a suburban elementary school», *Am. J. Epidemiol.*, fasc. 107, Art. fasc. 107, 1978.
[214] M. Abbas e D. Pittet, «Surfing the COVID-19 scientific wave», *Lancet Infect. Dis.*, pp. S1473-3099(20)30558–2, giu. 2020, doi: 10.1016/S1473-3099(20)30558-2.
[215] V. Stadnytskyi, C. E. Bax, A. Bax, e P. Anfinrud, «The airborne lifetime of small speech droplets and their potential importance in SARS-CoV-2 transmission», *Proc. Natl. Acad. Sci.*, vol. 117, fasc. 22, Art. fasc. 22, giu. 2020, doi: 10.1073/pnas.2006874117.
[216] W. Yang e L. C. Marr, «Dynamics of Airborne Influenza A Viruses Indoors and Dependence on Humidity», *PLOS ONE*, vol. 6, fasc. 6, Art. fasc. 6, giu. 2011, doi: 10.1371/journal.pone.0021481.
[217] E. Lavezzo *et al.*, «Suppression of a SARS-CoV-2 outbreak in the Italian municipality of Vo'», *Nature*, giu. 2020, doi: 10.1038/s41586-020-2488-1.
[218] Y. Pan, D. Zang, P. Yang, L. M. Poon, e Q. Wang, «Viral load of SARS-CoV-2 in clinical samples Yang Pan Daitao Zhang Peng Yang Leo L M Poon Quanyi Wang», *The Lancet*, 2020.
[219] C. Rothe *et al.*, «Transmission of 2019-nCoV Infection from an Asymptomatic Contact in Germany», *N. Engl. J. Med.*, vol. 382, fasc. 10, Art. fasc. 10, gen. 2020, doi: 10.1056/NEJMc2001468.
[220] K. K.-W. To *et al.*, «Temporal profiles of viral load in posterior oropharyngeal saliva samples and serum antibody responses during infection by SARS-CoV-2: an observational cohort study», *Lancet Infect. Dis.*, vol. 20, fasc. 5, Art. fasc. 5, mag. 2020, doi: 10.1016/S1473-3099(20)30196-1.
[221] R. Woelfel *et al.*, «Clinical presentation and virological assessment of hospitalized cases of coronavirus disease 2019 in a travel-associated transmission cluster», *medRxiv*, p. 2020.03.05.20030502, gen. 2020, doi: 10.1101/2020.03.05.20030502.
[222] S. N. Rudnick e D. K. Milton, «Risk of indoor airborne infection transmission estimated from carbon dioxide concentration.», *Indoor Air*, vol. 13, fasc. 3, Art. fasc. 3, set. 2003, doi: 10.1034/j.1600-0668.2003.00189.x.

[223] G. N. Sze To e C. Y. H. Chao, «Review and comparison between the Wells–Riley and dose-response approaches to risk assessment of infectious respiratory diseases», *Indoor Air*, vol. 20, fasc. 1, Art. fasc. 1, feb. 2010, doi: 10.1111/j.1600-0668.2009.00621.x.
[224] T. Watanabe, T. A. Bartrand, M. H. Weir, T. Omura, e C. N. Haas, «Development of a dose-response model for SARS coronavirus.», *Risk Anal. Off. Publ. Soc. Risk Anal.*, vol. 30, fasc. 7, Art. fasc. 7, lug. 2010, doi: 10.1111/j.1539-6924.2010.01427.x.
[225] C. N. Haas, «Estimation of risk due to low doses of microorganisms: a comparison of alternative methodologies.», *Am. J. Epidemiol.*, vol. 118, fasc. 4, Art. fasc. 4, ott. 1983, doi: 10.1093/oxfordjournals.aje.a113662.
[226] W. F. Wells, «On airborne infection: study II. Droplets and Droplet nuclei», *Am. J. Epidemiol.*, vol. 20, fasc. 3, Art. fasc. 3, nov. 1934, doi: 10.1093/oxfordjournals.aje.a118097.
[227] S. Cui, M. Cohen, P. Stabat, e D. Marchio, «CO2 tracer gas concentration decay method for measuring air change rate», *Build. Environ.*, vol. 84, pp. 162–169, gen. 2015, doi: 10.1016/j.buildenv.2014.11.007.
[228] Y. S. Cheng, W. E. Bechtold, C. C. Yu, e I. F. Hung, «Incense smoke: Characterization and dynamics in indoor environments», *Aerosol Sci. Technol.*, vol. 23, fasc. 3, pp. 271–281, 1995.
[229] W. W. Nazaroff, «Indoor particle dynamics», *Indoor Air Suppl.*, vol. 14, fasc. SUPPL. 7, pp. 175–183, 2004.
[230] L. Stabile, F. C. Fuoco, e G. Buonanno, «Characteristics of particles and black carbon emitted by combustion of incenses, candles and anti-mosquito products», *Build. Environ.*, vol. 56, fasc. 0, Art. fasc. 0, 2012, doi: 10.1016/j.buildenv.2012.03.005.
[231] International Agency for Research on Cancer, «IARC Monographs on the Evaluation of carcinogenic Risks to Humans», Lyon, France, ott. 2013.
[232] International Agency for Research on Cancer, «International Agency for Research on Cancer. Agents classified by the IARC monographs, volumes 1-130.», Lyon, France, dic. 2021. [Online]. Disponibile su: https://monographs.iarc.who.int/agents-classified-by-the-iarc/.
[233] Office of Environmental Health Hazard Assessment, *Technical Support Document for Cancer Potency Factors: Methodologies for Derivation, Listing of Available Values, and Adjustments to Allow for Early Life Stage Exposures*. 2009.
[234] C. Andersen *et al.*, «Emissions of soot, PAHs, ultrafine particles, NOx, and other health relevant compounds from stressed burning of candles in indoor air», *Indoor Air*, vol. 31, fasc. 6, pp. 2033–2048, 2021.
[235] T.-S. Lin, «Indoor Air Pollution: Unusual Sources», in *Encyclopedia of Environmental Health*, J. O. Nriagu, A c. di, Burlington: Elsevier, 2011, pp. 201–207. doi: 10.1016/B978-0-444-52272-6.00710-8.
[236] T. T. Yang, S. T. Lin, H. F. Hung, R. H. Shie, e J. J. Wu, «Effect of relative humidity on polycyclic aromatic hydrocarbon emissions from smoldering incense», *Aerosol Air Qual. Res.*, vol. 13, fasc. 2, Art. fasc. 2, 2012.
[237] T.-T. Yang, S.-T. Lin, T.-S. Lin, e H.-Y. Chung, «Characterization of polycyclic aromatic hydrocarbon emissions in the particulate and gas phase from smoldering mosquito coils containing various atomic hydrogen/carbon ratios», *Sci. Total Environ.*, vol. 506, pp. 391–400, 2015.
[238] G. Shen *et al.*, «Emissions of PAHs from indoor crop residue burning in a typical rural stove: emission factors, size distributions, and gas− particle partitioning», *Environ. Sci. Technol.*, vol. 45, fasc. 4, pp. 1206–1212, 2011.

[239] M. D. Hays, N. D. Smith, J. Kinsey, Y. Dong, e P. Kariher, «Polycyclic aromatic hydrocarbon size distributions in aerosols from appliances of residential wood combustion as determined by direct thermal desorption—GC/MS», *J. Aerosol Sci.*, vol. 34, fasc. 8, pp. 1061–1084, 2003.

[240] T. V. Vu, J. Ondracek, V. Zdímal, J. Schwarz, J. M. Delgado-Saborit, e R. M. Harrison, «Physical properties and lung deposition of particles emitted from five major indoor sources», *Air Qual. Atmosphere Health*, vol. 10, fasc. 1, pp. 1–14, 2017.

[241] J. Osán *et al.*, «Experimental evaluation of the in-the-field capabilities of total-reflection X-ray fluorescence analysis to trace fine and ultrafine aerosol particles in populated areas», *Spectrochim. Acta Part B At. Spectrosc.*, vol. 167, p. 105852, mag. 2020, doi: 10.1016/j.sab.2020.105852.

[242] S. Seeger *et al.*, «Quantification of Element Mass Concentrations in Ambient Aerosols by Combination of Cascade Impactor Sampling and Mobile Total Reflection X-ray Fluorescence Spectroscopy», *Atmosphere*, vol. 12, fasc. 3, 2021, doi: 10.3390/atmos12030309.

[243] C. Sophonsiri e E. Morgenroth, «Chemical composition associated with different particle size fractions in municipal, industrial, and agricultural wastewaters», *Chemosphere*, vol. 55, fasc. 5, pp. 691–703, mag. 2004, doi: 10.1016/j.chemosphere.2003.11.032.

[244] International Commission on Radiological Protection, «Human respiratory tract model for radiological protection. A report of a Task Group of the International Commission on Radiological Protection.», *Ann. ICRP*, vol. 24, fasc. 1–3, pp. 1–482, 1994, doi: 10.1016/0146-6453(94)90029-9.

[245] Office of Environmental Health Hazard Assessment, *Technical Support Document for Cancer Potency Factors: Methodologies for Derivation, Listing of Available Values, and Adjustments to Allow for Early Life Stage Exposures.* 2009.

[246] L. Stabile, F. C. Fuoco, e G. Buonanno, «Characteristics of particles and black carbon emitted by combustion of incenses, candles and anti-mosquito products», *Build. Environ.*, vol. 56, fasc. 0, pp. 184–191, 2012, doi: 10.1016/j.buildenv.2012.03.005.

[247] E. J. Carlton *et al.*, «Relationships between home ventilation rates and respiratory health in the Colorado Home Energy Efficiency and Respiratory Health (CHEER) study», *Environ. Res.*, vol. 169, pp. 297–307, 2019.

[248] W. W. Nazaroff, «Residential air-change rates: A critical review», *Indoor Air*, vol. n/a, fasc. n/a, gen. 2021, doi: 10.1111/ina.12785.

[249] C. Howard-Reed, L. A. Wallace, e S. Emmerich, «Deposition rates of fine and coarse particles in residential buildings: literature review and measurements in an occupied townhouse», *Natl. Inst. Stand. Technol.*, 2003.

[250] L. A. Wallace, S. J. Emmerich, e C. Howard-Reed, «Effect of central fans and in-duct filters on deposition rates of ultrafine and fine particles in an occupied townhouse», *Atmos. Environ.*, vol. 38, fasc. 3, pp. 405–413, 2004.

[251] S. W. See e R. Balasubramanian, «Risk assessment of exposure to indoor aerosols associated with Chinese cooking», *Environ. Res.*, vol. 102, fasc. 2, pp. 197–204, 2006.

[252] M. Derudi *et al.*, «Emissions of air pollutants from scented candles burning in a test chamber», *Atmos. Environ.*, vol. 55, pp. 257–262, 2012.

[253] T. T. Yang, S. T. Lin, H. F. Hung, R. H. Shie, e J. J. Wu, «Effect of Relative Humidity on Polycyclic Aromatic Hydrocarbon Emissions from Smoldering Incense», *Aerosol Air Qual. Res.*, vol. 13, fasc. 2, pp. 662–671, 2013, doi: 10.4209/aaqr.2012.07.0182.

[254] L. Stabile, G. Buonanno, G. Ficco, e M. Scungio, «Smokers' lung cancer risk related to the cigarette-generated mainstream particles», *J. Aerosol Sci.*, vol. 107, pp. 41–54, mag. 2017, doi: 10.1016/j.jaerosci.2017.02.005.

[255] M. Scungio, L. Stabile, e G. Buonanno, «Measurements of electronic cigarette-generated particles for the evaluation of lung cancer risk of active and passive users», *J. Aerosol Sci.*, vol. 115, p. 1, 2018.
[256] S. E. Chatoutsidou, J. Ondráček, O. Tesar, K. Tørseth, V. Ždímal, e M. Lazaridis, «Indoor/outdoor particulate matter number and mass concentration in modern offices», *Build. Environ.*, vol. 92, pp. 462–474, 2015, doi: 10.1016/j.buildenv.2015.05.023.
[257] J. Qian, J. Peccia, e A. R. Ferro, «Walking-induced particle resuspension in indoor environments», *Atmos. Environ.*, vol. 89, pp. 464–481, giu. 2014, doi: 10.1016/j.atmosenv.2014.02.035.
[258] C. Howard-Reed, L. A. Wallace, e S. Emmerich, «Deposition rates of fine and coarse particles in residential buildings: literature review and measurements in an occupied townhouse», *Natl. Inst. Stand. Technol.*, 2003.
[259] M. Tiwari, S. K. Sahu, R. C. Bhangare, A. Yousaf, e G. G. Pandit, «Particle size distributions of ultrafine combustion aerosols generated from household fuels», *Atmospheric Pollut. Res.*, vol. 5, fasc. 1, pp. 145–150, gen. 2014, doi: 10.5094/APR.2014.018.
[260] F. d'Ambrosio Alfano, M. Dell'Isola, G. Ficco, e F. Tassini, «Experimental analysis of air tightness in Mediterranean buildings using the fan pressurization method», *Build. Environ.*, vol. 53, pp. 16–25, 2012.
[261] M. Carlsson, M. Touchie, e R. Richman, «A Compartmentalization & Ventilation System Retrofit Strategy for High-Rise Residential Buildings in Cold Climates», *Energy Procedia*, vol. 132, pp. 867–872, ott. 2017, doi: 10.1016/j.egypro.2017.09.682.
[262] UNI/TS 11300-1, «UNI/TS 11300-1. Prestazioni energetiche degli edifici. Parte 1: Determinazione del fabbisogno di energia termica dell'edificio per la climatizzazione estiva ed invernale», 2014.
[263] K. M. Smith e S. Svendsen, «Development of a plastic rotary heat exchanger for room-based ventilation in existing apartments», *Energy Build.*, vol. 107, pp. 1–10, 2015.
[264] T. Petry *et al.*, «Human health risk evaluation of selected VOC, SVOC and particulate emissions from scented candles», *Regul. Toxicol. Pharmacol.*, vol. 69, fasc. 1, pp. 55–70, 2014.
[265] J. P. Zacny e M. L. Stitzer, «Human smoking patterns», in *Monograph 7: The FTC Cigarette Test Method for Detemining Tar, Nicotine, and Carbon Monoxide Yields of U.S. Cigarettes*, N. I. of Health, A c. di, U.S. Department of health and human services, 1988, pp. 151–160.
[266] D. Rim, L. Wallace, S. Nabinger, e A. Persily, «Reduction of exposure to ultrafine particles by kitchen exhaust hoods: the effects of exhaust flow rates, particle size, and burner position», *Sci. Total Environ.*, vol. 432, pp. 350–356, 2012.
[267] A. Pacitto *et al.*, «Effect of ventilation strategies and air purifiers on the children's exposure to airborne particles and gaseous pollutants in school gyms», *Sci. Total Environ.*, vol. 712, p. 135673, apr. 2020, doi: 10.1016/j.scitotenv.2019.135673.
[268] S. Schumacher, D. Spiegelhoff, U. Schneiderwind, H. Finger, e C. Asbach, «Performance of New and Artificially Aged Electret Filters in Indoor Air Cleaners», *Chem. Eng. Technol.*, vol. 41, fasc. 1, pp. 27–34, gen. 2018, doi: 10.1002/ceat.201700105.
[269] J. M. Hammersley e D. C. Handscomb, *Monte Carlo Methods*. London & New York: Chapman and Hall, 1964.
[270] S. W. See e R. Balasubramanian, «Chemical characteristics of fine particles emitted from different gas cooking methods», *Atmos. Environ.*, vol. 42, fasc. 39, pp. 8852–8862, 2008.
[271] F. Arpino, G. Cortellessa, e A. Mauro, «Transient Thermal Analysis of Natural Convection in Porous and Partially Porous Cavities», *Numer. Heat Transf. Part Appl.*, vol. 67, fasc. 6, pp. 605–631, mar. 2015, doi: 10.1080/10407782.2014.949133.

[272] V. Martins *et al.*, «Relationship between indoor and outdoor size-fractionated particulate matter in urban microenvironments: Levels, chemical composition and sources», *Environ. Res.*, vol. 183, p. 109203, apr. 2020, doi: 10.1016/j.envres.2020.109203.
[273] C. Kakoulli, A. Kyriacou, e M. P. Michaelides, «A Review of Field Measurement Studies on Thermal Comfort, Indoor Air Quality and Virus Risk», *Atmosphere*, vol. 13, fasc. 2, p. 191, 2022.
[274] C. Peretti e S. Schiavon, «Indoor environmental quality surveys. A brief literature review.», 2011.
[275] S. Kim, E. Paulos, e J. Mankoff, «inAir: a longitudinal study of indoor air quality measurements and visualizations», *Proceedings of the SIGCHI Conference on Human Factors in Computing Systems*. Association for Computing Machinery, Paris, France, pp. 2745–2754, 2013. [Online]. Disponibile su: https://doi.org/10.1145/2470654.2481380
[276] S. E. West *et al.*, «Particulate matter pollution in an informal settlement in Nairobi: Using citizen science to make the invisible visible», *Appl. Geogr.*, vol. 114, p. 102133, 2020.
[277] N. C. Jenn, «Designing A Questionnaire.», *Malays. Fam. Physician Off. J. Acad. Fam. Physicians Malays.*, vol. 1, fasc. 1, pp. 32–35, 2006.
[278] C. Asbach *et al.*, «Comparability of portable nanoparticle exposure monitors», *Ann. Occup. Hyg.*, vol. 56, fasc. 5, pp. 606–621, 2012.
[279] I. Rivas *et al.*, «Identification of technical problems affecting performance of DustTrak DRX aerosol monitors», *Sci Total Env.*, vol. 584–585, pp. 849–855, apr. 2017, doi: 10.1016/j.scitotenv.2017.01.129.
[280] T. Hussein, A. Wierzbicka, J. Löndahl, M. Lazaridis, e O. Hänninen, «Indoor aerosol modeling for assessment of exposure and respiratory tract deposited dose», *Atmos. Environ.*, vol. 106, pp. 402–411, apr. 2015, doi: 10.1016/j.atmosenv.2014.07.034.
[281] C. Chen e B. Zhao, «Review of relationship between indoor and outdoor particles: I/O ratio, infiltration factor and penetration factor», *Atmos. Environ.*, vol. 45, fasc. 2, pp. 275–288, 1, doi: 10.1016/j.atmosenv.2010.09.048.
[282] S. B. Idso, C. D. Idso, e R. C. Balling, «Seasonal and diurnal variations of near-surface atmospheric CO2 concentration within a residential sector of the urban CO2 dome of Phoenix, AZ, USA», *NADP 2000 - Ten Years Clean Air Act Amend.*, vol. 36, fasc. 10, pp. 1655–1660, apr. 2002, doi: 10.1016/S1352-2310(02)00159-0.
[283] B. Stephens e J. A. Siegel, «Ultrafine particle removal by residential heating, ventilating, and air-conditioning filters», *Indoor Air*, vol. 23, fasc. 6, pp. 488–97, dic. 2013, doi: 10.1111/ina.12045.
[284] A. Pacitto *et al.*, «Effect of ventilation strategies and air purifiers on the children's exposure to airborne particles and gaseous pollutants in school gyms», *Sci. Total Environ.*, vol. 712, p. 135673, apr. 2020, doi: 10.1016/j.scitotenv.2019.135673.
[285] A. Persily e L. de Jonge, «Carbon dioxide generation rates for building occupants», *Indoor Air*, vol. 27, fasc. 5, pp. 868–879, 2017, doi: 10.1111/ina.12383.
[286] G. Shen *et al.*, «Quantifying source contributions for indoor CO2 and gas pollutants based on the highly resolved sensor data», *Environ. Pollut.*, vol. 267, p. 115493, 2020.
[287] B. C. Singer, R. Z. Pass, W. W. Delp, D. M. Lorenzetti, e R. L. Maddalena, «Pollutant concentrations and emission rates from natural gas cooking burners without and with range hood exhaust in nine California homes», *Build. Environ.*, vol. 122, pp. 215–229, 2017.
[288] K. Teinilä *et al.*, «Characterization of particle sources and comparison of different particle metrics in an urban detached housing area, Finland», *Atmos. Environ.*, vol. 272, p. 118939, mar. 2022, doi: 10.1016/j.atmosenv.2022.118939.

[289] E. G. Cauda, B. K. Ku, A. L. Miller, e T. L. Barone, «Toward developing a new occupational exposure metric approach for characterization of diesel aerosols», *Aerosol Sci. Technol.*, vol. 46, fasc. 12, pp. 1370–1381, 2012.
[290] V. Rizza, L. Stabile, G. Buonanno, e L. Morawska, «Variability of airborne particle metrics in an urban area», *Environ. Pollut.*, vol. 220, Part A, pp. 625–635, 1, doi: 10.1016/j.envpol.2016.10.013.
[291] W. H. Kruskal e W. A. Wallis, «Use of Ranks in One-Criterion Variance Analysis», *J. Am. Stat. Assoc.*, vol. 47, fasc. 260, pp. 583–621, dic. 1952, doi: 10.1080/01621459.1952.10483441.
[292] G. Buonanno, G. Johnson, L. Morawska, e L. Stabile, «Volatility characterization of cooking-generated aerosol particles», *Aerosol Sci. Technol.*, vol. 45, fasc. 9, pp. 1069–1077, 2011.
[293] L. A. Wallace, W. R. Ott, e C. J. Weschler, «Ultrafine particles from electric appliances and cooking pans: experiments suggesting desorption/nucleation of sorbed organics as the primary source», *Indoor Air*, vol. 25, fasc. 5, pp. 536–46, ott. 2015, doi: 10.1111/ina.12163.
[294] L. Wallace e W. Ott, «Personal exposure to ultrafine particles», *J. Expo. Sci. Environ. Epidemiol.*, vol. 21, fasc. 1, pp. 20–30, 2011.
[295] G. Ma, J. Lin, e N. Li, «Longitudinal assessment of the behavior-changing effect of app-based eco-feedback in residential buildings», *Energy Build.*, vol. 159, pp. 486–494, gen. 2018, doi: 10.1016/j.enbuild.2017.11.019.
[296] J. Kim, S. Kim, S. Bae, M. Kim, Y. Cho, e K.-I. Lee, «Indoor environment monitoring system tested in a living lab», *Build. Environ.*, vol. 214, p. 108879, apr. 2022, doi: 10.1016/j.buildenv.2022.108879.
[297] Y. N. Golumbic, B. Fishbain, e A. Baram-Tsabari, «User centered design of a citizen science air-quality monitoring project», *Int. J. Sci. Educ. Part B*, vol. 9, fasc. 3, pp. 195–213, lug. 2019, doi: 10.1080/21548455.2019.1597314.
[298] E. Gramsch *et al.*, «Citizens' Surveillance Micro-network for the Mapping of PM2.5 in the City of Concón, Chile», *Aerosol Air Qual. Res.*, vol. 20, fasc. 2, pp. 358–368, 2020, doi: 10.4209/aaqr.2019.04.0179.
[299] E. Gramsch *et al.*, «Influence of Particle Composition and Size on the Accuracy of Low Cost PM Sensors: Findings From Field Campaigns», *Front. Environ. Sci.*, vol. 9, 2021, doi: 10.3389/fenvs.2021.751267.
[300] H. Fritz *et al.*, «Design, fabrication, and calibration of the Building EnVironment and Occupancy (BEVO) Beacon: A rapidly-deployable and affordable indoor environmental quality monitor», *Build. Environ.*, vol. 222, p. 109432, ago. 2022, doi: 10.1016/j.buildenv.2022.109432.
[301] I. Demanega, I. Mujan, B. Singer, A. Andelkovic, F. Babich, e D. Licina, «Performance assessment of low-cost environmental monitors and single sensors under variable indoor air quality and thermal conditions», *Build. Environ.*, 2021, doi: 10.1016/j.buildenv.2020.107415.
[302] J.-B. Renard *et al.*, «LOAC: a small aerosol optical counter/sizer for ground-based and balloon measurements of the size distribution and nature of atmospheric particles – Part 1: Principle of measurements \hack\newlineand instrument evaluation», *Atmospheric Meas. Tech.*, vol. 9, fasc. 4, pp. 1721–1742, 2016, doi: 10.5194/amt-9-1721-2016.
[303] G. Buonanno, E. R. Jayaratne, L. Morawska, e L. Stabile, «Metrological Performances of a Diffusion Charger Particle Counter for Personal Monitoring», *Aerosol Air Qual. Res.*, vol. 14, pp. 156–167, 2014, doi: 10.4209/aaqr.2013.03.0085.
[304] H. Kaminski *et al.*, «Comparability of mobility particle sizers and diffusion chargers», *J. Aerosol Sci.*, vol. 57, pp. 156–178, 2013.

[305] Z. Xu, «Sampling Theory», in *Fundamentals of Air Cleaning Technology and Its Application in Cleanrooms*, Z. Xu, A c. di, Berlin, Heidelberg: Springer Berlin Heidelberg, 2014, pp. 729–776. doi: 10.1007/978-3-642-39374-7_16.

[306] S.-L. von der Weiden, F. Drewnick, e S. Borrmann, «Particle Loss Calculator – a new software tool for the assessment of the performance of aerosol inlet systems», *Atmos Meas Tech*, vol. 2, fasc. 2, pp. 479–494, set. 2009, doi: 10.5194/amt-2-479-2009.

[307] W. C. Driscoll, «Robustness of the ANOVA and Tukey-Kramer statistical tests», *Proc. 19th Int. Conf. Comput. Ind. Eng.*, vol. 31, fasc. 1, pp. 265–268, ott. 1996, doi: 10.1016/0360-8352(96)00127-1.

[308] E. L. Mendes Tavares, A. G. Brasolotto, S. A. Rodrigues, A. B. Benito Pessin, e R. H. Garcia Martins, «Maximum Phonation Time and s/z Ratio in a Large Child Cohort», *J. Voice*, vol. 26, fasc. 5, p. 675.e1-675.e4, set. 2012, doi: 10.1016/j.jvoice.2012.03.001.

[309] G. Koch, S. Poulsen, I. Espelid, e D. Haubek, *Pediatric Dentistry: A Clinical Approach*. Wiley, 2017. [Online]. Disponibile su: https://books.google.it/books?id=IxFSDQAAQBAJ

[310] P. H. Burri, «Fetal and postnatal development of the lung.», *Annu. Rev. Physiol.*, vol. 46, pp. 617–628, 1984, doi: 10.1146/annurev.ph.46.030184.003153.

[311] J. C. Kahane, «A morphological study of the human prepubertal and pubertal larynx», *Am. J. Anat.*, vol. 151, fasc. 1, pp. 11–19, gen. 1978, doi: 10.1002/aja.1001510103.